# SYNTHESIS OF METAKAOLIN-BASED GEOPOLYMER AND ITS PERFORMANCE AS SOLE STABILIZER OF EXPANSIVE SOILS

by

RINU ANN SAMUEL

Presented to the Faculty of the Graduate School of

The University of Texas at Arlington

in Partial Fulfillment of the Requirements

for the Degree of

DOCTOR OF PHILOSOPHY

THE UNIVERSITY OF TEXAS AT ARLINGTON

December 2019

*This work is dedicated to my loving husband, Sonu.*

ACKNOWLEDGEMENTS

I am sincerely grateful to my research advisor, Dr. Anand Puppala for the opportunity to pursue my doctoral research under his guidance. His mentorship, supervision, encouragement, and earnest care were extremely valuable to me during my time at UTA. I would also like to thank my committee members – Dr. Laureano Hoyos, Dr. Xinbao Yu, and Dr. Erick Jones for their valuable advice, assistance and support.

This research was funded by the Transportation Consortium of the South-Central States (TranSET) under the projects 17GTTAMU02 and 18CTAMU04. Additional funding was provided by the Department of Civil Engineering through GTA and GRA scholarships. I would also like to thank the Dwight D. Eisenhower Transportation Fellowship Program (DDETFP) under the U.S. Department of Transportation for granting me the doctoral research fellowship for two years.

I would like to thank Dr. Miladin Radovic and Oscar Huang, our research collaborators at the Texas A&M University, for their cooperation and insight on geopolymer synthesis. I would like to thank to James Hutt of TEAM Consultants, Inc., Arlington, TX for providing the Lewisville soil for this research.

I would like to express my sincere thanks to Dr. Aritra Banerjee, for his immense help and guidance during the course of the research. I would also like to thank my colleagues Dr. Sayantan Chakraborty, Dr. Surya Congress, Dr. Jasaswee Das, Dr. Santiago Caballero, Dr. Ali Shafikhani, Dr. Anu George, Dr. Shi He,

Manikanta Kartik, Leila Mosadegh, Ashrafuzzaman Khan, Nripojyoti Biswas, Puneet Bhaskar, Burak Boluk, and Prince Kumar for their support, assistance and encouragement during my time at UTA. Special thanks to Nice Kaneza, Sandesh Gautam, Lam Le, Jacque Bussey, Jose Bautista, and Harshwardhan Sawaitul, for their assistance with laboratory testing.

Words cannot express my gratitude towards my family for their love and support throughout this research. I am grateful for my parents, Omana and Madhu Samuel, for their constant encouragement and advice. I am eternally grateful to my husband, Sonu Varghese, for being my constant support, biggest believer, and best partner, who was patient and encouraging of the long hours and commitment to my research. And above all, I am thankful to Almighty God for opportunities, and life experiences beyond my wildest dreams.

November 30, 2019

ABSTRACT

SYNTHESIS OF METAKAOLIN-BASED GEOPOLYMER AND ITS PERFORMANCE AS SOLE STABILIZER OF EXPANSIVE SOILS

Rinu Ann Samuel

The University of Texas at Arlington, 2019

Supervising Professor: Dr. Anand J. Puppala

Expansive soils have been stabilized using conventional soil stabilizers such as lime and cement for many decades. These conventional stabilizers form cementitious productions that enhance the strength properties and reduce the swelling and shrinkage potential of expansive soils. However, the energy-intensive production operations of conventional soil stabilizers release substantial amounts of harmful greenhouse gases into the atmosphere. In addition, conventional soil stabilizers are also prone to durability issues, which make them somewhat ineffective as long-term solutions. Furthermore, the use of calcium-based stabilizers cause excessive swelling and shrinkage in sulfate-bearing subgrade soils due to the formation of highly expansive minerals like Ettringite.

This study investigates the use of geopolymers as an alternative soil stabilizer for expansive soils. Geopolymers are alumino-silicate binders that have received much attention as a sustainable alternative to conventional chemical additives. Geopolymers have high compressive strengths and can be processed at room temperatures from aqueous solutions by utilizing waste materials (e.g. fly

ash) or abundant natural sources (e.g. clay). Geopolymers have been investigated by a few researchers for the purpose of soil stabilization, although most studies were performed on non-expansive soils and focused solely on the ability of geopolymers to enhance soil strength. This study evaluates the performance of a metakaolin-based geopolymer in enhancing strength/stiffness, volume change, and long-term performance characteristics of expansive soils.

The objective of this research is to synthesize a metakaolin-based geopolymer and evaluate its efficiency as the sole binder to stabilize expansive soils. Two expansive soils from north Texas were obtained and treated with the in-house synthesized metakaolin-based geopolymer at different dosages for different curing periods. The following tasks were outlined to accomplish the objectives of this research: (1) synthesize metakaolin-based geopolymer and treat expansive soils with three different dosages, (2) perform basic, chemical, engineering, and mineralogical testing of control and geopolymer-treated soils, (3) treat expansive soils with lime to compare with geopolymer treatment, (4) analyze test results to evaluate efficiency of geopolymer to improve expansive soils, and (5) assess and compare sustainability and resiliency benefits of geopolymer and lime treatment for expansive soils.

Three dosages of the in-house synthesized metakaolin-based geopolymer was applied to both expansive soils and tested for different properties. The geopolymer dosages applied in this study are defined as the percentage weight of

metakaolin in the geopolymer, with respect to the dry weight of soil to be treated. Geopolymer treatment was found to decrease the plasticity index of the expansive soils, with increasing dosage and curing period. Significant strength and stiffness enhancement was observed in geopolymer-treated soils. Negligible swelling and shrinkage potential were observed in soils treated with just low geopolymer dosages. Modified durability and leachability tests conducted revealed low strength loss in geopolymer-treated soils. Strength, swell, and modified durability test results of lime-treated soils were found to be comparable to results from geopolymer-treated soils.

Microstructural studies provided insight into geopolymer gel formation that explains the enhanced macro-behavior of geopolymer-treated soils. Additionally, sustainability and resiliency assessment studies showed that geopolymers have a much lower impact on the environment than lime. Metakaolin-based geopolymers are evidently found to be quite efficient in stabilizing expansive soils.

It is expected that the present research findings will be valuable for future investigations and design implementations of geopolymers as a more sustainable and ‘green’ alternative to conventional soil stabilizers.

TABLE OF CONTENTS

LIST OF FIGURES

LIST OF TABLES

# CHAPTER 1

# INTRODUCTION

## 1.1 Background

Expansive soils are soils that have a tendency to undergo significant changes in volume due to variations in moisture content. The volume changes in expansive soils may result in heaving and cracking that lead to infrastructure damages worth several billions of dollars each year all over the world. In the United States (US) alone, annual damages due to expansive soils are projected to cost more than $7 Billion (Wray and Meyer 2004) and are classified as a geohazard by the Federal Emergency Management Agency (FEMA). Texas and its surrounding states are known to have a prevalence of expansive soils, in spite of which transportation infrastructure has been frequently built on them for decades. In addition to the presence of expansive soils, wet periods in Texas are followed by hot arid conditions, which significantly aggravates the problem. Alternating seasons of rain and drought result in recurring cycles of swelling and shrinking movements, which impose additional stresses to the infrastructure. In Texas, more than a billion dollars has been spent for the restoration of damages for infrastructure built on expansive soils (Punthutaecha et al. 2006).

Over the last several decades, several types of stabilization techniques – including physical, mechanical, and chemical methods were developed to treat expansive soils (Hausmann 1990). Of these methods, chemical stabilization,

particularly using calcium-based stabilizers, proved to be more reliable and capable of stabilizing soils effectively (Petry and Little 2002, Chakraborty and Nair 2017, 2018, Puppala et al. 2019a). Conventionally, chemical stabilization methods use cementitious materials such as lime and cement to enhance unconfined compressive strength and stiffness properties of expansive soils. Although these calcium-based stabilizers are widely used, they are limited by issues caused due to formation of the mineral Ettringite in sulfate-rich soils, which is known to cause excessive swelling resulting in infrastructure failure. Moreover, conventional soil stabilizers do not offer sustainable and eco-friendly treatments, as their production has been flagged as major contributors of carbon dioxide emissions worldwide (Zhang et al. 2013). As such, there is a need for soil stabilizers that are sustainable and durable as well as capable to significantly improve engineering properties of expansive soils.

Non-traditional stabilizers are therefore being investigated as improved alternatives for soil stabilization. The use of non-traditional stabilizers is usually prompted when traditional calcium-based stabilizers are unavailable or lacking in quality. While most non-traditional stabilizers are usually classified as either polymeric, ionic, or enzymatic in nature, many can be classified as recycled waste materials that are industry by-products. As a result, many non-traditional stabilizers are inherently more eco-friendly in nature, although they are not widely accepted for soil stabilization procedures. The reluctance to accept non-traditional stabilizers

for mainstream work can be attributed to the stabilizers being too novel in most places and the lack of comprehensive, peer-reviewed research on their ability to enhance multiple engineering properties of soils.

A relatively new class of materials known as ‘geopolymers’ have been hailed as sustainable alternatives to Ordinary Portland Cement (OPC) and Lime additives (Davidovits 2008, Provis and van Deventer 2009). Geopolymers can be synthesized from by-products of existing industrial processes and are known to have high compressive strength, low shrinkage, as well as heat and fire-resistant properties. Geopolymers have a much lower carbon footprint than lime and OPC (Gartner 2004), and are therefore being considered as an alternative to conventional soil stabilizers. While much information is available on the synthesis of geopolymers for use in the ceramics and resin industries, very few studies have investigated their viability as soil stabilizers. Additionally, the few studies that do explore the ability of geopolymers to stabilize soils mostly tend to focus only on the enhancement of the unconfined compressive strength of soil on geopolymer treatment, or do not consider their ability to stabilize expansive soils (Cristelo et al. 2012, Liu et al. 2016, Phummiphan et al. 2016).

This study makes an attempt to address some of the limitations in this regard. In this study, geopolymers are synthesized in-house and applied in different dosages as the sole stabilizer to two different expansive soils found in the North Texas area. In addition to considering enhancement of unconfined compressive

strength of soils, the effect of geopolymers on volume-change, stiffness and long-term performance characteristics of expansive soils is also investigated. Additionally, geopolymer-treated soils were compared to lime-treated soils, to evaluate their comparative effects on expansive soils.

## 1.2 Research Objectives

The primary objective of this study is to synthesize a metakaolin-based geopolymer and assess its effectiveness as the sole binder in stabilizing expansive soils. Specific objectives of this study are listed below:

1. Treat two expansive soils with the metakaolin-based geopolymer at different dosages. Perform engineering and microstructural characterization tests on geopolymer-treated soils to detect and quantify enhancement of soil properties.
2. Treat control soils with a conventional stabilizer like lime, to compare improvement in soil properties of geopolymer treatment versus lime treatment of soils.
3. Analyze results to evaluate the efficiency of geopolymers as the sole soil stabilizer, and determine optimum geopolymer dosage for volume change, strength/stiffness and long-term performance properties.
4. Assess sustainability and resiliency benefits of using metakaolin-based geopolymer as sole stabilizer of expansive clays, in comparison to lime.

Figure 1.1 presents a schematic of the experimental program that was performed to accomplish the above research objectives.

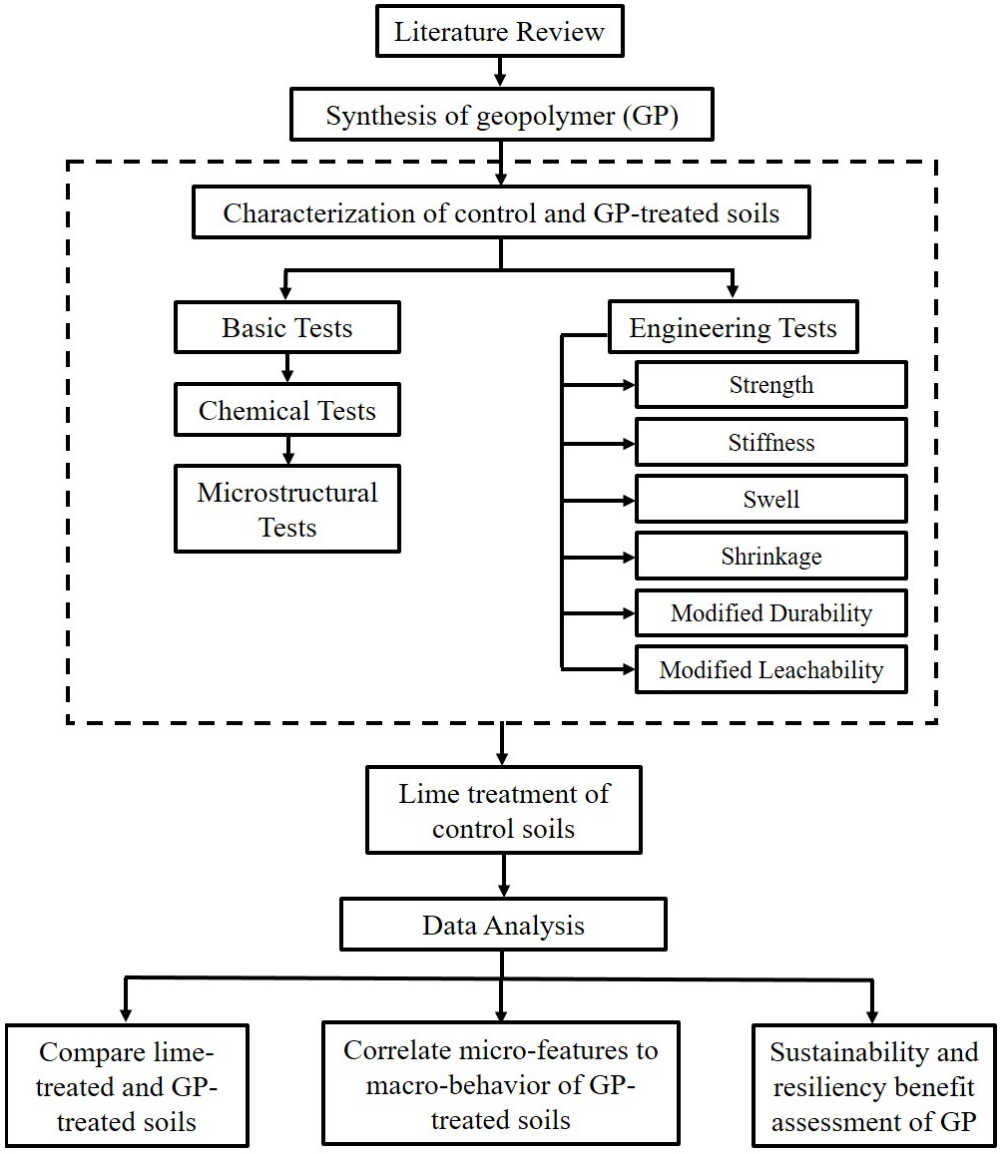


Figure 1.1 Schematic of experimental program followed in this study

## 1.3 Organization of Dissertation

This dissertation is the final culminating product of this research study and is categorized into seven chapters. This section provides a brief outline to the organization and contents of this dissertation.

Chapter 1 provides an introduction to the research with some background illuminating the necessity and relevance of this work, as well as the specific research objectives and tasks detailed to accomplish the goal. A brief description to each chapter details the organization of the presented dissertation.

Chapter 2 provides a review of existing literature on expansive soils, conventional soil stabilization techniques and their limitations, an introduction to geopolymers and their characteristics, as well as their use as soil stabilizers in the past.

Chapter 3 describes in detail the steps undertaken to synthesize a metakaolin-based geopolymer, including the selection of raw materials, mix proportioning, and curing conditions needed to optimize the geopolymer composition for this study.

Chapter 4 details the experimental methodology and test procedures conducted to accomplish the research objectives of this study. This chapter elaborates on the selection of expansive soils used in the study, basic soil characterization tests, microstructural and engineering characterization tests followed to determine the behavior of control and geopolymer-treated soils, and

steps undertaken to treat and cure geopolymer-treated soils for this study. Furthermore, some additional tests conducted on lime-treated soils are discussed as well.

Chapter 5 presents the results of all the basic and engineering characterization tests of control and geopolymer-treated soils, and analyzes improvement of strength/stiffness, volume-change and long-term performance of geopolymer-treated soils with respect to control soils. Additionally, a comparison of geopolymer-treated soils with lime-treated soils were presented in this chapter.

Chapter 6 discusses the results of microstructural tests and attempts to correlate micro characteristics geopolymer-treated soils to their macro behavior. Additionally, sustainable benefits of geopolymers are evaluated in this chapter.

Chapter 7 summarizes the major findings and conclusions from this study, in addition to addressing future research needs and recommendations.

# CHAPTER 2

# LITERATURE REVIEW

## 2.1 Introduction

Expansive soils demonstrate swelling and shrinkage due to variations in moisture content (Adem and Vanapalli 2015, Soltani et al. 2017, Julina and Thyagaraj 2019). These soils pose a threat to existing infrastructures and prospective developments and require recurring reconstruction and restoration costs worth billions of dollars (Jones and Holtz 1973, Puppala and Cerato 2009, Atahu et al. 2019). Expansive soil stabilization techniques were extensively researched due to their ability to potentially reduce construction and maintenance costs. Various techniques including the use of chemical additives have been used for the last several decades to stabilize expansive soils (Tayabji et al. 1982). Conventional stabilizers such as lime and cement, have proven to reduce swelling and shrinkage potential of expansive soils, in addition to enhancing its strength and stiffness properties (Little 1996, Prusinski and Bhattacharja 1999).

However, calcium-based stabilizers are known to cause excessive heaving and volume change in sulfate-rich soils due to the formation of the mineral known as Ettringite (Katz et al. 2001, Puppala et al. 2005, Zhang et al. 2015). Additionally, production of lime and cement are major contributors in escalating carbon dioxide emissions worldwide, due to the high energy requirement during production (Chen et al. 2010, Provis and van Deventer 2014, Garcia-Lodeiro et al. 2015).

Furthermore, conventional stabilizers are also limited due to their durability and leaching issues, which affect their long-term performance.

This chapter reviews available literature for information on expansive soils, ways to stabilize them and identifies issues regarding stabilization of expansive soils. Section 1 describes expansive soils and its association with clay mineralogy. Section 2 elaborates on conventional soil stabilization techniques. Sections 3 and 4 introduce geopolymers and present previous research conducted on stabilizing soils using geopolymers.

## 2.2 Expansive soils

Expansive soils exhibit susceptibility to swelling and shrinking due to moisture fluctuations. Expansive soils are prevalent all over the world, mostly in areas with semi-arid to arid climates where the annual evapo-transpiration rates are higher than the annual precipitation (Jones and Holtz 1973, Puppala et al. 2005, 2013, Talluri et al. 2013, Banerjee and Puppala 2015, Banerjee 2017, Congress and Puppala 2019). The swelling and shrinking nature of the expansive soils makes them quite erratic and are not suitable to be built on. In spite of their notoriety, expansive soils cannot be bypassed due to aggressive urbanization and rapid population growth (Williams 2003) or simply because of their sheer pervasiveness. Infrastructure damage caused by expansive soils have been reported by many countries such as Australia, Canada, China, India, Israel, South Africa, and the United States (Nelson and Miller 1992, Steinberg 1998, Saride et al. 2010).

The extent of swelling clays in the conterminous United States is shown in Figure 1 (Olive et al. 1989); areas with high swelling potential are colored as pink and blue. While almost half of the conterminous U.S. is observed to have expansive clays, the majority of the state of Texas is shown to have a prevalence of clays with high swelling potential. As such, it makes it virtually impossible to avoid expansive soils while constructing necessary infrastructure within the state of Texas. Each wet and dry season causes considerable infrastructure distress to foundations, pavements, buried utilities and other structures built on expansive soils, due to the volume changes and movements from shrinking and swelling of soils (George et al. 2018, Huang et al. 2019, Chakraborty et al. 2019).

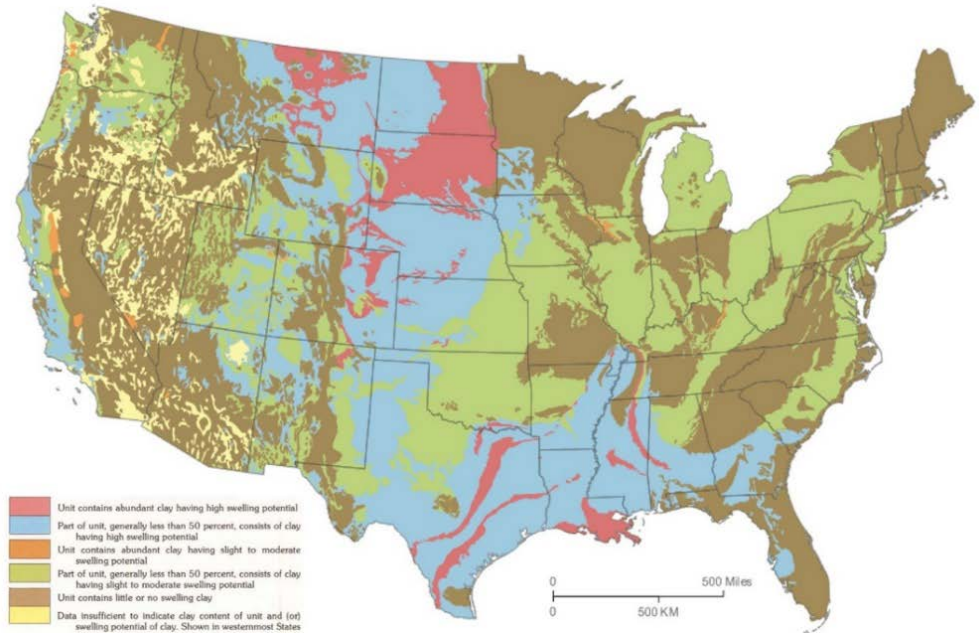


Figure 2.1 Swelling clays map of the conterminous United States (Olive et al. 1989).

The swelling and shrinking potential of expansive clays is mainly governed by three factors: soil properties, environmental influences and state of stresses (Nelson and Miller 1992). Soil properties affecting the shrink-swell potential of soils include clay mineralogy, soil-water chemistry, soil suction, plasticity, soil structure and fabric, permeability, as well as dry density; while influential environmental factors include moisture variations, climate, groundwater, drainage, vegetation, temperature, loading and stress history (Nelson and Miller 1992).

Clay mineralogy plays a substantial role in establishing the shrink-swell potential of soils. Some of the main types of clay minerals that have been classified include: Kaolinite, Illite, Smectite, Vermiculite, Chlorite and Halloysite, of which the first three are most commonly found (Bailey 1980). Montmorillonite, the most common mineral of the smectite clay mineral group, is the dominant source of swelling in expansive soils found prevalent all over the world (Mitchell and Soga 2005). As such smectite is often referred to as Montmorillonite. Montmorillonites are held together by very weak van der Waals forces and have the least basal spacing (9.6 Å) of the three major clay minerals. Different clay mineral exhibit different measures of swelling and shrinking potential due to the variations in their individual electrical fields.

Clay minerals usually have a net negative charge due to their intrinsic physico-chemical properties, thus drawing dipolar water molecules and salt cations such as sodium (Na), calcium (Ca), potassium (K), and magnesium (Mg) to

maintain charge neutrality. Large amounts of water can be accumulated between clay particles as a result of the hydration of cations and adsorptive forces of clay crystals; this hydrophilic nature of clay minerals forms a double-layer water around the clay minerals resulting in volume change (Snethen 1980, Nelson and Miller 1992). The negatively charged clay particle along with the solution at its interface that contains the exchangeable cations is referred to as the diffuse double layer or DDL (Bohn et al. 1985). According to Nelson and Miller (1992), the overlapping DDLs between clay particles generate repulsive forces that can be considered to be micro-scale swelling pressures, therefore the swelling potential of soils increase with the increase in the thickness of their DDLs.

The quantity of exchangeable cations required to balance the negative charge on the surface of the clay particle in the soil is known as the cation exchange capacity (CEC), and is expressed as milliequivalents (meq) per gram of dry clay. To determine CEC in the laboratory, the adsorbed cations are replaced by saturating the exchange sites with a known chemical species; the known cations required to saturate the exchange sites are then determined analytically (Nelson and Miller 1992). The CEC of a soil is closely related to its clay mineralogy and is a good indicator of the swell potential of soils, as high CEC values correspond to high surface activity resulting in high swell potential. Table 2.1 shows typical values of CEC for common clay minerals, where Montmorillonite known to have high

swelling potential is shown to have the highest CEC values among other clay minerals.

Table 2.1: Typical CEC values for major clay minerals (Nelson and Miller 1992)

| Clay Mineral | CEC (meq/100g) |
|---|---|
| Kaolinite | 3 - 15 |
| Illite | 10 - 40 |
| Montmorillonite | 80 - 150 |

Other properties that significantly influence the swelling potential of expansive soils are plasticity and density. Atterberg limits provide a quantification of the plasticity or the consistency of soils. Table 2.2 provides a summary of the classification of swelling potential made by different researchers based on the plasticity index (PI) of soil. While there is no definitive agreement on the limits of PI that conforms to a specific swelling potential, most researchers concur that a soil with PI of over 20 can have high swelling potential (Seed et al. 1962, Raman 1967, Terzaghi and Peck 1967). It is also understood that high soil density leads to higher swell potential.

Table 2.2: Classification of swell potential based on PI by different researchers

| Swelling Potential | Seed et al., 1962 | Terzaghi & Peck, 1967 | Raman, 1967 | Nelson & Miller, 1992 |
|---|---|---|---|---|
| Low | 0-10 | 0-15 | 0-12 | 0-18 |
| Medium | 10-20 | 10-35 | 12-23 | 15-28 |
| High | 20-35 | 20-55 | 23-32 | 25-41 |
| Very High | > 35 | > 55 | >32 | >35 |

## 2.3 Conventional Soil Stabilization Techniques

The impact of expansive soils is most discernible near the ground surface where confining stresses are low enough to be overcome by swell pressures exerted by expansive soils, resulting in uplift and damage of overlying infrastructure (Punthutaecha et al. 2006). Damage caused by expansive soils include but are not limited to foundation failure due to differential settlement or uplift, slope failures due to desiccation cracks, and pavement distress and failure due to soil heave and cracking (Congress et al. 2019, Jafari et al. 2019a, 2019b, Puppala et al. 2019c). As such, stabilization techniques are applied to expansive soils to mitigate volume change and movements.

Problematic soils are usually stabilized by means of moisture-control methods, ponding or prewetting, removal and replacement of soils, and other mechanical or chemical stabilization techniques. Moisture-control methods try to sustain the initial water content in a soil mass, so as to avert water content variations that may lead to swelling and shrinking of soils. While it is extremely difficult to prevent changes in water content of soil, it is possible to regulate its rate of change to minimize seasonal fluctuations over a period of time (Nelson and Miller 1992). Moisture barriers or drains are usually employed for this purpose. Moisture-control methods prove quite ineffective in expansive soils as they are known to have low permeability and high soil suction, which would significantly increase the time required to regulate moisture change. Similarly, the idea behind ponding or

prewetting of soils is to induce most of the potential heave prior to construction. While this method could be used successfully for a soil with decent permeability and rapid swell properties, it proves quite impractical in expansive soils due to the extended period of time required for prewetting as well as the significant loss in bearing capacity.

### *2.3.1 Mechanical Stabilization*

Mechanical stabilization refers to the technique where mechanical improvements are conducted on the soil using materials that do not alter inherent soil properties (Bell 1993, Nazarian et al. 2015). Some of the methods performed as part of mechanical stabilization of soils include deep densification, precompression, and reinforcement. Deep densification increases the density of the soil mass by expelling the air within the soil voids in a rapid manner, resulting in increased shear strength and decreased permeability thereby reducing its chance of settlement. Two main types of deep densification techniques used to stabilize soils are dynamic compaction and vibro-compaction (Kirsch and Bell 2012).

Dynamic compaction is used to densify loose granular soils by high energy impact. The appropriate density is achieved based on the weight of the tamper, the height of drop, and the number of drops onto a grid that covers most of the soil that required compaction. Dynamic compaction improves the engineering properties of soil by decreasing its void ratio and increasing its bearing capacity and strength. Dynamic compaction is most effective in cohesionless soils, and is considered

inappropriate for clayey soils (Nicholson 2014). Vibro-compaction techniques employ the use of vibratory techniques that eliminate excess pore water pressure enabling consolidation and consequently an increase in shear strength. Furthermore, it increases the bearing capacity of the soil, decreases settlement and mitigates liquefaction potential (Nicholson 2014, Banerjee et al. 2018a). Vibro-compaction could be used to stabilize expansive soils as it facilitates soil drainage but has proved more effective in cohesionless soils (Nicholson 2014). In addition, low-density compaction of soils could minimize heave of expansive soils, but special attention must be paid to ensure that the soil has adequate strength at the low density. Densification of soils using both dynamic compaction and vibro-compaction are especially effective in cohesionless soils, however in cohesive soils particle rearrangement and interlocking through compaction is quite difficult to attain. Reinforcement is another way to stabilize soils and reinforcement is provided using geosynthetics, such as geotextiles, geogrids, and Geocells, for various types of structures (El Sawwaf 2007, Biswas and Ghosh 2018, 2019, George et al. 2019c, 2019a, 2019b). Reinforcements have been utilized to reinforce pavements, slopes, earth-retaining walls and others.

Removal of problematic soils and their replacement with non-expansive compacted fills is another approach with expansive soils. Some of the major factors that should be considered for this method are the amount and depth of material to be removed, the location of site, and the cost of fill placement. Usually the extensive

spread of expansive soils and the cost associated with removal and replacement of soils makes it an impractical option.

### *2.3.2 Chemical Stabilization*

Chemical stabilization refers to the mixing of chemical additives to the soil that alter the physico-chemical properties of the soil thereby enhancing its engineering properties. Chemical stabilization of soils improve its strength and stiffness properties, such as unconfined compressive strength, and resilient modulus, as well as reduces its swelling potential (Puppala et al. 2003a, 2011, Khoury et al. 2012). It is a very common and effective type of stabilization employed for expansive soils over the last several decades (Madhyannapu and Puppala 2014, Puppala 2016, Firoozi et al. 2017). The type of stabilizer to be used is determined based on the type of soil to be treated, its clay content, mineralogy, as well as its plasticity. Chemical stabilizers can be broadly categorized as traditional and non-traditional stabilizers, which are explained in more detail in the following sections.

#### 2.3.2.1 Traditional Stabilizers

Conventionally, lime, cement, and fly-ash are the most commonly used chemical soil stabilizers. The stabilizing mechanism for these additives are based on cation exchange and pozzolanic reactions with soil minerals. Traditional stabilizers have proven to be quite effective and a reasonably economical solution to treat expansive soils.

2.3.2.1.1 Lime

Lime has been used since ancient times by the Romans, the Chinese and the people of the Indian subcontinent for construction purposes. Lime is especially effectively implemented in stabilizing expansive soils. Lime used for stabilization purposes is usually either calcium oxide (CaO) known as quicklime or calcium hydroxide ($Ca(OH)_2$) known as hydrated lime. Quicklime is produced by calcining high quality limestone at extremely high temperatures and eliminating the carbon dioxide in it by vaporization as shown in equation 2.1:

$$\underset{Limestone}{CaCO_3} \xrightarrow[Heat\ (\geq 1000℃)]{} \underset{Quicklime}{CaO} + \underset{Carbon\ Dioxide}{CO_2} \qquad \text{(Eqn. 2.1)}$$

The quicklime produced is then slaked with water to produced hydrated lime. The hydration process is shown in equation 2.2:

$$\underset{Quicklime}{CaO} + \underset{Water}{H_2O} \longrightarrow \underset{Calcium\ Hydroxide}{Ca(OH)_2} + Heat \qquad \text{(Eqn. 2.2)}$$

While both quicklime and hydrated lime are relatively stable compounds, they do react with carbon dioxide to reverse the reaction and form calcium carbonate (Boynton 1980). Quicklime is highly reactive with water, and reacts with moisture from the atmosphere resulting in the formation of hydrated lime, which has a slightly higher solubility in water than quicklime.

Lime treatment of expansive soils is a very widely accepted and effective method for soil stabilization that is also economically feasible. The stabilization of soils with lime is a complex process and consists of a two-step process. The initial

stage comprises of the cation exchange and flocculation-agglomeration reactions, which cause an immediate change in texture and plasticity of the soils (Little 1995). Flocculation or agglomeration is the process in which clay particles reorganize to form loosely held micro-clumps or flocs, and is heavily influenced by soil mineralogy and soil-water chemistry. These reactions result in the formation of larger clay clusters that make the soils friable, workable and compactable. The second stage is a long-term pozzolanic reaction that cements the flocculated particles and subsequently enhances soil strength. Pozzolans are essentially finely divided siliceous or aluminous materials which react with water and calcium hydroxide to form strong cementitious compounds (Little 1995). The silicate and aluminate-rich minerals in clay are the pozzolan phases here and the cementitious compounds formed are calcium-silicate-hydrate (CSH) or calcium-aluminate-hydrate (CAH). The primary mechanism in a pozzolanic reaction is the migration of calcium hydroxide via water within the soil to associate with the aforementioned pozzolans (Duxson et al. 2007a). Pozzolanic reactions can take months or even years to complete, depending on the reactivity and solubility of the pozzolans as well as the soil pH.

The treatment of expansive soils with lime causes several effects that improve soil properties such as decreased plasticity index and swelling potential as well as increased unconfined compressive strength (UCS), shear strength, California Bearing Ratio (CBR), resilient modulus ($M_R$), durability and workability

(Thompson 1966, 1969, 1970; Holtz 1969; Little et al. 1995; Little 1996; Puppala et al. 1996). While lime is known to significantly improve the soil properties of expansive soils, it also has its limitations. Lime treatment is not effective in granular soils, and also encounters leaching and long-term durability issues. In sulfate-rich soils, lime treatment causes excessive heaving and distress resulting in infrastructure damage (Puppala et al. 2019b). In addition, the production of lime is an energy-intensive process that releases several tens of million metric tons of carbon dioxide emissions per year, and therefore has severe negative impact on the environment.

2.3.2.1.2 Cement

Ordinary Portland Cement (OPC) commonly referred to as ‘cement’ is another common binder consisting of cementitious products used to stabilize problematic soils. Cement production requires three major raw materials: limestone, clay, and gypsum. Limestone provides lime (CaO), while clay is usually the source for silica ($SiO_2$), alumina ($Al_2O_3$) and iron ($Fe_2O_3$). Cement production consists of three major steps: (1) the proportioning and mixing of limestone and clay, (2) calcination of limestone and clay to form cementitious products, known as ‘clinker’, and (3) the grinding of clinker along with the addition of retarding agent gypsum. While there are several chemical reactions that occur to produce several different cementitious compounds that form cement, the process can be summarized in an elementary manner as shown in equation 2.3:

$$Limestone + Clay + Gypsum \xrightarrow[Heat \geq 1300℃]{} Cement \quad \text{(Eqn. 2.3)}$$

Cement has been successfully used to modify and stabilize soils for the past several decades. Cement stabilization involves the mixing of the appropriate amount of cement with water and soil. The stabilization mechanism of cement and soils is similar to that of lime and involves: cation exchange, flocculation and agglomeration, cementitious hydration and pozzolanic reactions. Cement is composed of four major oxide phases: tricalcium silicate ($3CaO.SiO_2$), dicalcium silicate ($2CaO.SiO_2$), tricalcium aluminate ($3CaO.\ Al_2O_3$) and tetracalcium aluminoferrite ($4CaO.Al_2O_3.\ Fe_2O_3$). Upon hydration, the two calcium-silicate phases release calcium hydroxide and calcium-silicate-hydrate initiating the process of stabilization (Prusinski and Bhattacharja 1999). The hydration reactions that form calcium hydroxide and calcium-silicate-hydrate are shown in equations 2.4 and 2.5:

$$2\ (3CaO.SiO_2) + 6\ H_2O \longrightarrow CSH + 3\ Ca(OH)_2 \quad \text{(Eqn. 2.4)}$$

$$2\ (2CaO.SiO_2) + 4\ H_2O \longrightarrow CSH + Ca(OH)_2 \quad \text{(Eqn. 2.5)}$$

Cement stabilization of soils is known to reduce plasticity index and volume change potential of soils as well as increase its UCS, shear strength, and CBR (Christensen 1969, Kézdi 1979, Chen 1988, Petry and Wohlgemuth 1988). Cement stabilization has proven more effective and economical in granular soils due to the lower quantity of cement required, as well as lower workability in cohesive soils.

Limitations of cement in stabilizing soils are similar to lime owing to the thermal energy intense production process which impacts the environment negatively; in addition to its susceptibility to cracking, brittle failures and sulfate attacks.

2.3.2.1.3 Fly ash

Fly ash is a fine, gray, dust-like pozzolanic material composed of tiny spheres of silica and alumina glass produced as a result of burning powdered coal (Mateos and Davidson 1962). Unlike lime and cement which are manufactured products, fly ash is a by-product of the coal-production industry. As a result, the chemical composition of fly ash can vary considerably depending on the source used and the manufacturing process. Fly ash is broadly classified into Class C (self-cementing) and Class F (non-self-cementing) fly ash based on AASHTO and ASTM standards. Class C fly ash contains a significant amount of lime, CaO, which enables it to work quite well as a sole binder in appropriate quantities; while Class F fly ash has very little lime and therefore requires an activator like cement or lime to initiate the stabilizing reactions.

Stabilization of soils with fly ash occurs in two steps: the immediate reaction that agglomerates soil particles to make it more workable, and the long-term pozzolanic reaction that forms cementitious products which enhance the engineering properties of the soil. The effectiveness of fly ash as a stabilizer and the rate of its reactions is heavily dependent on the chemical composition of fly ash, the amount of fly used, soil type, temperature and moisture content of mixture

(Usmen and Bowders Jr 1990). Fly ash is known to reduce plasticity index and increase the UCS and CBR properties of treated soils (Zulkifley et al. 2014); although swell potential is found to be minimal in high PI soils (PI = 30) treated with Class C fly ash (Parsons 2002). Limitations of using fly ash for soil stabilization include its questionability as an effective sole binder in reasonable amounts, varying setting time and reaction times, air-quality concerns in immediate area of use, as well as respiratory problems in workers.

2.3.2.2 Non-traditional Stabilizers

While traditional stabilizers are used extensively in most parts of the world to effectively stabilize problematic soils, non-traditional stabilizers have been used in cases when traditional stabilizers are not readily available, or are not of acceptable quality. In addition, concerns with traditional stabilizers regarding escalating costs, long curing times, adverse chemical reactions in high-sulfate soils and negative environmental impacts have led agencies to seek alternative stabilization methods, generally classified as non-traditional stabilizers.

Non-traditional stabilizers used include a variety of materials such as granulated blast furnace slag, mine tailings, kiln dust, enzymes, polymers, salts, sulfonated oils, resins, rubber tires, rice husk and fibers (Petry and Little 2002, Tingle and Santoni 2003, Kumar and Singh 2008, Little and Nair 2009a, Karatai et al. 2016, Caballero et al. 2016, Diniz et al. 2017, He et al. 2018). Most non-traditional stabilizers are by-products of other industries or waste materials that

require safe and effective disposal techniques. Non-traditional stabilizers mixed with complementary additives or activating agents have been shown to stabilize soils, albeit not to the extent of traditional stabilizers (Tingle et al. 2007, Sharma and Sivapullaiah 2016). While research on non-traditional stabilizers is increasing, existing literature is minimal and focuses mostly on its performance rather than stabilization mechanisms. Performance evaluation of non-traditional stabilizers is found to be inadequate as most of them focus exclusively on UCS and swell reduction, while most other engineering properties are left uninvestigated.

## 2.4 Introduction to Geopolymers

Geopolymers are a relatively new class of binder materials based on alkali-aluminosilicate reactions and are known to have properties comparable to OPC but with a much lower carbon footprint. Geopolymers are formed by the alkali-activation of aluminosilicate-rich materials and consist of large three-dimensional (3-D) networks of covalently bonded alumino-silicates and are known for their high compressive strength, low shrinkage and durability properties (Duxson et al. 2007a). These alkali activated materials can be formed from relatively inexpensive aluminosilicate precursors (clay, metakaolin, fly ash, and others) (Davidovits 1991, van Jaarsveld et al. 2002, Cheng and Chiu 2003, Gordon et al. 2005), harden at ambient temperatures in a relatively short amount of time (Lizcano et al. 2012a) and are therefore considered to be a more eco-friendly and sustainable alternative to conventional building materials.

### *2.4.1 Historical Background*

The formation of alkali-activated materials (AAMs) comparable to Portland cement was first patented by German researcher Kuhl in 1908 when he combined an alumino-silicate precursor (vitreous slag) with an alkali source (alkali sulfate or carbonate) (Provis and van Deventer 2013). The fundamentals of AAMs were further developed by Purdon, when he tested several different blast furnace slags activated by sodium hydroxide (NaOH) and calcium hydroxide ($Ca(OH)_2$) solutions to form materials with comparable tensile, flexural and final strengths as that of Portland cements (Purdon 1940). In the 1950s, Glukhovsky found that alkali-activated binder materials could be created using low-calcium or calcium-free aluminosilicates (clay); these binders were called ‘soil cements’ and ‘soil silicates’ to reflect their similarity to natural minerals (Krivenko 2017). Glukhovsky’s discovery is believed to be the first recorded synthesis of what is now known as geopolymers.

In the 1980s, French material scientist Joseph Davidovits created geopolymer binders by alkali activation of naturally occurring materials like kaolinite, limestone and dolomite (Davidovits 1991). Significant interest was sparked in geopolymers once Davidovits patented several aluminosilicate compositions and marketed them as fire-resistant resins. Since then geopolymers and their uses have been explored in many disciplines such as chemistry, mineralogy, material sciences, and engineering applications, for a wide variety of

uses such as fire-resistant materials, thermal insulation, containment of radioactive materials, corrosion-resistant coatings and adhesives, cements, concretes, as well as composites for infrastructure applications (Davidovits 1991, Van Jaarsveld et al. 1999, Hussain et al. 2004, Duxson et al. 2007a, Provis and van Deventer 2009, Temuujin et al. 2009, 2011).

### *2.4.2 Terminology*

The term ‘geopolymer’ was coined by Davidovits in the 1980s. Geopolymers are defined as a class of inorganic, alumino-silicate based ceramics charge balanced by group I or II (Na, K, Ca, etc.) oxides; they are rigid gels, made under ambient temperature and pressure conditions to form near-net dimension bodies, subsequently converted to crystalline or amorphous materials (Bell et al. 2009). Geopolymers are considered to be a subset of a class of materials known as AAMs. AAMs are formed by the combination of an aluminosilicate precursor and an alkaline activator and have properties comparable to those of a traditional cement binder; whereas geopolymers are essentially AAM binders formed using little to no calcium, and is often developed using metakaolin or fly ash as the aluminosilicate precursor (Provis and van Deventer 2014).

It is important to note that while research on geopolymer binders have been going on for the past several decades, there is still some misperception in regards to the correct terminology of these materials, as no official nomenclature system has yet been set up. These innovative binders are most commonly referred as either

an ‘alkali-activated material’, an ‘inorganic polymer’ or a ‘geopolymer’. While it would require extensive research to correctly classify and designate each binder material, a widely acknowledged categorization of AAMs as provided by van Deventer is shown below in Figure 2.2, where the darker shading indicates higher concentrations of Na and/or K. Figure 2.2 also compares Portland-based cements and calcium sulfo-aluminate cements with AAMs based on their calcium and aluminum contents. When referring to geopolymers in this study, they will be considered a subset of inorganic polymers which are in turn a subset of AAMs, as illustrated in Figure 2.3.

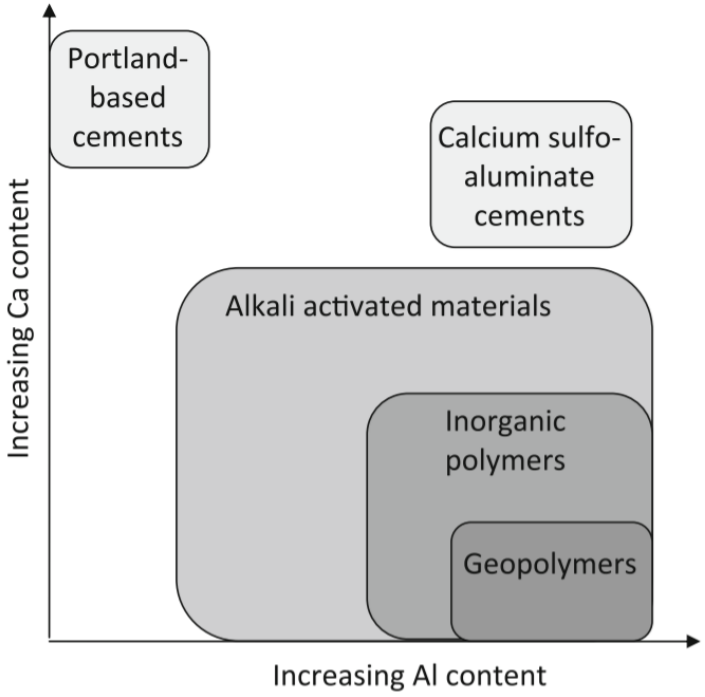


Figure 2.2: General classification of AAMs and its subsets (Van Deventer, Provis, Duxson, and Brice, 2010)

### *2.4.3 Conceptual Structure of Geopolymers*

Chemically, Geopolymers are identified as polysialates. The term 'sialate' is the abbreviation of the term 'silicon-oxo-aluminate'. Polysialates are described as chain or ring polymers where $Si^{4+}$ and $Al^{3+}$ are present in IV-fold coordination with oxygen (see Figure 2.3), and range from amorphous to semi-crystalline in nature (Davidovits 1991). Geopolymers can be represented by the empirical formula of polysialates as shown in Equation 2.6.

$$M_n[-(SiO_2)_z - AlO_2]_n.wH_2O \quad \text{(Eqn. 2.6)}$$

Where, *M* is the alkali metal cation (such as Na, K, or Ca), *n* is the degree of polycondensation, *z* is the silicon to aluminum (Si:Al) ratio (usually 1, 2, or 3), and *w* is the molar water amount. The oligomeric units of polysialates classified according to the Si:Al atomic ratio (*z*) of 1, 2, and 3 are notated as poly(sialate) (PS), poly(sialate-siloxo) (PSS), and poly(sialate-disiloxo) (PSDS), respectively and are shown in Figure 2.3.

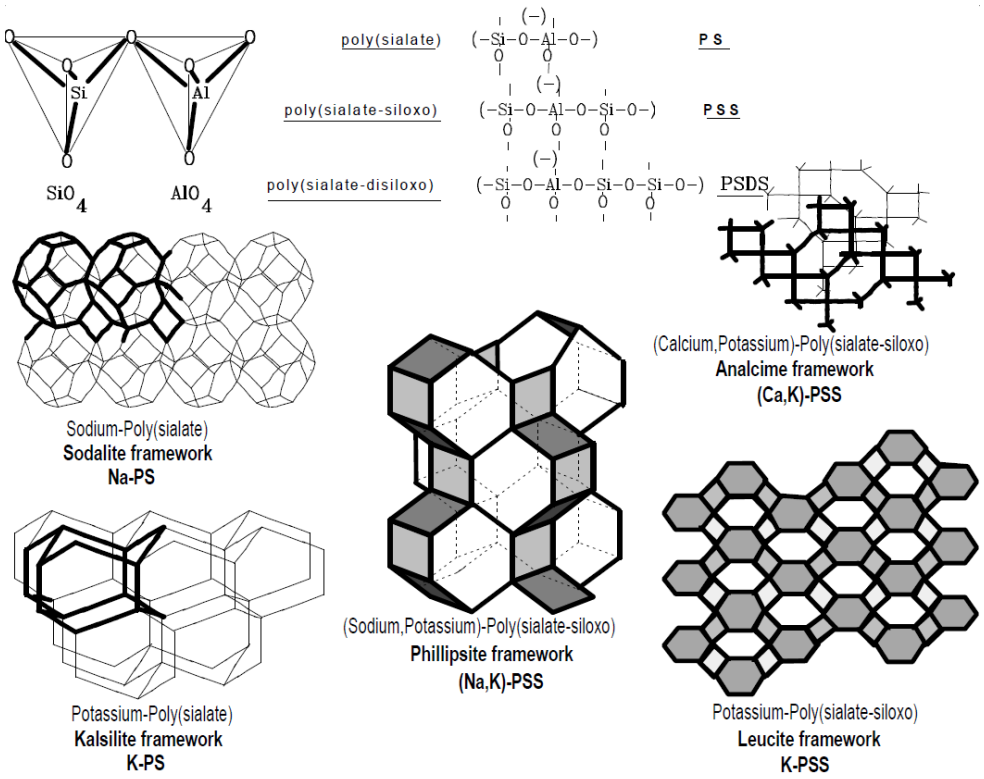


Figure 2.3: Molecular framework of geopolymers and their associated crystalline structures (Davidovits 1991).

Most geopolymers are non-crystalline in nature and are usually described to have an X-ray amorphous structure, as a result of which X-ray diffraction (XRD) of geopolymers results in what is called a 'broad diffuse halo' instead of the usually expected sharp diffraction peaks (Davidovits 1991). Figure 2.4 shows the X-ray diffractograms of geopolymers with their characteristic broad diffuse halo. Geopolymers are usually amorphous when cured at temperatures below 80°C (Davidovits 1991, Kriven et al. 2004), but form crystalline phases at elevated temperatures (Barbosa and MacKenzie 2003), which are shown to have structural similarities to zeolitic minerals at atomic scales (Provis and van Deventer 2009).

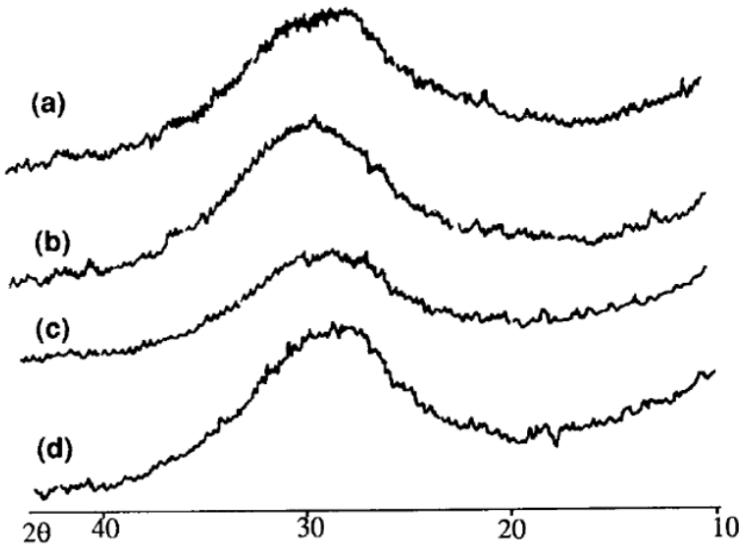


Figure 2.4: X-ray diffractograms of two types of [Na,K]-PSS (a, b), and [K]-PSS (c, d) (Davidovits 1988).

Davidovits asserts that unlike the representative crystalline formations that are shown in Figure 2.3, which are evidently the final structures of completed crystallization processes at elevated temperatures; most geopolymers are cured at much lower temperatures, are therefore non-crystalline in structure and are actually a long network of aluminosilicate chain or ring polymers as shown below in Figure 2.5 (Davidovits 1991). A geopolymer that has not fully reacted with its components would have free aluminate and silicate groups within the partially formed ring or chain structures, which will eventually polycondense to complete the links.

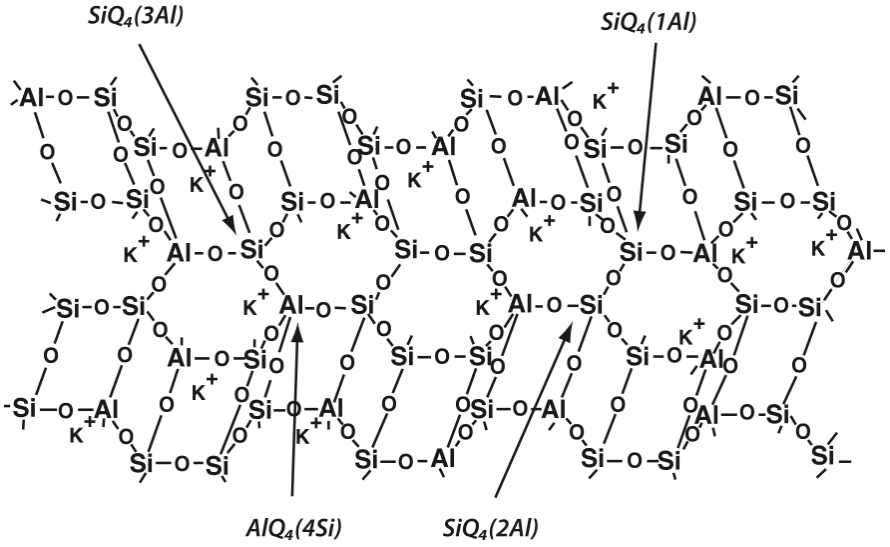


Figure 2.5: Theoretical 3-D structural model of a fully reacted Potassium-based geopolymer (Davidovits 1991).

### *2.4.4 Conceptual Geopolymerization Process*

The formation of geopolymers is essentially an alkali-activated polycondensation reaction process. Polycondensation reaction is a method of forming polymers by the bonding of monomers usually resulting in the release of water or other condensed molecules in the process (Bhat and Kandagor 2014). Glukhovsky proposed a general geopolymerization mechanism in the 1950s which comprised of three major steps: (a) destruction–coagulation, (b) coagulation–condensation, and (c) condensation–crystallization. Over the years, researchers have attempted to describe the geopolymerization process more comprehensively in view of various technological advancements that have enabled an improved insight into the process (Davidovits 1991, Provis and van Deventer 2009).

Figure 2.6 provides a schematic showing a simplified summary of the conceptual geopolymerization process, and delineates major processes involved. Geopolymerization can be effectively summarized into the following five stages: (a) dissolution, (b) speciation equilibrium, (c) gelation, (d) reorganization, and (e) polymerization and hardening (Duxson et al. 2007a, Medri et al. 2010). It should be noted that while the different stages of geopolymerization are shown to be successive reactions, they are generally overlapping reactions that occur concurrently.

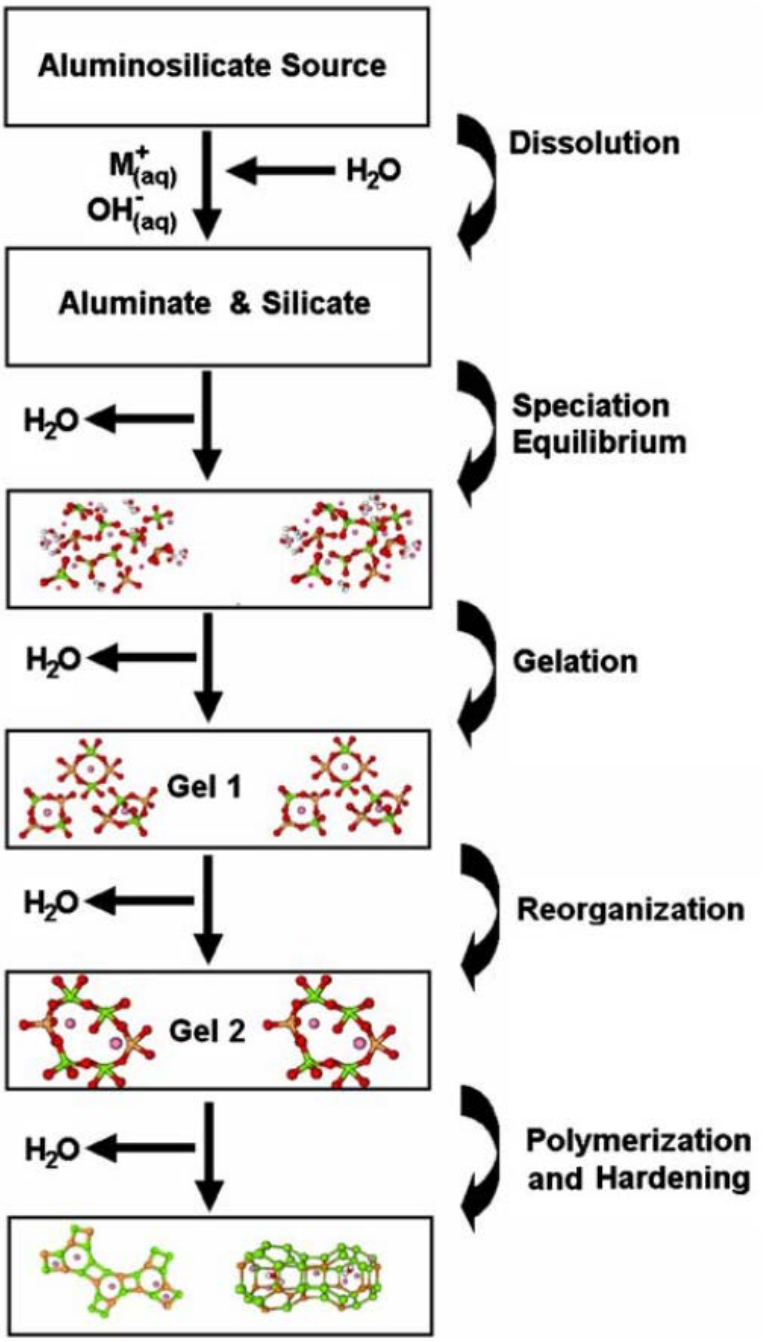


Figure 2.6: Schematic of geopolymerization process (Duxson et al., 2007).

The dissolution process begins when the aluminosilicate precursor is mixed with the alkaline activator solution which contains the metal cation, water, and additional silica. At high pH, the water rapidly dissolves the aluminosilicate precursor forming monomeric aluminate ($Al(OH)_4^{3-}$) and silicate ($Si(OH)_4^{2-}$) species through hydrolysis (consumption of water). Dissolution of the aluminate and silicate species into the aqueous solution that contains the silicate from the alkaline activator solution results in the formation of a complex supersaturated aluminosilicate solution. Subsequently, polycondensation reactions of monomeric/oligomeric units in the concentrated solution forms large networks or chains resulting in gelation. The water released during this process resides within the pores of the gel, but is not chemically bound to the geopolymer structure (Duxson et al. 2007a). Rearrangement and reorganization of the gel system continues as it develops into a complex 3-D structure with extensive networks of aluminosilicates indicative of geopolymers. Further curing results in hardening, and formation of much significantly evolved polymeric networks that eventually crystallize.

Gelation of dissolved aluminosilicate species is significantly dependent on various factors such as concentration of reactive species in solution, raw material type and quality, processing conditions, and time. Therefore, different geopolymer formulations gel and harden at different rates, depending on the type and quality of raw materials used for geopolymer synthesis.

### *2.4.5 Geopolymer Synthesis and Influencing Factors*

The synthesis of geopolymers requires four main components: (1) an aluminosilicate source or precursor, (2) an alkali-metal cation source, (3) additional silica source (if needed), and (4) water. The alkali metal cation source, the additional silica source and water are combined in the required proportions to form the alkaline activator solution. Subsequently, the aluminosilicate precursor is mixed with the alkaline activator solution to form a slurry, which is then cured to form the hardened geopolymer. One of the major benefits of geopolymers is its ease of synthesis and application.

The term geopolymer was first applied by Davidovits to alkali hydroxide/silicate activated metakaolin (calcined clay) (Provis et al. 2009). The most commonly used raw materials for the production of geopolymers are calcined clays, fly ashes, and slags (Duxson 2009). The time required for the geopolymer to gel and subsequently solidify, is significantly dependent on mix design, presence of contaminants, and curing environment. Geopolymer properties are significantly affected by seemingly trivial factors such as purity of precursor, addition of alkaline activator, availability of reactive alumina and water content (Rowles and O'connor 2003, Fletcher et al. 2005, Buchwald et al. 2007, Lizcano et al. 2012a). The following sections elaborate on some of these influencing factors that affect geopolymer properties.

2.4.5.1 Aluminosilicate Precursor

While there are a myriad of aluminosilicate precursors available for geopolymer synthesis, metakaolin is considered to be an ideal raw material due to the purity and high reactivity of its alumina and silicate content. Metakaolin (MK) is a pozzolanic material produced by the calcination of kaolinite at temperatures ranging from 500°C to 800°C. Metakaolin production generates 80-90% less $CO_2$ than lime and cement as it requires lower calcining temperatures, and is therefore more environmentally friendly (Davidovits 1994). The quality of metakaolin can vary depending on the particle size, purity, and crystallinity of the precursor clay, and is therefore crucial to be considered for geopolymer synthesis. The achievable extent of geopolymerization in metakaolin-based geopolymers is noted to be quite high compared to other aluminosilicate precursors, especially when cured in sealed environments with elevated temperatures (Provis et al. 2009). Metakaolin is known for its sheet-like particle shape and very high surface area resulting in high water demand for reactions, which might be a disadvantage for large-scale operations. In addition, efflorescence issues are observed in metakaolin-based geopolymers due to its high alkali content (Provis et al. 2009). A Scanning Electron Microscopy (SEM) image of metakaolin-based geopolymer is shown in Figure 2.7, giving an insight into its microstructure.

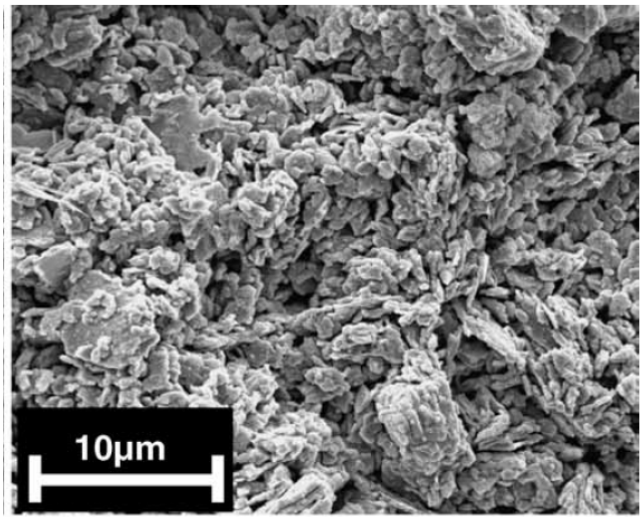


Figure 2.7: SEM image of metakaolin-based geopolymer (Duxson et al. 2005).

Fly ash is another common precursor used for geopolymer synthesis. While fly ash is a relatively easily available and economical precursor, it is an extremely variable material. The properties of fly ash are dependent heavily on the quality of coal it is obtained from, as well as the production process. As such, the alumina/silicate content in fly ashes as well as their reactivity vary considerably from one to the other. This results in a more complex process of mix design proportioning using fly ashes. In general, the release of alumina from fly ash is found to occur at a much slower rate than from metakaolin, and is significantly affected by the type and concentration of alkali present (Van Jaarsveld et al. 1999, Fernández-Jiménez and Palomo 2003). Despite these deficiencies of fly ash, researchers are working toward linking theories of geopolymer chemistry and ash dissolution. Figure 2.8 shows a SEM image of a fly ash-based geopolymer.

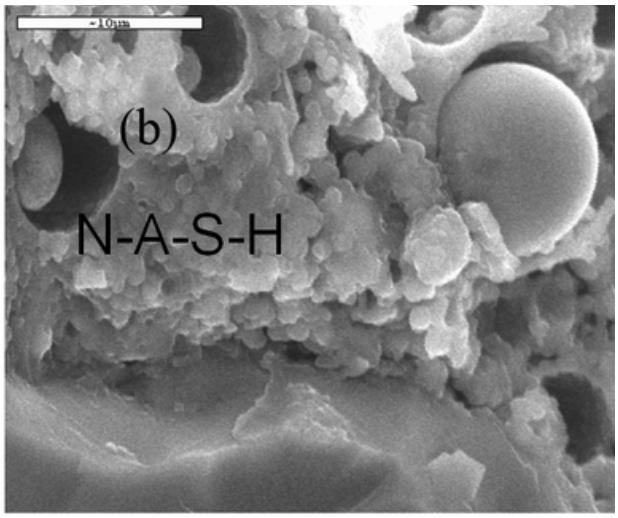


Figure 2.8: SEM image of fly ash-based geopolymer (Garcia-Lodeiro et al. 2015)

2.4.5.2 Alkali Metal Cation

The alkaline activator solution is a mixture of the alkali metal cation source, additional silica source and water. Alkali metal cations (M) are used to balance the negative charge of the tetra-coordinated aluminate in the geopolymer structure. Commonly used cations include $Na^+$, and $K^+$ ions, while rubidium ($Rb^+$), and cesium ($Cs^+$) are also used to a lesser extent. The type of cations used affect the reactivity, geopolymerization rate, and porosity of the geopolymer systems. An increase in cation size ($Na^+ \rightarrow K^+ \rightarrow Cs^+$) was found to decrease the rate of geopolymerization, due to slower dissolution of the aluminosilicate precursor (Steins et al. 2012). Slight difference in reaction times were observed when activation energies were observed to decrease with increasing cation sizes for Na and K-based geopolymers (Poulesquen et al. 2011).

2.4.5.3 Si:Al ratio

The most influential parameters governing geopolymer characteristics are arguably the Si:Al ratio in its structure and the amount of water consumed during the process; these parameters dictate the formation of polysialates, the building blocks of the geopolymer framework (Xu and Van Deventer 2000, Phair and Van Deventer 2002, Davidovits 2008, Lizcano et al. 2012a). Higher Si:Al ratio corresponds to higher compressive strength due to the more complex networks of polysialates formed during polycondensation (Duxson et al. 2005). Based on previous studies, significant improvement in geopolymer strength properties is noticed when Si:Al ratio is between 1 and 3 (Davidovits 1991).

2.4.5.4 Water

The water content in a geopolymer mix is known to affect the general workability of the initial mixture as well as the density, strength, microstructure, and durability characteristics of the final hardened geopolymer (Rangan 2008, Provis and van Deventer 2009, Lizcano et al. 2012a). High water content results in more widely-spaced geopolymer chains. As the excess water evaporates during gelation and curing, it leaves behind a more open geopolymer framework with lower density. A decrease in density results in geopolymer with lower compressive strength and increased porosity, which can also result in lower thermal conductivity (Lizcano et al. 2012a). Presence of excess water in the system also decreases the pH of the aqueous solution, resulting in an insufficiently alkaline environment that

deters the dissolution process. This issue can be resolved by the addition of excess hydroxide ions that would balance the solution and form the optimal geopolymer.

2.4.5.5 Alumina Content

The amount of aluminum available in the geopolymer gel is another critical determinant of geopolymer properties such as strength, acid resistance, microstructure, as well as its curing and strength development profile (Weng et al. 2005, Fernández-Jiménez et al. 2006). The rate of release of alumina from different aluminosilicate precursors can become the deciding factor for the rate of geopolymerization and its final curing time (Rees et al. 2008). Alumina in metakaolin-based geopolymers is known to be more readily available than in fly-ash based geopolymers, where it is released at a much slower rate (Duxson et al. 2005).

The aluminum content in relation with the alkali cation (Na, K, etc.) is also an important factor in geopolymer synthesis. The alkali metal cation to aluminum (M:Al) ratio of 1:1 is the recommended stoichiometric balance for optimal geopolymer formation (Barbosa et al. 2000), as the positive charge on the $Al^{3+}$ ion is balanced by the $Na^{+}$ or $K^{+}$ ions loosely connected to the aluminosilicate framework (Provis et al. 2005). An increase in M:Al ratio is hypothesized to prevent the complete development of geopolymer chains (Provis and van Deventer 2009, Lizcano et al. 2012a).

2.4.5.6 Curing Environment

The structural and mechanical properties of geopolymers are significantly affected by its curing environment. Initial curing temperatures for geopolymers were quoted to be around 150°C to 180°C (Davidovits 1982), while more recent studies show researchers curing geopolymers at lower temperatures ranging from 20°C to 90°C (Duxson et al. 2005, Rangan 2008, Bell et al. 2009, Chindaprasirt et al. 2011, Deb and Sarker 2016, Shadnia and Zhang 2017). Researchers have effectively cured geopolymers at room temperatures (20-23°C) making the synthesis process simpler and quite energy efficient; although geopolymers cured at lower temperatures are known have slower setting times and low-strength at early stages (Provis and Bernal 2014). Various studies have shown that an increase in curing temperature has shown to result in higher compressive strength and lower setting times up to a certain temperature (85-95°C), after which no increase in strength is observed (Duxson et al. 2005, Rangan 2008, Shadnia and Zhang 2017). Researchers have also studied the effect of elevated temperatures on different geopolymers, wherein crystalline phases are observed to start forming around 120°C (Duxson et al. 2007a). Specimen curing has been carried out in either sealed or unsealed environments where relative humidity ranges from 40-90%. Since curing environments play a significant role in geopolymer properties, they should be assessed critically based on the required application and strength needs of the geopolymer to be formed.

## 2.5 Geopolymer stabilized soil

Over the years, many types of geopolymers have been formulated for a variety of applications in the engineering and construction industry, such as fire and acid-resistant materials, high-tech resins, composites for infrastructure repair and reinforcement, low-tech building materials, and 'green' cements and concrete. Geopolymers are most notably promoted as alternatives to OPC due to comparable properties and recent advocacy for use of more innovative and sustainable materials in construction. In more recent years, geopolymers have been proposed as an alternative material for stabilization of problematic soils. This premise gained popularity particularly since 2010, when researchers began investigating the efficiency of geopolymers to stabilize an assortment of soils. It is important to note that while there is sizeable literature available on the formulation of different types of geopolymers for various applications, research on geopolymers as soil stabilizers is sparse and is mostly from other countries.

Several types of fly ash-based (single-precursor) geopolymers have been used to improve strength properties of silty and clayey sands (Cristelo et al. 2012, Rios et al. 2016, Dungca and Codilla 2018), as well as some low-plasticity (Liu et al. 2016), and high-plasticity clays (Phetchuay et al. 2014). The few studies conducted in the US used metakaolin-based (single-precursor) geopolymers to improve the strength and swell of a synthetic lean clay (Zhang et al. 2013, 2015) and a high plasticity clay (Khadka et al. 2018). Researchers also developed

geopolymers from multiple precursors by combining fly ash (FA) with ground-granulated blast-furnace slag (GGBFS) (Mohammadinia et al. 2016, Abdullah et al. 2017) or calcium carbide residue (CCR) (Phetchuay et al. 2016, Phummiphan et al. 2016) to enhance both coarse and fine-grained soils. Other single-precursor materials used for geopolymer development for the purpose of soil improvement include GGBFS (Du et al. 2016), palm-oil fuel ash (POFA) (Pourakbar et al. 2016), and volcanic ash (VA) (Miao et al. 2017). The tests conducted on geopolymer-stabilized soils at UTA also showed some promising results which have been described in detail in subsequent chapters (Samuel et al. 2019, Huang et al. 2019).

Table 2.3 below provides a compilation of the current available literature on geopolymer stabilization of soils used for this study, which reveals that most research regarding stabilization of soils using geopolymers were conducted within the last few years. The ability of geopolymers to stabilize soils has been demonstrated in most cases exclusively through the enhancement of UCS, and in a few cases by means of swell, shrinkage or California Bearing Ratio (CBR) testing. Geopolymer treatment of soils has shown to significantly increase the UCS of all treated soils, while other engineering properties such as volume-change (shrinkage and swell) and durability characteristics still need to be explored further. In addition to the engineering properties tested, most researchers conducted microstructural analyses through mineralogical and elemental characterization as well as microscopic observations in the form of either SEM, XRD, X-ray Fluorescence

(XRF), or energy dispersive X-ray spectroscopy (EDS) tests, in an effort to better understand the stabilizing mechanism of geopolymers.

Table 2.3: Compilation of peer-reviewed articles on geopolymer-stabilized soils

| **Author(s) & Publication Year** | **Soil Type (USCS)** | **Geopolymer Precursor** | **Engineering Properties Tested** |
|---|---|---|---|
| Cristelo et al. (2012) | SM | Class-F FA | UCS |
| Zhang et al. (2013) | CL | MK | UCS, Shrinkage |
| Phetchuay et al. (2014) | CH | FA | UCS, LL, PL |
| Zhang et al. (2015) | CL | MK | UCS, 1-D Swell |
| Du et al. (2016) | CL | GGBFS | UCS, Hydraulic Conductivity |
| Liu et al. (2016) | CL | Class-F FA | UCS |
| Mohammadinia et al. (2016) | GW | Class-F FA + GGBFS | UCS, $M_R$ |
| Phetchuay et al. (2016) | CH | Class-F FA + CCR | UCS |
| Phummiphan et al. (2016) | SC-SM | Class-C FA + CCR | UCS |
| Pourakbar et al. (2016) | CH | POFA | UCS, Bearing Capacity (lab load test) |
| Rios et al. (2016) | SM | Class-F FA | UCS, Durability, S and P-wave velocity |
| Abdullah et al. (2017) | CH | Class-F FA + GGBFS | UCS, LL, PL |
| Miao et al. (2017) | CH | VA | UCS, Swell, LL, PL |
| Dungca & Codilla (2018) | SM | Class-F FA | UCS, CBR |
| Khadka et al. (2018) | CH | MK | UCS, Swell |

LL: Liquid Limit
PL: Plastic Limit
USCS: Unified Soil Classification System
UCS: Unconfined Compressive Strength
CBR: California Bearing Ratio
$M_R$: Resilient Modulus
S and P-wave: Shear and Compression Waves

The improvement in strength properties of geopolymer-treated soil is attributed to the formation of geopolymer gel that grows during the curing period and physically binds adjacent soil particles to form a solid binder (Liu et al. 2016). Researchers claim that no direct chemical reaction occurs between the geopolymer precursors and soil minerals, since no new mineral formation is observed in the microstructural analysis of geopolymer-treated soil (Zhang et al. 2013). A comparison between potassium hydroxide (KOH) and sodium hydroxide (NaOH) as the cation sources in the alkaline activator solution showed that the KOH activated geopolymer provides a higher UCS value than the NaOH activated geopolymer for mixtures with the same fly ash/soil ratio (Liu et al. 2016, Pourakbar et al. 2016). This increase in strength can be explained by the smaller hydration sphere of K+ ions as compared to Na+ ions, that allows for more close-knit and intervolved polycondensation reactions, resulting in higher overall strength of geopolymer-treated soil (Pourakbar et al. 2016).

Higher strength and lower swell reduction was observed in soils treated with MK-based geopolymers than FA-based geopolymers (Khadka et al. 2018). It is important to note that there was no consistency in curing temperatures and methods. Some geopolymer-treated soil specimens were cured at room temperature (19°C-23°C), while others were at higher temperatures (23°C-60°C) and lower relative humidity. Specimens cured in higher temperatures and lower relative humidity

conditions resulted in dehydrated specimens that provide misleading results for strength gain (Cristelo et al. 2012, Zhang et al. 2013, 2015, Phetchuay et al. 2014).

Most research on geopolymer treatment of soils has been conducted on sandy or clayey silts, and low-plasticity clays (CL) from all around the globe, while limited research has been focused on severely problematic expansive clays that are mostly classified as high-plasticity clays (CH). Although significant improvements are observed in tested properties, it has proved challenging to quantify, compare and reproduce similar results due to the large range of variabilities including but not limited to soil type, precursor and activator type, silica and alumina content, water content, geopolymer dosages, curing environments, as well as variations in testing standards. Therefore, further studies are required to understand the behavior of expansive soils to geopolymer treatment, optimize curing methods, as well as to study the effects of durability testing on geopolymer-treated soils.

## 2.6 Summary

This chapter reviewed the available literature on expansive soils and their characteristics. The swelling potential of expansive clays is inherent to the clay mineralogy. Of the major clay minerals, Montmorillonite is known to have the highest swelling potential. The various conventional stabilization techniques used to treat expansive soils and their mechanisms were explored in detail. Calcium-based stabilizers are known to be quite effective in reducing swelling and shrinkage potential in expansive soils. The need for alternative stabilizers were discussed due

to the negative impacts of calcium-based stabilizers on the environment, as well as their limitations in sulfate-rich soils.

Subsequently, the materials known as Geopolymers were introduced, where their historical background, conceptual structure and synthesis process were presented. Finally, the limited past research using geopolymers as soil stabilizers were presented and discussed. Very few studies were conducted on expansive soils, and when available focused solely on strength enhancement. Multiple precursor materials used to synthesize geopolymers were combined in varying proportions, and were found to vary drastically in properties from region to region. This dissertation study focuses on the synthesis of a metakaolin-based geopolymer that is applied to two expansive soils in different dosages. The metakaolin-based geopolymer is then evaluated for its performance as a sole stabilizer of the expansive soils using a more extensive laboratory characterization of geopolymer-treated expansive soils.

# CHAPTER 3

# GEOPOLYMER SYNTHESIS

## 3.1 Introduction

One of the benefits of geopolymers is that they can be easily synthesized at room temperature from a myriad of different sources, as discussed in the previous chapter. Consequently, there is a very diverse collection of geopolymers in published literature formulated from an assortment of raw materials available to researchers, due to the lack of standardized experimental compositions and processing techniques. Regrettably, the variation in the geopolymer synthesis process makes it challenging to effectively correlate the properties of the different geopolymers and their comparative efficiency in various applications.

This chapter details the synthesis of geopolymers used for this study. It will describe the selection of its raw materials, preparation of the geopolymer mix, curing conditions, mix proportioning, comparative analysis of different geopolymer mixes, and finally reveal the geopolymer composition selected for this study. The formulation of geopolymers was conducted in collaboration with the research team at the Material Science Department at Texas A&M University, College Station, Texas.

## 3.2 Raw Material Selection

As stated previously, the four main components necessary for geopolymer synthesis are: (1) an aluminosilicate source or precursor, (2) an alkali-metal cation

source, (3) additional silica source (if needed), and (4) water. The selection of proper raw materials depends on the desired qualities of the geopolymer required for an application, as well as the availability and cost-effectiveness of the raw materials. For a pioneering study such as this, where soil stabilization using geopolymers is still being investigated, the reliability and purity of its ingredients is imperative for correlations and reproducibility for future studies.

### *3.2.1 Aluminosilicate precursor*

While there are numerous aluminosilicate precursors that can be attained relatively easily to synthesize geopolymers, metakaolin is chosen as the sole aluminosilicate precursor for this study. Metakaolin is considered an ideal precursor as it usually contains very small amounts of impurities as compared to other potential precursors. Metakaolin is a highly reactive pozzolanic material which has a relatively well-defined chemical composition of $2SiO_2.Al_2O_3$, and is a good source of reactive alumina and silica needed for geopolymerization. Compared to other commonly used precursors such as fly ash, metakaolin is known to have increased strength, reduced permeability, and excellent workability (Caldrone et al. 1994, Thomas et al. 1999, Gruber et al. 2001). Additionally, metakaolin has significantly lower quantities of calcium oxide than fly ash, which can typically contain calcium oxide in the range of 10 to 40% (McManis and Arman 1989, Fan et al. 2015). In an effort to mitigate the negative effects of calcium-based

stabilizers in presence of potentially sulfate-rich soils, metakaolin was chosen as the sole aluminosilicate precursor for geopolymer synthesis in this study.

The metakaolin used in this study is commercially known as MetaMax® and was procured from BASF Catalysts LLC, New Jersey. The chemical composition of MetaMax® metakaolin was provided by the manufacturer and is presented in Table 3.1, where its calcium oxide content was observed to be less than 0.5%. The MetaMax® metakaolin is a white-colored, fine powder, with a pH of 6, specific gravity of 2.5, and bulk unit weight of 30 pcf (4.71 kN/m$^3$). According to the manufacturer, the particle size for the MetaMax® metakaolin ranges from 0.2 µm to 10 µm, with 100% passing the No. 325 sieve.

Table 3.1: Chemical composition of metakaolin used in this study

| **Chemical composition** | **Results (wt %)** |
|---|---|
| Silicon Dioxide ($SiO_2$) | 50.75 |
| Aluminum Oxide ($Al_2O_3$) | 45.91 |
| Titanium Dioxide ($TiO_2$) | 1.87 |
| Iron Oxide ($Fe_2O_3$) | 0.45 |
| Sodium Oxide ($Na_2O$) | 0.23 |
| Sulfur Trioxide ($SO_3$) | 0.08 |
| Calcium Oxide (CaO) | 0.06 |

### *3.2.2 Alkali metal cation and silica source*

The aqueous alkaline activator solution (AAS) formulated for this study is a combination of an alkali metal cation source, an additional silica source and deionized water. The effect of two different alkali metal cations, $Na^+$ and $K^+$, were

considered for geopolymer synthesis. Laboratory grade NaOH (99% pure) and KOH (99% pure) as shown in Figure 3.1 were obtained from Noah Technologies Corporation, Texas, to make separate Na-based and K-based aqueous AAS.

The additional silica source used to formulate the AAS was silica fume ($SiO_2$). For this purpose, amorphous fumed silicon (IV) oxide with a surface area of 350-410 $m^2/g$ was obtained from Alfa Aesar, Massachusetts. According to the manufacturer, the silica fume has a specific gravity of 2.2, molecular weight of 60.09, and is insoluble in water.

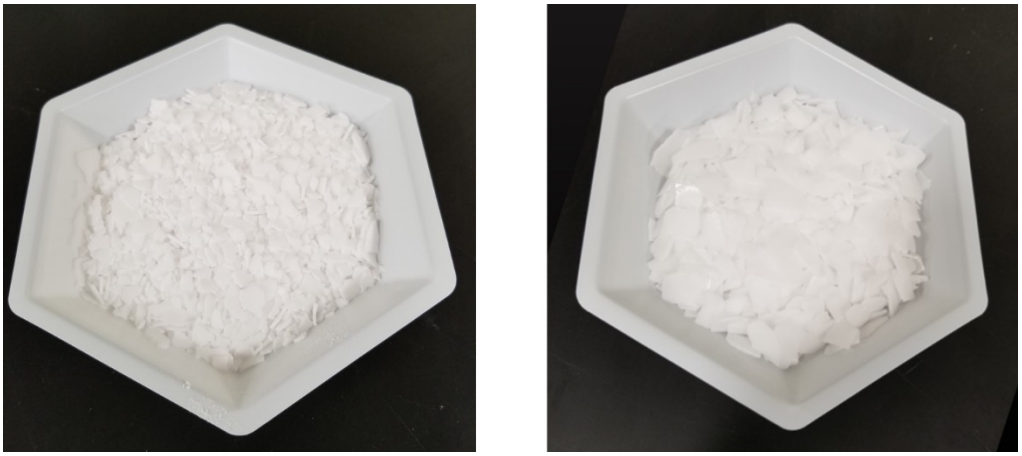

(a) (b)

Figure 3.1: (a) KOH and (b) NaOH flakes obtained to make AAS

## 3.3 Preparation of Geopolymer

Geopolymer preparation can be performed as a two-step process. The initial step involves the mixing of the relevant ingredients to create the AAS with a specific mix proportion. The second and final step involves the process of mixing

the AAS and metakaolin in the required proportions to prepare the geopolymer slurry. A simplified schematic of the geopolymer synthesis process is shown in Figure 3.2.

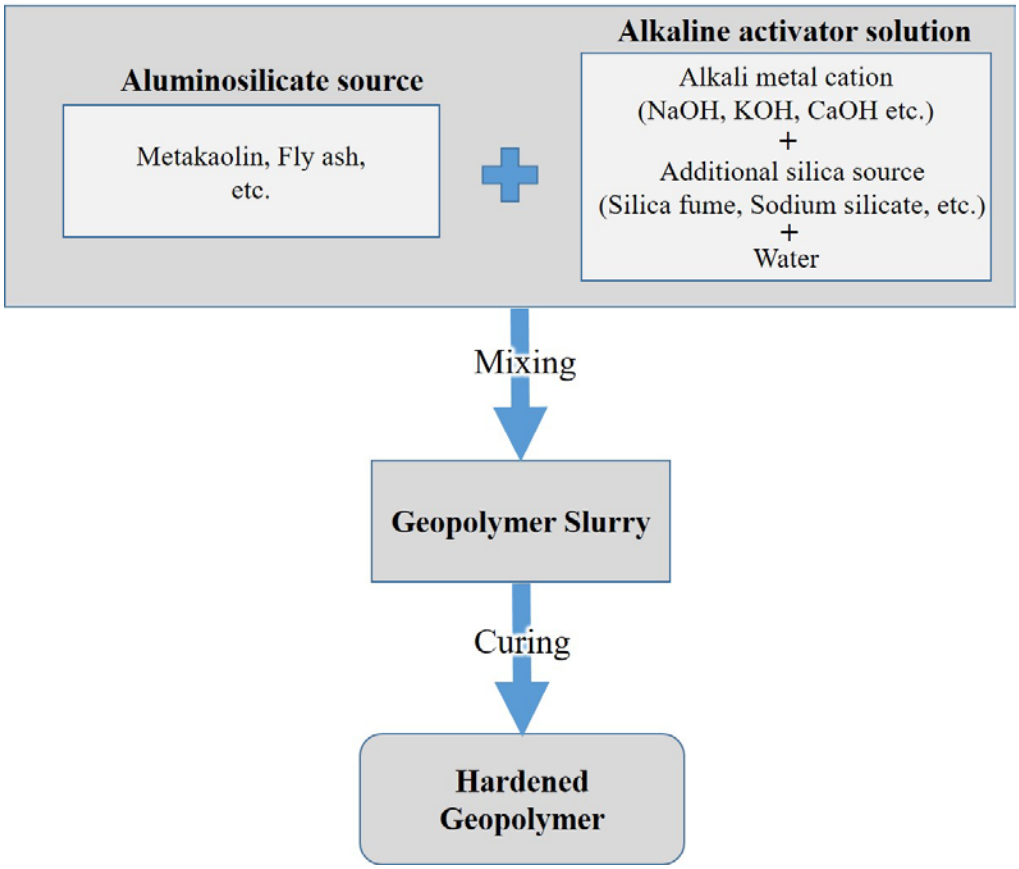


Figure 3.2: Simplified schematic of geopolymer synthesis

### *3.3.1 Alkaline Activator Solution*

Initially, a specified mass of the NaOH or KOH flakes were dissolved in deionized water to create a highly alkaline solution to process the alkali metal cations. This exothermic reaction produced a heated solution that was left to cool to room temperature for a few hours. Subsequently, the amorphous fumed silicon

oxide was added in different proportions to adjust the Si:Al ratio of the final product as desired, to create different AAS mixes for the synthesis of geopolymer. The aqueous AAS was mixed using a magnetic stirrer for a period of 48 hours at room temperature, resulting in a slightly viscous solution with a yellowish hue (Figure 3.3). All aqueous AAS mixes were prepared ahead of time and stored in sealed containers to minimize contamination by atmospheric carbonation.

### *3.3.2 Geopolymer slurry*

The high-purity, high-reactive metakaolin and aqueous AAS were mechanically mixed in a high-sheared mixer for 3 minutes at 400 revolutions per minute (RPM) to create a homogenized slurry (Figure 3.4). Depending on the desired mix proportioning and strength of geopolymer, water may be added to adjust the final strength and workability of the geopolymer mix. Since metakaolin has a fixed $SiO_2$:$Al_2O_3$ ratio, the type, concentration and amount of AAS is varied to attain the desired final mix design.

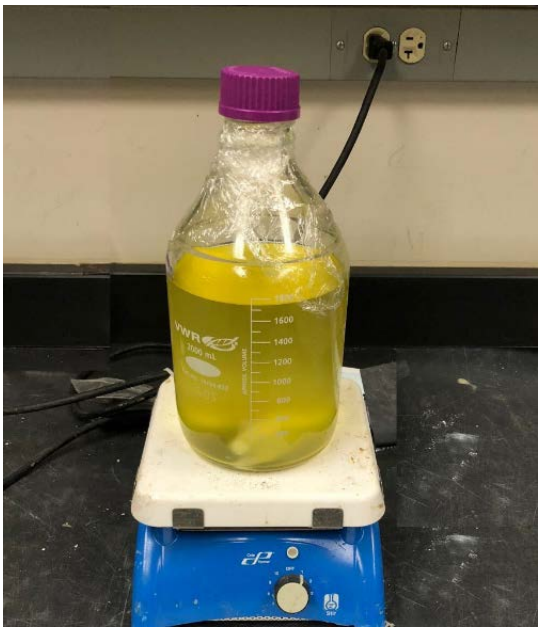


Figure 3.3: AAS being magnetically stirred at room temperature

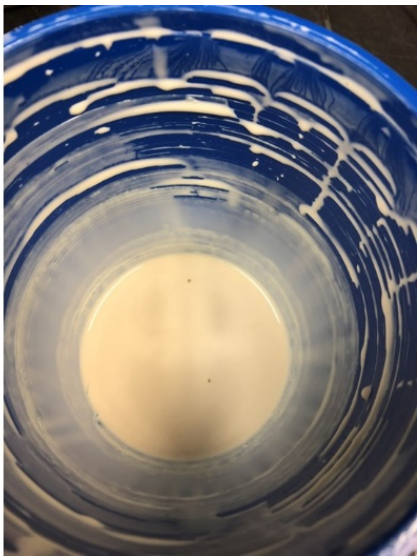

(a) (b)

Figure 3.4: Use of (a) high-sheared mixer to create (b) homogenous GP slurry

## 3.4 Curing Conditions

Curing conditions are crucial in the process of geopolymer formation. Elevated curing temperatures are known to usually increase the mechanical strength of geopolymers (Fernández-Jiménez et al. 2005, Škvára et al. 2005, Mo et al. 2014). Although elevated temperatures are known to accelerate the rate of geopolymerization and therefore reduce setting time, they do not guarantee a higher degree of geopolymerization (Rovnaník 2010, Granizo et al. 2014). Additionally, lower humidity results in large pores and shrinkage cracks in geopolymers due to rapid water loss (Kovalchuk et al. 2007, Zuhua et al. 2009).

Based on recommendations from previous researchers for metakaolin-based geopolymers, and the intention of this study in using these geopolymers for soil stabilization, all geopolymers synthesized were cured at room temperature and humidity of around 72°F (22°C) and 50% relative humidity (RH), respectively. The geopolymer slurry was poured into PVC molds that were sealed using plastic wrap and placed at room temperature. After the required curing period, hardened geopolymer specimens (Figure 3.5) were demolded and placed back into the curing room, where they were maintained until compressive strength testing. Before curing, all specimens were vibrated in molds for about two minutes to remove air bubbles introduced during mixing and pouring. Dehydration of specimens during curing determined by transient weight loss was found to be negligible (<1%).

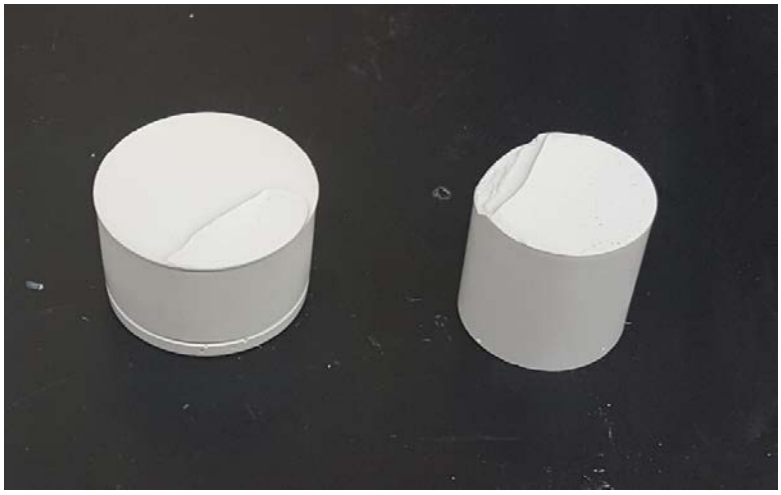

Figure 3.5: Hardened geopolymer specimens used for strength testing

## 3.5 Mix Proportioning

The most common technique of varying geopolymer composition when using a single aluminosilicate precursor, is by manipulating the aqueous AAS. The concentrations of the alkali metal cation, reactive alumina and silica, and water can be varied to produce desirable proportions of compounds for different geopolymer compositions (Duxson et al. 2007b, Lizcano et al. 2012b). The manipulation of silicon content in geopolymers is restricted by the physical limits of silicon solubility in alkaline solutions. The proportions of AAS that are varied to create different geopolymer compositions in this study are as follows:

(1) Silicon dioxide to aluminum oxide ratio [$SiO_2$:$Al_2O_3$], and

(2) Water to solids ratio [$H_2O$:($Al_2O_3$+$SiO_2$)], and

Eight different AAS mixes were formulated for this study as part of the geopolymer synthesis process, and are shown in Table 3.2. Four of the AAS mixes were

formulated using potassium as the alkali metal cation, while the other four used sodium. The different AAS mixes were combined with the required amount of metakaolin to produce eight different geopolymer mixes.

Table 3.2: MK-based geopolymer compositions synthesized as part of this study

| **M** | **$SiO_2$: $Al_2O_3$** | **$H_2O$: ($Al_2O_3$+$SiO_2$)** | **$M_2O$: $Al_2O_3$** | **GP - ID** |
|---|---|---|---|---|
| Na | 2 | 4 | 1 | Na241 |
| Na | 2 | 5 | 1 | Na251 |
| Na | 4 | 2 | 1 | Na421 |
| Na | 4 | 3 | 1 | Na431 |
| K | 2 | 3 | 1 | K231 |
| K | 2 | 4 | 1 | K241 |
| K | 4 | 2 | 1 | K421 |
| K | 4 | 3 | 1 | K431 |

The alkali metal cation to aluminum oxide ratio [$M_2O$:$Al_2O_3$] was kept at a constant value of 1, to ensure stoichiometric balance for optimal geopolymer formation (Barbosa et al. 2000). The higher the water to solids ratio, the lower the compressive strength of the geopolymer (Lizcano et al. 2012a); as such, the water to solids ratio was kept as low as possible while still maintaining reasonable workability of the geopolymer slurry.

### 3.6 Comparative analysis of different geopolymers

Eight different MK-based geopolymer mixes were synthesized as part of this study (Table 3.2). Each of these geopolymer mixes were analyzed for their setting time, workability and compressive strength, which are important parameters for the purpose of soil stabilization. These parameters are known to be significantly

affected by the variation in $SiO_2$:$Al_2O_3$ and water to solids ratio of the geopolymer mix. The following sections present the results of these analyses. Multiple specimens of each geopolymer mix were created to test for the different parameters.

### *3.6.1 Setting time*

The setting time of the geopolymer specimens were determined using a Vicat apparatus based on ASTM C191-04a developed for cement (Figure 3.6). The penetration resistance of the Vicat needle to the geopolymer specimen determined its final setting time. The geopolymer was considered completely hardened or set, when the Vicat needle did not leave an impression on the surface of the geopolymer specimen, or shows a maximum penetration of 0 mm. The test was conducted every 6 hours during the initial 24-hr curing period, and then every 24 hours thereon.

The setting times obtained for the different geopolymer mixes are presented in Table 3.3. The setting time of the geopolymer mixes were observed to increase with increasing $SiO_2$:$Al_2O_3$ and water to solids ratios. A high $SiO_2$:$Al_2O_3$ ratio decreases the degree of polycondensation, resulting in a longer setting time (Cioffi et al. 2003). All GP mixes with the $SiO_2$:$Al_2O_3$ ratio of 4, were observed to have a final setting time of 7 ± 2days. The maximum final setting time required was a period of 8 days for the K431 GP mix. Overall, the setting time was observed to be longer for K-based geopolymer mixes than Na-based geopolymer mixes.

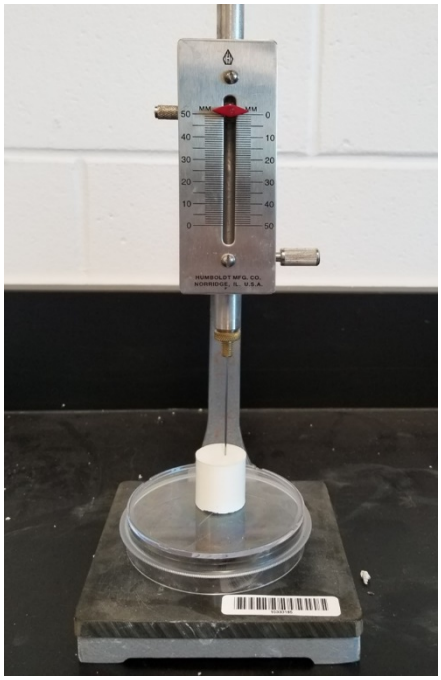

Figure 3.6: Vicat apparatus used to test setting time of geopolymer specimens

### *3.6.2 Workability*

According to the American Concrete Institute (ACI), workability is the property of freshly mixed concrete that determines the ease with which it can be mixed, placed, consolidated, and finished to a homogeneous condition (Scanlon 1994). It involves not only the concept of a consistency of concrete, but also the condition under which it is to be placed — size and shape of the member, spacing of reinforcing, or other details interfering with the ready filling of the forms. This definition is very close to the concept of workability of geopolymer mixes for this study. Geopolymers to be used as soil stabilizers need to have a certain consistency so that they are able to be mixed easily with soils.

The workability of different geopolymer mixes was determined qualitatively using freshly made geopolymer slurry. The geopolymer slurry is checked for its ability to flow or pour freely, when transferring it from one container to the other, after a period of 15 minutes. Additionally, it is also checked that large amounts of the geopolymer slurry does not adhere to the walls of the container. In this study, the workability of the geopolymer slurry is classified into four categories as: very low, low, moderate, and high. The workability assessment of the different geopolymer mixes are presented in Table 3.3. Overall, Na-based geopolymer mixes were observed to have lower workability than K-based geopolymer mixes for the same water to solids ratio

Table 3.3: Setting time and workability of different MK-based GP mixes

| GP - ID | Setting time (days) | Workability |
|---|---|---|
| Na241 | 1 | Low |
| Na251 | 2 | Moderate |
| Na421 | 5 | Very low |
| Na431 | 7 | Low |
| K231 | 1 | Very low |
| K241 | 2 | Moderate |
| K421 | 7 | Low |
| K431 | 8 | High |

The workability of a geopolymer mix is usually directly proportional to its water to solids ratio, although an increase in water to solids ratio has been known to decrease the mechanical strength of geopolymers (Van Jaarsveld et al. 1999, Steveson and Sagoe-Crentsil 2005). As such, it is important to maintain a low water

to solids ratio as possible, while ensuring adequate workability of geopolymer slurry.

### *3.6.3 Unconfined compressive strength testing*

The different geopolymer specimens were tested for unconfined compressive strength once they reached a curing period of 7 days. Compressive strength testing conducted was based on ASTM C150-19 established for Portland cement, and was performed on the 810 Material Testing System (MTS Corporation, MN) at a constant strain rate of 0.60 mm/minute (Figure 3.7). Testing specimens were 1 inch (25.4 mm) high with a diameter of 1 inch (25.4 mm), and were lightly buffed at the top and bottom to ensure uniform loading. The maximum value at which the geopolymer specimen fails is recorded as its UCS. Further details of UCS testing are presented in Chapter 4.


Figure 3.7: 810 MTS system used for strength testing of geopolymer specimens

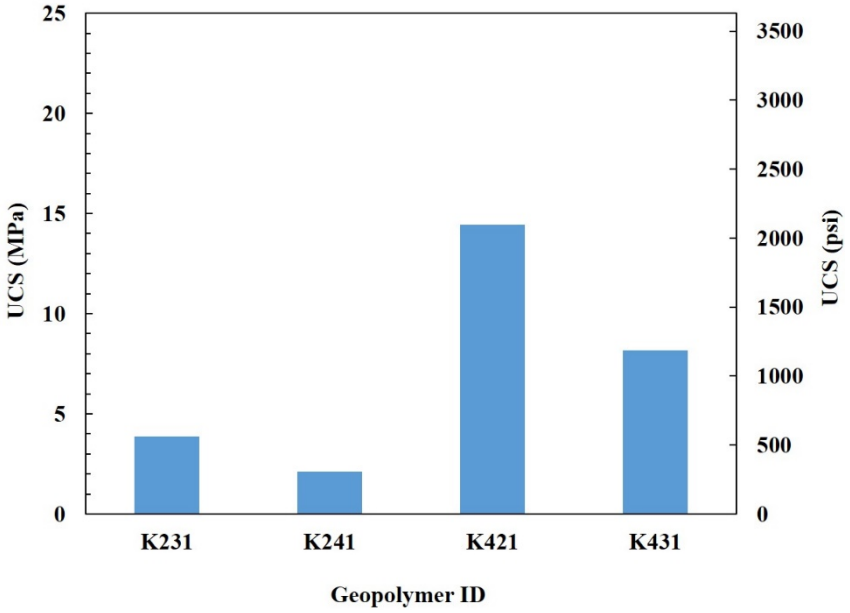


Figure 3.8: UCS of K-based geopolymer specimens

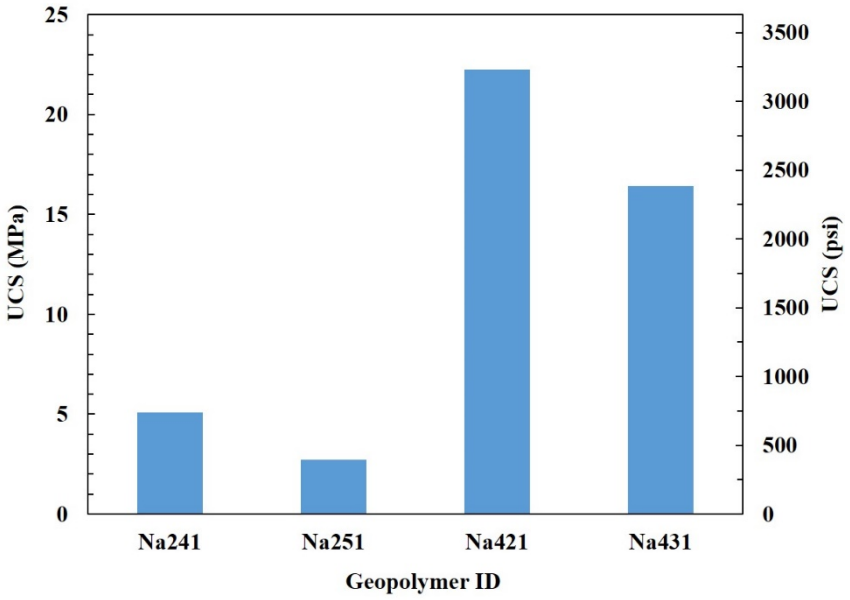


Figure 3.9: UCS of Na-based geopolymer specimens

The UCS test results for K-based and Na-based geopolymers are presented in Figures 3.8 and 3.9, respectively. Overall, Na-based geopolymers were observed to have higher UCS values than K-based geopolymers. As expected, increasing $SiO_2$:$Al_2O_3$ and decreasing water to solids ratios were observed to increase UCS values. UCS values of geopolymer specimens with $SiO_2$:$Al_2O_3$ ratio of 4 range from 1160 psi (8 MPa) to 3190 psi (22 MPa), which is comparable to the range of compressive strengths of most Portland cement mortars as indicated by ASTM C150-19.

### *3.6.4 Selection of geopolymer for soil stabilization*

In this study, eight different MK-based geopolymers with different alkali metal cations, $SiO_2$:$Al_2O_3$ and water to solids ratio were synthesized. These geopolymers were assessed for their setting time, workability and compressive strength. Ideally the geopolymer mix to be selected should have the fastest setting time, high workability, and high compressive strength, in order to be deemed a worthy competitor alongside conventional soil stabilizers. Such a geopolymer mix was challenging to synthesize due to the different variables involved in the process. As such, a suitable geopolymer mix to be used for soil stabilization purposes in this study would have a reasonable final setting time, good workability and decent compressive strength.

A setting time of 5 to 10 days is considered reasonable, while workability of the geopolymer mix is necessary to be either moderate or preferably high for this

study. Compressive strength tests show K421, K431, Na421, and Na431 geopolymer mixes to have the higher range of UCS values. Despite their high UCS values, both Na-based geopolymer mixes were observed to be quite viscous with low to very low workability, which made it challenging to place and mix them in with the soils. After careful deliberation, the K431 geopolymer mix was selected to be used as the MK-based geopolymer for stabilization of expansive soils in this study. Henceforth, the term geopolymer corresponds to the use of the K431 geopolymer mix in this study.

## 3.7 Summary

This chapter discusses the process of synthesis of metakaolin-based geopolymers used in this study. An aluminosilicate precursor, an alkali-metal cation source, a silica source and water are the four main components needed to synthesize geopolymers. Metakaolin was chosen as the aluminosilicate precursor due to its high reactivity, purity and low calcium oxide component. Two alkali metal cation sources (KOH and NaOH) were used to prepare eight AAS mixes with different $SiO_2$:$Al_2O_3$ and water to solids ratio. All geopolymer specimens were cured at room temperature at about 50% RH, and assessed for their final setting time, workability and compressive strength. The metakaolin-based K431 geopolymer mix was selected as the stabilizer for this study. The purpose of this study is to evaluate the performance of the selected geopolymer as the sole stabilizer of expansive.

# CHAPTER 4

# EXPERIMENTAL METHODOLOGY

## 4.1 Introduction

The purpose of this study is to assess the effectiveness of a metakaolin-based geopolymer as the sole stabilizer of expansive clays. Two expansive soils were treated with a metakaolin-based geopolymer at three different dosages. Control soils and geopolymer-treated soils were subjected to an array of characterization tests to understand the effects of geopolymer treatment on expansive soils. In addition, the expansive soils were treated with lime to compare how the different treatments affect the engineering properties of soils. The experimental methodology for this study is categorized into the following sub-sections:

1) Selection of expansive soils
2) Soil characterization tests,
3) Engineering characterization tests,
4) Geopolymer treatment of expansive soils, and
5) Lime treatment of expansive soils

Soil characterization tests include basic, chemical, and microstructural tests, while engineering characterization tests include strength, stiffness, volume change, and long-term performance tests. The microstructural tests are expected to yield a better understanding of the probable stabilization mechanisms as well as provide a

coherent justification for the macro behavior of geopolymer-treated soils. Additionally, durability tests performed on geopolymer-treated soils will further help in the determination of optimum geopolymer dosage rates. The procedures conducted to evaluate the effectiveness of GP as the sole stabilizer of expansive soils are detailed in the following sections.

## 4.2 Expansive Soil Selection

Texas has a prevalence of expansive soils as was shown in Figure 2.1. North Texas in particular is covered by the Blackland Prairie, Eastern Cross Timbers, and Grand Prairie soil units that are made of a mixture of clay, silt, and loam (Strong 1938). These soil units are derived from the disintegration of underlying geological formations such as the Eagle Ford shale, Austin chalk and Taylor marl, which are known to form soils that cake and crack during the summer (Winton and Scott 1912, Shuler 1918, Winton 1925). Due to the prevalence of expansive soils in Texas, it was imperative that this study focused specifically on stabilization of expansive soils.

The sole criteria for the procurement of soils was its plasticity index (PI), as higher PI is known to be an indicator of higher swelling potential (see Table 2.2) and therefore the expansive nature of soils. Two types of subgrade soils commonly found in North Texas were obtained from Lewisville, TX (Denton County) and Alvarado, TX (Johnson County) to be stabilized with geopolymer (Figure 4.1). The Lewisville soil was provided to UTA for this study by TEAM Consultants Inc.,

Arlington, TX; while the Alvarado soil was obtained from an excavation site in Alvarado.

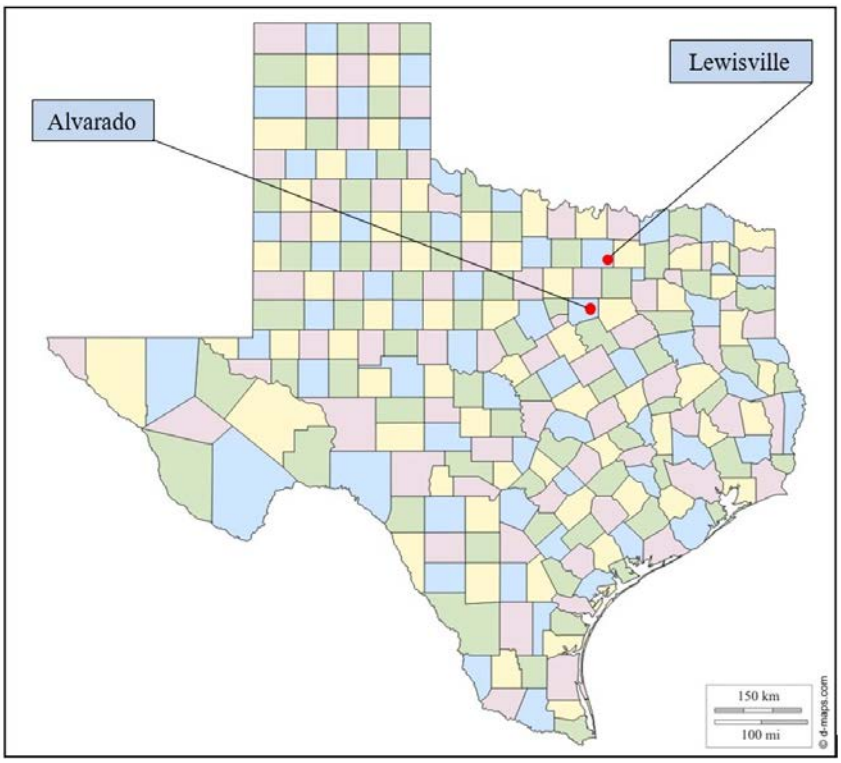


Figure 4.1: Map of Texas, showing locations from where expansive clays were obtained for this study

The soils were tested for particle size distribution and Atterberg limits and classified as per the Unified Soil Classification System (USCS). The Lewisville soil is brown in color with a PI of 53%, while the Alvarado soil is yellowish tan in color with a PI of 25% (Figure 4.2). Based on Table 2.2, the Alvarado soil is found to have medium swelling potential, while the Lewisville soil is found to have very high swelling potential, thereby classifying them to be expansive in nature. All soil

testing and treatments were conducted on oven-dried, crushed, and pulverized soils, and are explained in detail in the following sections.

(a) (b)

Figure 4.2: (a) Alvarado and (b) Lewisville soil in native state as was obtained.

## 4.3 Soil Characterization Tests

Both soils obtained for the study were subjected to a series of basic, chemical, and microstructural characterization tests that helped to better understand the geotechnical properties as well as the chemical composition of the soils. Both soils were initially oven-dried in batches at 110°C for a period of 24 to 48 hours, then crushed in a Massco Crusher to a size of about ¼ to ½ inches, and subsequently pulverized to a fine powder (Figure 4.3), before being subjected to tests or treatments. The soil characterization tests were primarily conducted on control (untreated) soils, although a few tests were conducted on geopolymer-treated soils to compare changes in properties upon geopolymer treatment.

Figure 4.3: Soils oven-dried, crushed, and pulverized before testing.

### *4.3.1 Basic Tests*

Basic geotechnical tests conducted as part of this study include specific gravity, Atterberg limits, gradation analyses, and moisture content – dry density relationship tests. The methodology followed for each test is detailed in the forthcoming sections.

#### 4.3.1.1 Specific Gravity Test

Specific gravity ($G_s$) is the ratio of the weight of a given volume of a material to the weight of the same volume of distilled water, and is important to determine the weight-volume relationships of soils. The specific gravity tests of control soils were conducted as per ASTM D854-14, and determined using a water pycnometer on soils passing the 4.75 mm (No. 4) sieve. Triplicate tests were conducted for each soil to ensure reliability of results. Specific gravity values were found to be slightly higher for the high-plasticity Lewisville soil, than the low-plasticity Alvarado soil. The specific gravity values for the control soils are shown in Table 4.1 and were found to be consistent with the expected values.

4.3.1.2 Atterberg Limits

The Atterberg limits or the 'limits of consistency' provide an insight into the plasticity and therefore the shrink and swell potentials of cohesive soils. The moisture content at which the cohesive soil passes from a liquid state to a plastic state is known as the liquid limit of the soil. Similarly, the moisture content at which the soil changes from a plastic to a semisolid state and from a semisolid state to a solid state are referred to as the plastic limit and the shrinkage limit, respectively. The liquid limit (LL) of the two soils was determined on the soil fraction that passes the 425-μm (No. 40) sieve, as per ASTM D4318-17 using a motorized Casagrande apparatus. Once the LL was determined, the plastic limit (PL) of the soils was determined by air drying and rolling the soil to the right consistency as per TEX 105-E. An E-180 PL rolling device developed by the Texas Department of Transportation (TxDOT) was used to roll the soils to the appropriate PL consistency. Equipment used for determining the Atterberg limits are shown in Figure 4.4. The Atterberg limit values for the control soils are shown in Table 4.1. Geopolymer-treated soils were also subjected to Atterberg limit tests after various curing periods, to assess changes in soil plasticity properties upon treatment.


Figure 4.4: (a) Casagrande apparatus and (b) E-180 PL rolling device used to determine Atterberg limits.

4.3.1.3 Gradation Analysis

The particle size distribution test provides a distribution of grain sizes within a soil mass and is used to classify soils for engineering purposes according to the Unified Soil Classification System (USCS). The sieve analysis and hydrometer tests on control soils were performed as per ASTM D6913-17 and D7928-17, respectively. Based on the particle size distribution tests and Atterberg limit tests, the Lewisville soil was classified as a high-plasticity clay (CH), while the Alvarado soil was classified as a low-plasticity clay (CL), as shown in Table 4.1. The gradation curves of both control soils are shown in Figure 4.5.

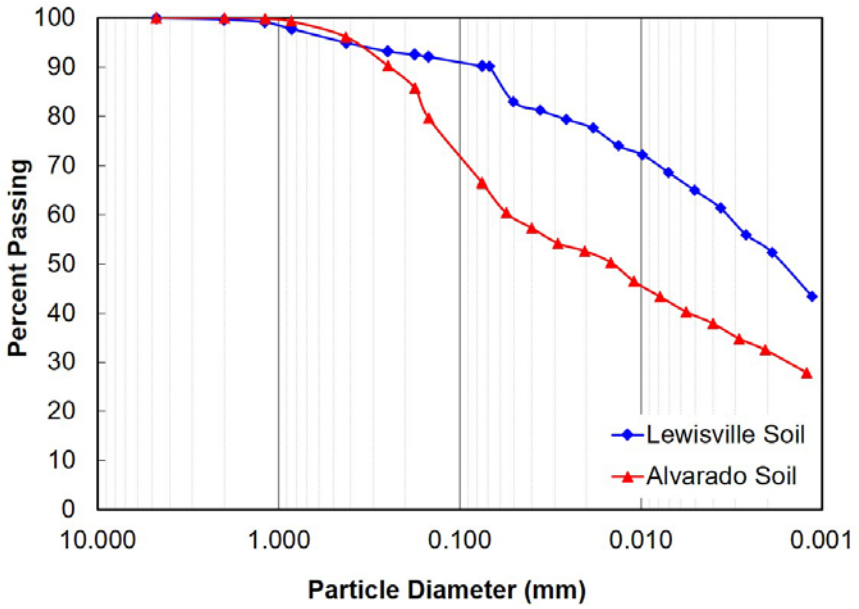


Figure 4.5: Gradation Analysis of control soils.

4.3.1.4 Moisture Content – Dry Density Relationship Test

Moisture content – dry density relationships of control soils were determined using the Harvard Miniature compaction test, as per ASTM D4609-94 and GR-84-14, to obtain the optimum moisture content (OMC) at which the soils were compacted to its maximum dry density (MDD). The Harvard miniature compaction apparatus was introduced by Wilson in 1950 as a means to obtain moisture content – dry density relationships of soils in a quicker manner using smaller amounts of soil (Scavuzzo 1984). The apparatus consists of a mold with an inner diameter of 1.31 inches (3.3 cm), height of 2.82 inches (7.2 cm) and volume of 1/454 $ft^3$ (62.3 $cm^3$), as well as a spring-loaded plunger and a sample extruder as shown in Figure 4.6. Harvard compaction closely resembles the kneading action of

a sheepsfoot roller (Lade 2016), and is therefore ideal for use in cohesive soils. The Harvard miniature compaction for this study was performed by preparing the soils at different moisture contents and molding specimens in three layers, by applying 25 tamps of 20 pound (89 N) force with the spring-loaded plunger to each of the three lifts in the Harvard compaction mold.

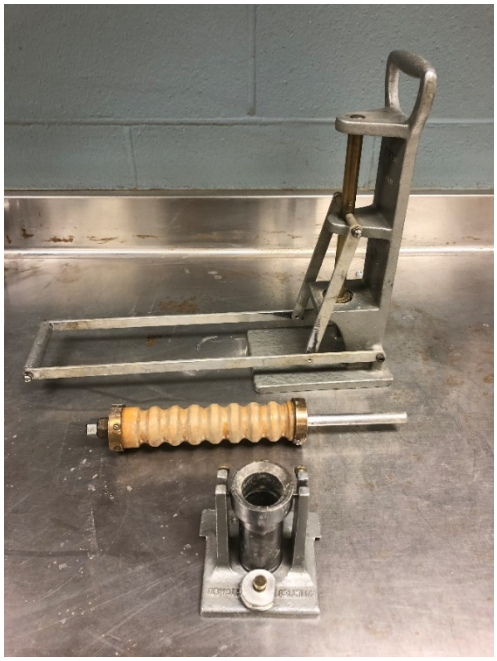

Figure 4.6: Harvard miniature compaction apparatus

It was ensured that the same compactive effort was applied to all soil specimens being compacted to maintain uniformity and accuracy for evaluation of results. According to TEX-113-E, compactive effort is the total energy used to compact a specimen and is usually expressed in kN-m/m$^3$ (or lb-ft/in$^3$). The compactive effort (CE) used to compact a specimen can be calculated using Equation 4.1 as follows:

$$CE = \frac{Drop\ height \times Hammer\ weight \times No.of\ drops \times No.of\ layers}{Volume\ of\ compaction\ mold} \quad \text{(Eqn. 4.1)}$$

The compactive effort applied to soil specimens in this study using the Harvard compaction method was calculated to be about 275 kN-m/m$^3$. The compactive effort applied using standard compaction equipment is usually about 600 kN-m/m$^3$, which is more than two times the compactive effort of the Harvard compaction method used in this study. A comparison between Standard compaction and Harvard compaction would yield an enhanced awareness of moisture content – dry density relationships of obtained soils from a prevailing point of view.

The compaction test results of the control soils are given in Table 4.1, and their moisture content – dry density relationship curves are shown in Figure 4.7. It is observed that the high-plasticity Lewisville soil has a higher MDD and lower OMC than the low-plasticity Alvarado soil. All specimens in this study molded to the dimensions of the Harvard compaction mold for engineering tests, whether treated or control, were compacted at its respective OMC to 95% of its MDD. Drier side of optimum moisture content were avoided to prevent flocculation (Banerjee et al. 2018c, 2019a).

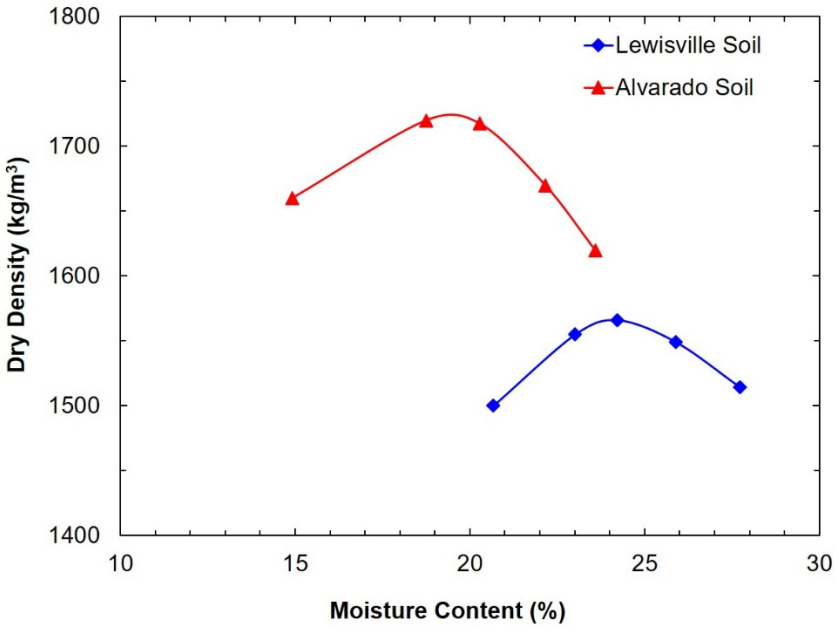


Figure 4.7: Moisture content – dry density relationship curves of control soils

Table 4.1: Basic geotechnical properties of control soils used in this study

| **Property** | **Alvarado Soil** | **Lewisville Soil** |
|---|---|---|
| Passing No. 10 sieve (%) | 100 | 99.7 |
| Passing No. 40 sieve (%) | 96.2 | 95.0 |
| Passing No. 200 sieve (%) | 66.5 | 90.2 |
| Silt content (75 – 2 μ) (%) | 33.9 | 37.8 |
| Clay content (< 2 μ) (%) | 32.6 | 52.4 |
| Liquid limit (%) | 40 | 80 |
| Plasticity Index (%) | 25 | 53 |
| Specific Gravity ($G_s$) | 2.69 | 2.78 |
| Max. Dry Density (kg/m$^3$) | 1720 | 1570 |
| Optimum Moisture Content (%) | 20 | 24 |
| Sulfate Content (ppm) | 100 | 7000 |
| USCS-ID | Low plasticity Clay (CL) | High Plasticity Clay (CH) |

### *4.3.2 Chemical and Microstructural Tests*

Chemical and microstructural tests conducted as part of this study include pH test, cation exchange capacity test, specific surface area tests, X-ray diffraction test, X-ray fluorescence test, as well as the field emission scanning electron microscopy test. The methodology followed for each test is detailed in the sections below.

#### 4.3.2.1 pH Test

Soil pH is a measure of the degree of acidity or alkalinity of a soil, and is useful in determining the solubility of soil minerals and mobility of ions in the soil. All pH tests in this study were measured as per ASTM D4972-19, using the Cole-Parmer P200 pH meter (Figure 4.8). The pH meter was calibrated before every test, as per the manufacturer's specifications. The pH of soils was measured in both distilled water and 0.01M calcium chloride ($CaCl_2$) solution, but only the pH values from the soil-$CaCl_2$ suspension were reported, as they were observed to provide more reliable values.

Equal amounts of soil and solution were mixed thoroughly in a glass beaker and allowed to stand for an hour, after which the pH reading was measured by immersing the pH electrode in the supernatant. pH tests were conducted on both control and treated soils after specific curing periods to ensure sufficient alkalinity for ongoing reaction processes, as well as to observe the variations in pH to get an

understanding of the long-terms effects of the treatments and potential advancing chemical reactions.


Figure 4.8: Cole-Parmer P200 pH meter

4.3.2.2 Cation Exchange Capacity Test

The cation exchange capacity (CEC) determines the amount of exchangeable cations a soil possesses, and is usually expressed as milliequivalents of charge per 100 g of dry soil (meq/100 g) (Ross and Ketterings 1995). Clay minerals have exchangeable cations due to the negative charge on the clay minerals. The higher the negative charge on the clay mineral, the more cations it can accommodate, therefore higher the CEC value. Typical CEC values for clay minerals presented earlier in Table 2.1, showed that higher CEC values correspond to the presence of the high swelling potential clay mineral montmorillonite in the

system. The CEC test can be used in conjunction with the specific surface area test to determine the montmorillonite content in a soil.

In this study, CEC of control soils is determined using the ammonium acetate method introduced by Chapman in 1965 (Ross and Ketterings 1995). This method involves the addition of a saturating solution and the subsequent extraction of adsorbed cations using an extraction solution. An ammonium acetate ($NH_4OAc$) solution at pH of 7 is used as the saturating solution, while a potassium chloride (KCl) solution functions as the extracting solution. Once the KCl extract is obtained by leaching through the soil, the ammonia-nitrogen ($NH_3$-N) concentration in the soil is determined using the Hach DR-2800 spectrophotometer by the Nessler colorimetric method (Hach 8038). The CEC of soil is calculated using Equation 4.2 as follows, and is shown in Table 4.2:

$$CEC\ (meq/100g) = \frac{NH_3\text{-}N\ (ppm)}{14} \times 4 \qquad \text{(Eqn. 4.2)}$$

Figure 4.9 shows some apparatus and chemicals used for CEC; steps followed in this study to determine CEC values of control soils are outlined in Figure 4.10.


Figure 4.9: Chemicals and apparatus used for CEC test

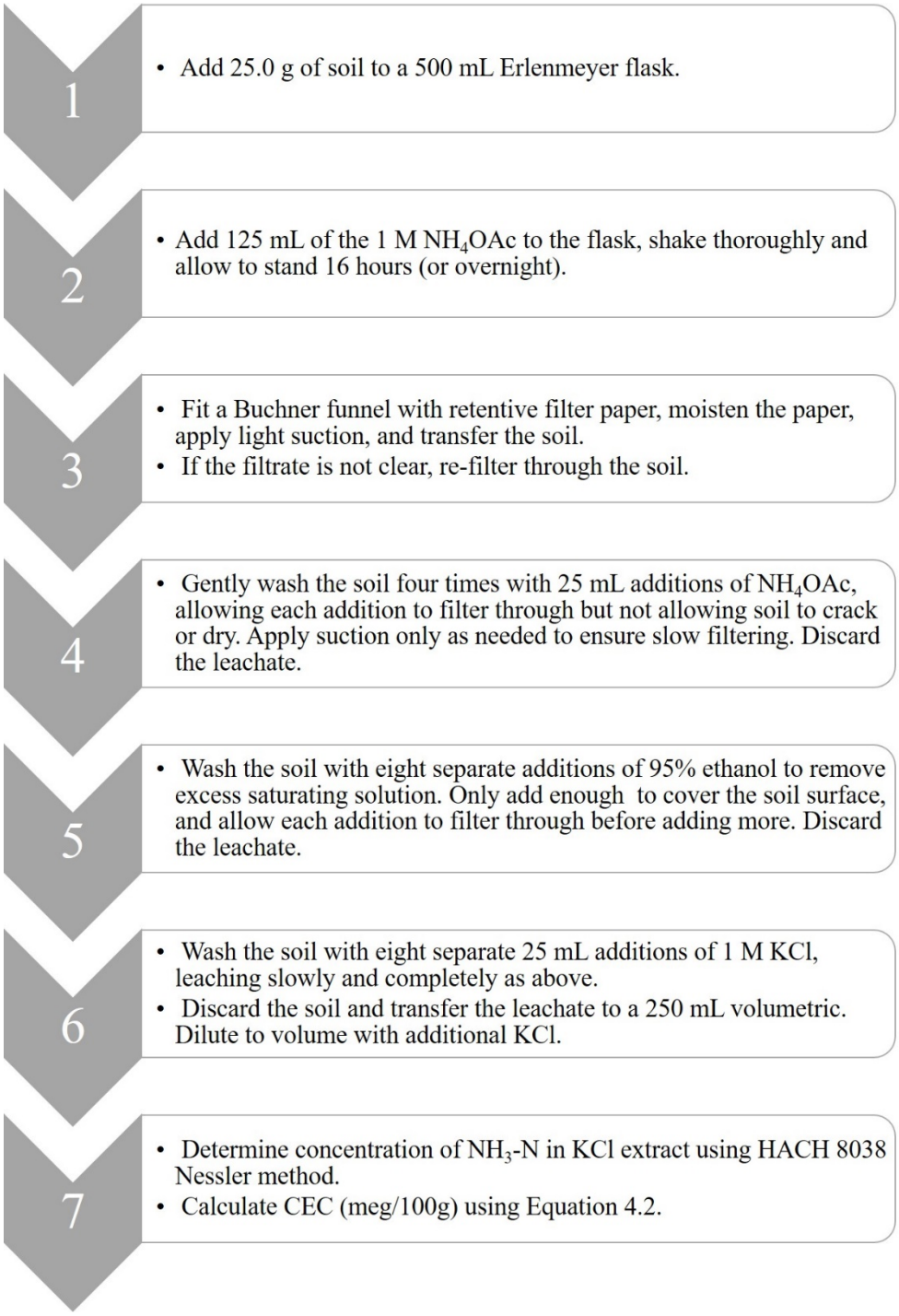


Figure 4.10: Flowchart of CEC test procedure (Chittoori 2009)

4.3.2.3 Specific Surface Area Test

The specific surface area (SSA) refers to the surface area per unit mass of soil and is usually expressed as cubic meters per gram ($m^2/g$) (Pennell 2002). Apart from CEC, SSA is a crucial influence on physical and chemical properties of soils. SSA of a soil is known to be closely associated with its water retention capacity as well as CEC. Soils with smaller particle size have higher specific surface areas, which translates to higher water retention capacity and therefore higher swelling potential (Carter et al. 1986).

SSA is usually determined by the adsorption of a solvent known as ethylene glycol monoethyl ether (EGME) (Diamond and Kinter 1956, Carter et al. 1986). The EGME method of determining SSA was verified for geotechnical use (Cerato and Lutenegger 2002), and is therefore used in this study. Figure 4.11 shows apparatus and chemicals used for SSA determination. The steps followed to determine SSA values of control soils are outlined in Figure 4.12.


Figure 4.11: Chemicals and apparatus used for *SSA* test

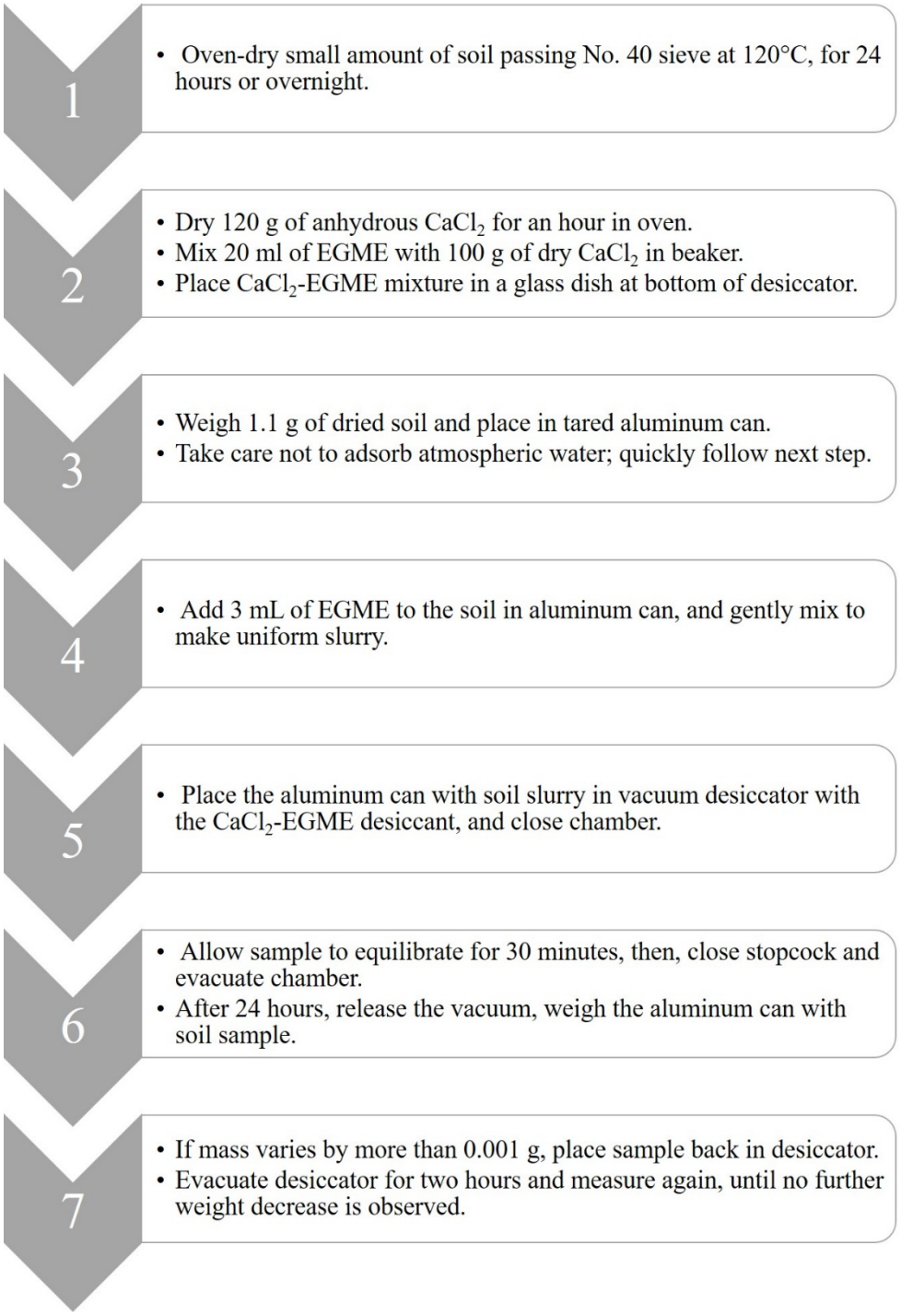


Figure 4.12: Flowchart of SSA test procedure (Chittoori 2009)

The soil specimen is initially saturated with EGME to create a slurry that is placed in a desiccator for a period of time unless no further drop in mass is observed. Mass of the soil specimen was obtained using an electronic analytical balance with an accuracy of 0.001 g. A $CaCl_2$-EGME mixture was used as the desiccant to adsorb the excess EGME from the soil. The SSA of soils is then calculated using Equation 4.3, as follows:

$$SSA\ (m^2/g) = \frac{W_a}{W_s \times 0.000286} \quad \text{(Eqn. 4.3)}$$

Where, $W_a$ is the weight of EGME retained by the specimen in grams (final slurry weight – $W_s$), $W_s$ is the initial soil weight (g), and 0.00286 is the weight of EGME required to form a monomolecular layer on a square meter of surface ($g/m^2$).

Chittoori established correlative equations to determine the montmorillonite content in soils using CEC and SSA values (Chittoori 2009, Chittoori and Puppala 2011). The montmorillonite content (%) in soils is calculated using Equation 4.4, as follows:

$$Montmorillonite\ (\%) = -2.87 + (0.08 \times SSA) + (0.26 \times CEC) \quad \text{(Eqn. 4.4)}$$

The SSA values of both control soils as well as their calculated montmorillonite content are given in Table 4.2. As expected, the low-plasticity Alvarado soil is observed to have both lower CEC and SSA values, resulting in a lower montmorillonite content of 44.7%, in comparison to the high-plasticity Lewisville soil with a 52.2% montmorillonite content.

Table 4.2: Mineralogical test results and montmorillonite content of control soils

| **Control Soil** | **CEC (meq/100g)** | **SSA ($m^2/g$)** | **Montmorillonite content (%)** |
|---|---|---|---|
| Alvarado soil (CL) | 152.9 | 98.0 | 44.7 |
| Lewisville soil (CH) | 172.9 | 126.8 | 52.2 |

4.3.2.4 X-Ray Diffraction Test

X-ray diffraction (XRD) tests were performed on metakaolin as well as the metakaolin-based K431 GP to get an insight into their qualitative mineral composition. XRD tests were conducted on Bruker D8 X-ray diffractometer (see Figure 4.13) using the powder XRD method. The specimens to be tested were oven-dried and pulverized to a fine powder passing the No. 200 sieve, and then scanned between 2θ values of 10° to 50°, at a speed of 0.01 degrees per second using Cu-Kα radiation with a wavelength of 1.5406 Å.

XRD curves for metakaolin and K431 GP are show in Figure 4.14. As expected, both metakaolin and K431 geopolymer produced characteristic broad diffuse halos instead of distinct peaks, due to their amorphous nature. As expected, the broad diffuse halo was observed for metakaolin between $2\theta_{max}$ values 21° to 23°, and for the K431 geopolymer between 27° to 31° (Williams et al. 2011). The the sharp peaks observed at $2\theta_{max}$ values of around 25°, 38°, and 48° correspond to the non-reactive, crystalline titanium oxide ($TiO_2$) in anatase phase, a known impurity in metakaolin (Lizcano et al. 2012b).

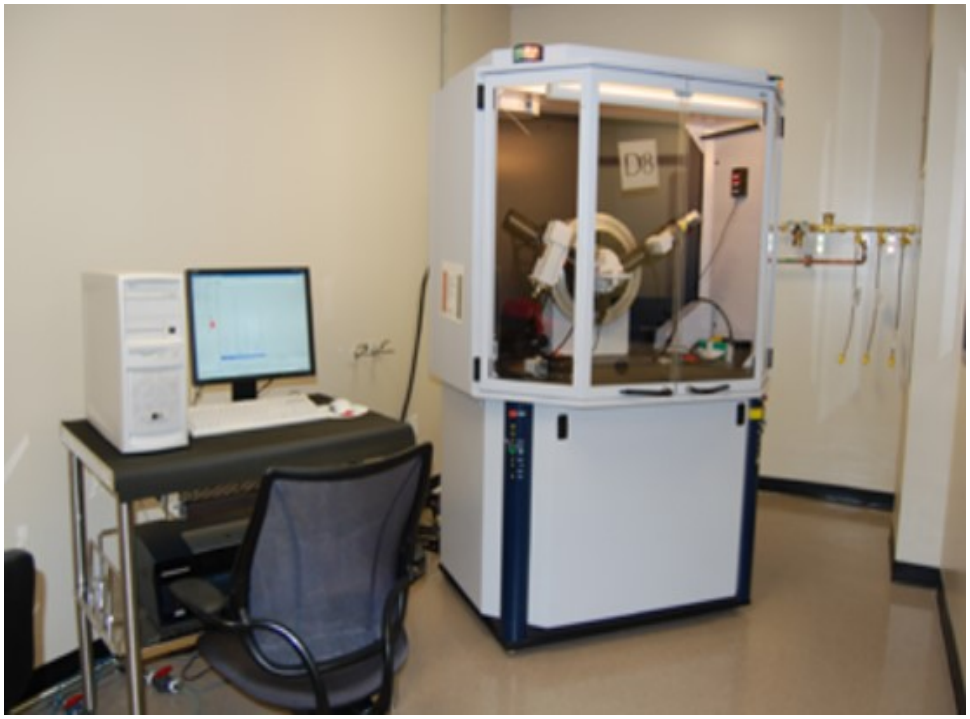


Figure 4.13: Bruker D8 X-ray diffractometer

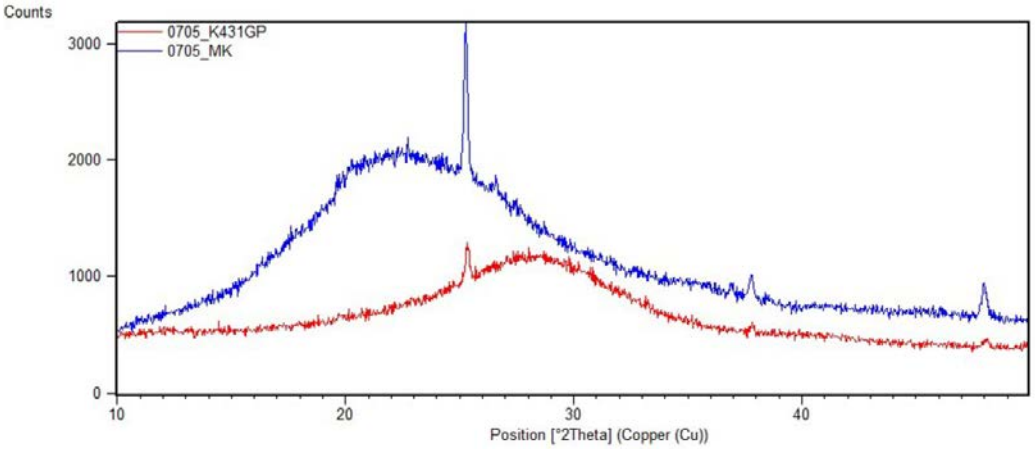


Figure 4.14: XRD curve for metakaolin (blue) and K431 GP (red).

Control soils were sent for XRD testing at the Mineral Lab Inc. (Golden, CO), where powder XRD was conducted on soil passing No. 400 sieve size. The fine powder was scanned with the Siemens D5000matic diffractometer using Cu-Kα radiation over a 2θ range of 3° to 61°. Estimates of approximate mineral weight percentages were made. Montmorillonite content of the clay size fractions (< 2 microns) tested was found to be 63% and 77% in Alvarado soil and Lewisville soil, respectively, while the kaolinite content was found to be only 13% and 8% in Alvarado soil and Lewisville soil, respectively. These results verify that montmorillonite content is higher in high-plasticity Lewisville soil than low-plasticity Alvarado soil, as was established from CEC and SSA tests.

4.3.2.5 X-Ray Fluorescence Test

X-ray fluorescence (XRF) tests were performed on control soils to determine their chemical composition. XRF analysis was performed using the Rigaku Supermini200 (Rigaku Corporation, Japan), and each specimen was scanned twice for qualitative as well as quantitative information (Table 4.3). The qualitative scan gives a general idea of the chemical composition of the specimen, but lacks $Na_2O$ values as it cannot detect light elements properly. Quantitative analysis gives a more accurate chemical composition, although it is observed to be quite similar to the qualitative values. The $TiO_2$ value is missing, as the required standard was not available. From Table 4.3, $SiO_2$, $Al_2O_3$, and CaO are observed to be the predominant minerals in both control soils.

Table 4.3: Chemical composition of control soils from XRF analysis

| | Alvarado clay (wt%) | | | | | | | | |
|---|---|---|---|---|---|---|---|---|---|
| | **MgO** | **$Al_2O_3$** | **$SiO_2$** | **$SO_3$** | **$K_2O$** | **CaO** | **$TiO_2$** | **$Fe_2O_3$** | **$Na_2O$** |
| ***Qual*** | 1.08 | 15.10 | 46.36 | 0.12 | 1.38 | 27.47 | 1.17 | 7.32 | - |
| ***Quan*** | 0.83 | 15.88 | 42.85 | -0.21 | 1.04 | 20.28 | - | 4.57 | 0.09 |
| | **Lewisville clay (wt%)** | | | | | | | | |
| | **MgO** | **$Al_2O_3$** | **$SiO_2$** | **$SO_3$** | **$K_2O$** | **CaO** | **$TiO_2$** | **$Fe_2O_3$** | **$Na_2O$** |
| ***Qual*** | 1.70 | 20.57 | 50.67 | 1.33 | 2.83 | 10.54 | 1.35 | 11.02 | - |
| ***Quan*** | 1.51 | 19.91 | 50.72 | 0.50 | 2.51 | 9.25 | - | 9.95 | 0.24 |

4.3.2.6 Field Emission Scanning Electron Microscopy Test

Field Emission Scanning Electron Microscopy (FESEM) tests were performed on control and geopolymer-treated soil as well as the K431 geopolymer, to qualitatively assess microstructural changes in soils upon treatment and to detect the potential formation of geopolymer gels. FESEM specimen scanning was performed on a Hitachi S-4800 II FESEM machine (Figure 4.15), either in powder form or as cubical specimen (Figure 4.16). Cubical FESEM specimens were prepared by cutting out small cubical specimen (approximately 1cm x 1cm x 0.5 cm) from a statically compacted specimen at its OMC and MDD. Care was taken to ensure that cubical specimens were more or less flat so they were stable enough to be placed on the aluminum stub to be scanned. Both powder and cubical specimens were dried using the desiccator method, as the slow removal of moisture preserves the microstructure of specimen and produces higher quality images (Gautam 2018).

Since soils and geopolymers are non-conductive in nature, silver sputter coating was applied on the specimen using a CrC-100 sputtering machine (Figure 4.17) to ensure there were no arching effects or image instability. Double-sided carbon tape was used to make sure the specimen were secured in place during scanning. The aluminum stubs with specimens were placed in the sputtering machine and sputter coated with silver in the presence of Argon gas at pressures between 5 and 10 millitorrs. Images obtained from FESEM of control and treated specimens were compared visually to determine morphological changes at a microscopic level that would indicate the presence of reaction products.

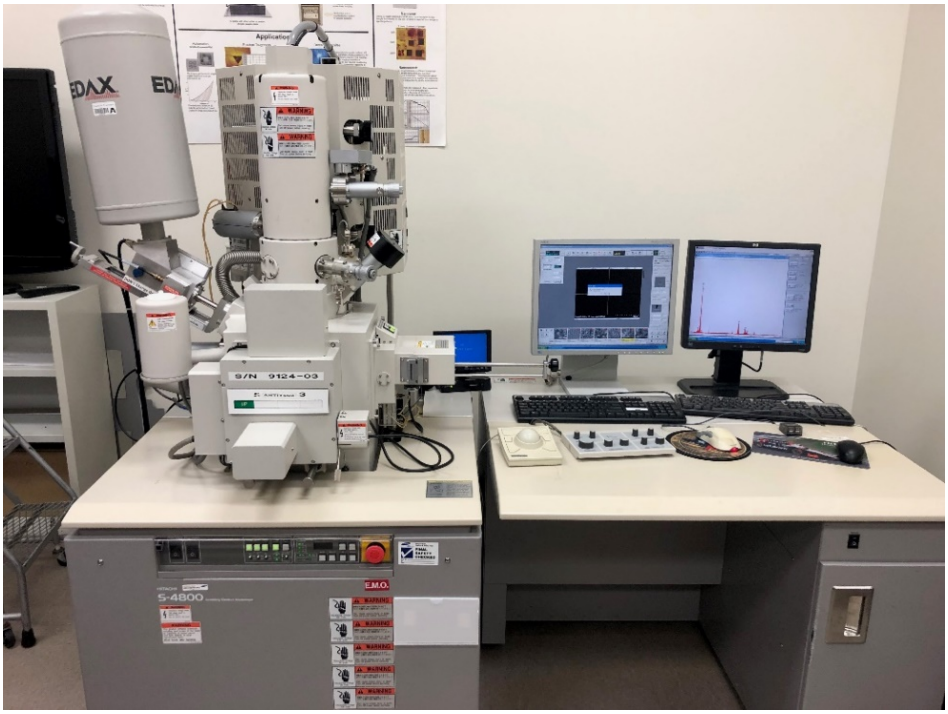


Figure 4.15: Hitachi S-4800 II FESEM system

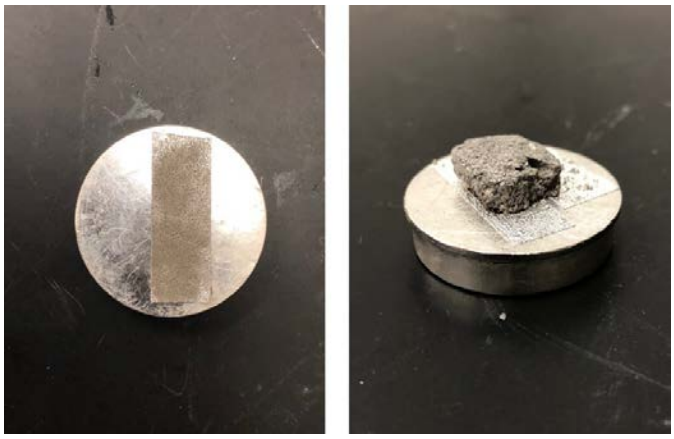

Figure 4.16: Sputter-coated powder and cubical FESEM specimen


Figure 4.17: CrC-100 sputter coating machine

## 4.4 Engineering Characterization Tests

Control and treated soil specimens were subjected to engineering tests to evaluate the effects of geopolymer treatment on the engineering characteristics of soils. This section presents detailed descriptions of the tests and their testing methodology. Triplicate tests were conducted for each specimen to ensure reliability of results.

### *4.4.1 Unconfined Compressive Strength Test*

Unconfined compressive strength (UCS) is the maximum axial compressive strength a soil mass can withstand before failing, when no confining stress is provided. It is a key geotechnical parameter used to assess the strength of a soil mass. In saturated condition, UCS ($q_u$) and undrained shear strength ($s_u$) of a cohesive soil are correlated by Equation 4.5 as follows (Das and Sobhan 2013):

$$s_u = \frac{q_u}{2} \qquad \text{(Eqn. 4.5)}$$

UCS tests were performed on control and treated soils to get a rough estimation of the soil strength before and after treatment, in accordance with ASTM D2166-16. UCS tests were conducted by applying strain-controlled uniaxial loads to right-cylindrical soil specimens until it failed. The stress at which the specimen fails is known as the UCS of the soil, which is also the maximum value of the stress-strain curve obtained from the UCS test.

Soil was statically compacted to cylindrical specimens with two dimensions: larger specimens with approximate diameter of 2.85 inches (72.4 mm)

and height of 5.85 inches (148.6 mm), and miniature specimens with approximate diameter of 1.31 inches (33.3 mm) and height of 2.85 inches (72.4 mm). Larger specimens were statically compacted in a split-mold using the Wykeham Farrance International automated compaction device at a strain rate of 2.7 mm/minute (Figure 4.18), while the miniature specimens where statically compacted in a Harvard miniature compaction mold using a mechanical tamper. All specimens were compacted at their OMC in three equivalent lifts to 95% of their respective MDD and have a height to diameter ratio of at least 2 to reduce errors due to end effects of the specimen. Results reported in the study are predominantly from miniature specimens, as they utilize much less soil than required to mold larger specimens and yield representative and reliable results.

Figure 4.18: Static compaction of specimens for engineering tests

Control soils were mixed with water to achieve the correct OMC and set in a moisture room to equilibrate for a minimum of 16 hours, after which they were compacted to cylindrical specimens as detailed above and tested for UCS. On the other hand, geopolymer-treated soils were immediately compacted to form cylindrical specimens. The molded geopolymer-treated specimens were extruded and set to cure in a moisture room with 100% relative humidity (RH) for a period of 0 (2 hours), 7 and 28 days. UCS testing of soil specimens was performed on the Geocomp Load Trac-II machine for larger specimens, and the Geotac Sigma-1 machine for miniature specimens (Figure 4.19). The UCS of control and geopolymer-treated soil specimen at three different dosages and curing periods were considered to evaluate the efficiency of geopolymers in improving the strength of the soils in this study.

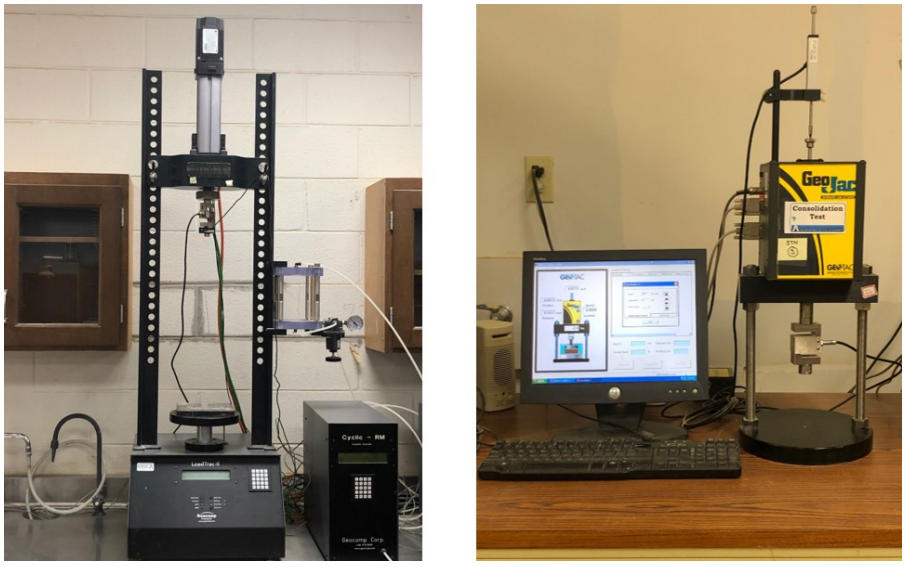


Figure 4.19: UCS equipment for large (left) and miniature (right) specimens

### *4.4.2 Repeated Load Triaxial Test to Determine Resilient Modulus*

Resilient modulus ($M_R$) is an important parameter of pavement materials (Puppala et al. 2003b). $M_R$ is defined as the ratio of the applied deviator stress ($\sigma_d$) to the recoverable or 'resilient' elastic strain ($\varepsilon_r$), as given in Eqn. 4.6:

$$M_R = \frac{\sigma_d}{\varepsilon_r} \quad \text{(Eqn. 4.6)}$$

The repeated load triaxial (RLT) test applies cyclic loading for specific time durations to simulate traffic loading providing insight into material response and stiffness, and is therefore an essential element in mechanistic-empirical pavement design.

RLT tests for this study were conducted on control soils and geopolymer-treated soil in accordance with AASHTO T307 using a cyclic triaxial setup (Figure 4.20). Soil specimens tested for $M_R$ were molded into cylindrical specimen with approximate diameter and height of 2.85 inches (72.4 mm) and 5.85 inches (148.6 mm), respectively using static compaction. The testing program as per AASHTO T307 includes 15 test sequences at specified confining pressures and deviator stresses as shown in Table 4.4. A conditioning test sequence of 500 repetitions was applied to each specimen to minimize errors due to specimen preparation and imperfect contact. Each test sequence consists of 100 loading cycles, wherein a haversine pulse load was applied for a period of 0.1 seconds followed by a rest period of 0.9 seconds. The $M_R$ value for a specific test sequence was calculated as a mean of its last five loading cycles (Buchanan 2007; Banerjee et al. 2018, 2019).

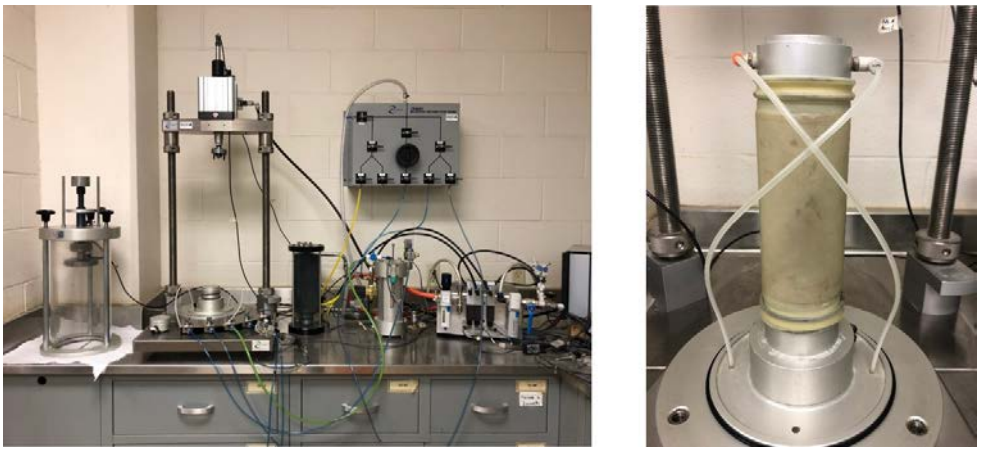

Figure 4.20: IPC Global RLT test setup with specimen prepared for testing

Table 4.4: Test sequence for RLT test as per AASHTO T307 used in this study

| Sequence # | Confining Pressure, (kPa) | Contact Stress, (kPa) | Cyclic Stress, (kPa) | Max. Axial Stress, (kPa) | No. of Load cycles |
|---|---|---|---|---|---|
| Conditioning | 41.4 | 2.8 | 24.8 | 27.6 | 500 |
| 1 | 41.4 | 1.4 | 12.4 | 13.8 | 100 |
| 2 | 41.4 | 2.8 | 24.8 | 27.6 | 100 |
| 3 | 41.4 | 4.1 | 37.3 | 41.4 | 100 |
| 4 | 41.4 | 5.5 | 49.7 | 55.2 | 100 |
| 5 | 41.4 | 6.9 | 62 | 68.9 | 100 |
| 6 | 27.6 | 1.4 | 12.4 | 13.8 | 100 |
| 7 | 27.6 | 2.8 | 24.8 | 27.6 | 100 |
| 8 | 27.6 | 4.1 | 37.3 | 41.4 | 100 |
| 9 | 27.6 | 5.5 | 49.7 | 55.2 | 100 |
| 10 | 27.6 | 6.9 | 62 | 68.9 | 100 |
| 11 | 13.8 | 1.4 | 12.4 | 13.8 | 100 |
| 12 | 13.8 | 2.8 | 24.8 | 27.6 | 100 |
| 13 | 13.8 | 4.1 | 37.3 | 41.4 | 100 |
| 14 | 13.8 | 5.5 | 49.7 | 55.2 | 100 |
| 15 | 13.8 | 6.9 | 62 | 68.9 | 100 |

RLT testing was performed on geopolymer-treated specimens cured for a period of 7 and 28 days at 100% RH, at three different geopolymer dosages, to study the impact of the variables on the stiffness of treated soils.

### *4.4.3 One-dimensional Swell Test*

The one-dimensional swell (1-D) test provides a quantification of the swelling potential of a soil. The free swell of a soil is defined as the percentage swell exhibited by a soil following water absorption at a seating pressure of 0.145 psi (1 kPa), and is determined in this study as per ASTM D4546-14e1 using a modified swell test setup (Figure 4.21). The specimens used for the 1-D swell tests were statically compacted in a ring mold at its OMC to 95% of its MDD, to form specimens with diameter and height of 2.5 inches (63.5 mm) and 1.13 inches (28.7 mm), respectively. The compacted specimens were cured in the ring molds at 100% RH for the required curing period and then tested for 1-D swell.

The ring mold with the compacted soil specimen was placed in a grooved consolidation cell, to ensure the ring mold remains stable. A filter paper and porous stone were placed on top of the soil specimen, over which a top cap applying a 0.145 psi (1 kPa) load was placed. A dial gauge was placed on the top cap to monitor the vertical strain due to water absorption. Subsequently the consolidation cell was inundated with water, and swell readings were recorded right away for a period of 24 hours or until no significant strain change was observed. The percentage of vertical swell strain was then plotted with respect to time on a semi-

logarithmic scale to obtain a swell curve. Swelling potential of a soil is equated to its percentage vertical swell strain. Swell specimens were always ensured to be completely submerged in water during the entire testing period. 1-D swell tests were performed on control soils and geopolymer-treated soils after curing periods of 0 (2 hours), 3 and 7 days at three different dosages.

Figure 4.21: Modified 1-D swell test setup

### *4.4.4 Linear Shrinkage Test*

The linear shrinkage test of soils was performed in accordance with TEX-107-E to determine the shrinking potential of control and geopolymer-treated soils. Soil fraction to be tested passing the 425-μm (No. 40) sieve was mixed thoroughly with water until it reached its liquid limit consistency. The proper molding consistency

of the soil required for this test was tested by shaping the soil specimen into a smooth layer about 0.5 inches (12.7 mm) thick and making a groove with the grooving tool. Once the material flowed on its own accord and just closed the groove, it was ready for the test. The soil slurry was then transferred to linear bar molds greased with petroleum jelly to ensure that soil did not adhere to the mold walls (Figure 4.22). The slurry in the mold was gently jarred to enable trapped air bubbles to escape, and smoothed with a straightedge. The mold with the soil slurry was placed at room temperature for two hours and then oven-dried at 230°F (110°C) till no further change in mass was observed. Once cooled, the length of the bars was measured to determine the percentage of linear shrinkage, given by Equation 4.7 as follows:

$$LS = 100 \times \frac{L_W - L_D}{L_W} \quad \text{(Eqn. 4.7)}$$

Where $LS$ is the linear shrinkage expressed as a percentage, $L_W$ is the length of the wet soil bar, 5 inches (127 mm), and $L_D$ is the length of the dry soil bar, inches (mm). Linear shrinkage tests were performed on control soils and geopolymer-treated soils after curing periods of 0 (2 hours), 3 and 7 days at three different dosages.

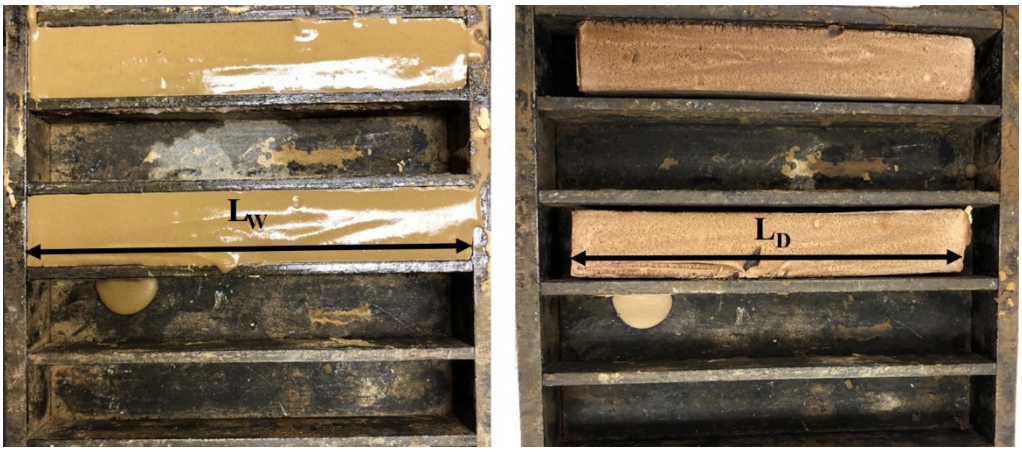


Figure 4.22: Linear shrinkage bar test setup

### *4.4.5 Modified durability test*

Durability tests are imperative to address the long-term performance of chemically-treated soils, especially in the arid to semi-arid climatic conditions of North Texas. These tests provide insight into the effects of seasonal moisture fluctuations on engineering properties of treated soils. Durability testing of soil-cement mixtures is usually conducted as per ASTM D559-15, where cured specimens with approximate diameter and height of 4 inches (101.6 mm) and 4.58 inches (116.3 mm), respectively, are subjected to 12 alternating cycles of wetting and drying. In addition, the specimen is also brushed with a wire-scratch brush to estimate soil-cement loss. This standard test was not performed for durability performance testing in this study.

In this study, durability testing of chemically treated soils were conducted using a modified durability testing approach known as capillary soaking. Capillary soaking replicates reasonable seasonal moisture fluctuations under typical

pavement conditions, such as increase in groundwater table; whereas the conventional method simulates intense cycles of flooding and drought. According to a technical brief published by the National Lime Association in 2006, if soils to be stabilized are known to be expansive in nature, capillary soaking is recommended to determine durability performance of treated soils (Little 1998). It was observed that geopolymer-treated miniature soil specimens when subjected to the first wetting cycle as per ASTM D559-15 disintegrated immediately. As such, modified durability testing in this study refers to the capillary soaking of miniature specimens.

The capillary soaking setup consisted of a container filled with coarse-grained sand filled with water up to the top of the sand layer, over which porous stones are placed. (Figure 4.23). After the prescribed days of curing, geopolymer-treated soil specimens are placed for capillary soaking on the porous stones for a period of 24 hours. The specimens are wrapped in absorptive paper that is constantly maintained to be moist throughout the 24-hour period. True capillary action was sustained by ensuring that while the water level reaches the middle of the porous stone, the soil specimen was never in direct contact with the water. A hollow PVC pipe was placed in the middle of the container to effectively monitor the water level at all times. The container was secured with a lid to maintain a stable environment during testing. The dimensions and mass of the soil specimen are recorded just before and after the 24-hour period, after which it is subjected to UCS

testing. Variations in mass and diameter of specimen due to ingress of water is analyzed to study the effects of geopolymer treatment on the soil's ability to absorb water.

Figure 4.23: Modified durability test setup using capillary soaking

### *4.4.6 Modified leachability test*

The leachability of a soil specimen is the ability of percolating water to leach out its soluble constituents. The volume of leachate produced in a certain time span provides insight into the presence of interconnected voids within the specimen, as larger void spaces presumably correspond to higher volumes of leachate produced (Chittoori et al. 2013). Leachability testing for this study is conducted using a modified leachate setup developed at UTA (Lad 2012). The schematic of the modified leachate setup in plan view and elevation view are shown

in Figures 4.24 and 4.25, respectively. The leachate setup consists of a transparent PVC casing with approximate diameter and height of 4 inches (101.6 mm) and 5 feet (1.524 m), respectively, secured into an 8 inches by 8 inches (203.2 mm x 203.2 mm) square PVC block. The PVC block encloses an elevated circular base pedestal with an approximate diameter of 2.8 inches (71.12 mm), on which two holes are drilled leading through to the PVC block and finally into a leachate outlet spout. Care was taken to ensure that no water was leaking from the system by sealing the casing threads.

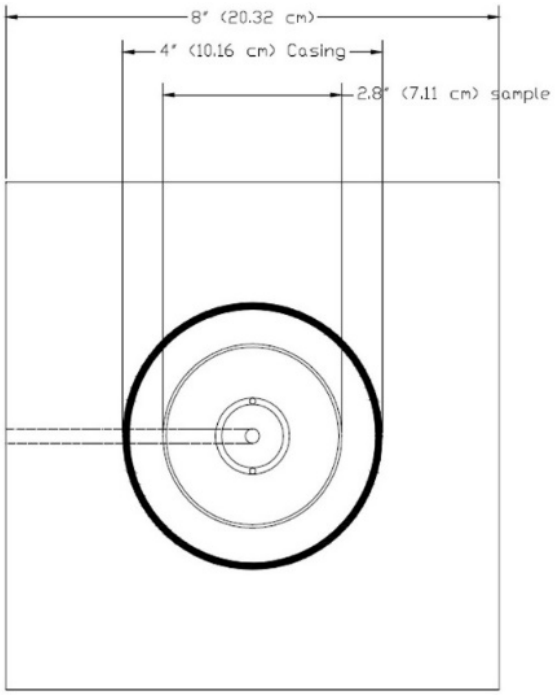


Figure 4.24: Schematic of modified leachate setup - plan view (Lad 2012)

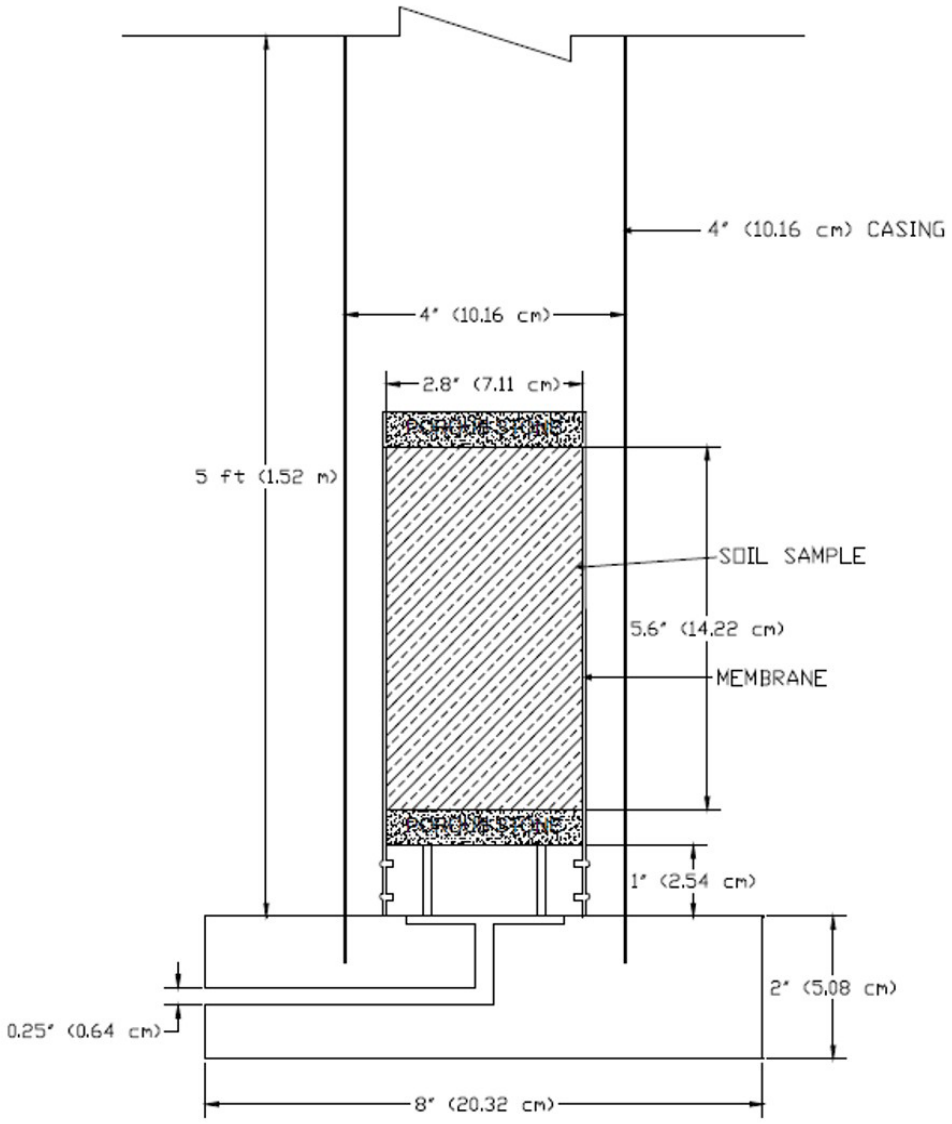


Figure 4.25: Schematic of modified leachate setup - elevation view (Lad 2012)

Porous stones and filter paper were placed on the top and bottom of the compacted specimen, which was then covered with a latex membrane and placed on the base pedestal. The latex membrane was secured to the base pedestal and top cap using O-rings to ensure that water percolates through the specimens only from

top to bottom. Once the PVC casing was threaded into the PVC block and sealed, water was poured into the casing from the top to maintain a hydrostatic pressure of 4 feet (1.2 m) of water (Figure 4.26). The leachate was collected through the outlet spout at the base until a period of five hours. The volume of leachate collected was recorded for each specimen. Subsequently, the potassium concentration in the leachate was determined using the Hach DR-2800 spectrophotometer by the tetraphenylborate method (Hach 8049). Both control soils were treated with the lowest and highest geopolymer dosages, cured for 7 and 28 days before being subject to leachate testing in this study.

Figure 4.26: Modified leachability test setup

## 4.5 Geopolymer treatment of expansive soils

A metakaolin-based geopolymer treatment was applied to both control soils obtained for the study. The K431 geopolymer, was synthesized in-house by combining metakaolin with the K431 AAS in predetermined amounts to treat expansive soils. The K431 AAS was prepared by combining potassium hydroxide, silica fume, and deionized water in specific proportions to yield ratios of $[SiO_2:Al_2O_3] = 4$, $[H_2O:(Al_2O_3+SiO_2)] = 3$, and $[K_2O:Al_2O_3] = 1$, as detailed in Chapter 3. Henceforth, the K431 GP will be referred to simply as 'geopolymer' or 'GP' in this study.

### *4.5.1 Dosages*

The geopolymer dosages in this study are presented as the percentage weight of metakaolin in the geopolymer, with respect to the dry weight of soil to be treated. Three dosages of 4%, 10%, and 15% metakaolin (MK) were applied to soils in this study. As such, a 4% dosage denotes that the amount of metakaolin in the geopolymer equals 4% of weight of dry soil, as shown in Table 4.5. Given 100 grams of dry soil, 4 grams of metakaolin and 6.5 grams of K431 AAS are required to apply a 4% dosage to the given soil. The 4%, 10% and 15% dosages translate to about 13%, 32%, and 47% of total geopolymer to dry soil, respectively, as shown in Table 4.6. Additional water is added as needed to the soil-geopolymer mix to bring the final moisture to its OMC. These dosages were chosen for this study, to

make sure a wide range of dosages were covered for an enhanced understanding of geopolymer-treated soils.

Table 4.5: Geopolymer dosage for soil treatment w.r.t. MK content.

| | **Dosage (% MK to dry wt. soil)** | **Dry mass of soil (g)** | **Mass of MK (g)** | **Mass of K431 AAS (g)** |
|---|---|---|---|---|
| ***Dosage 1*** | 4% | 100 | 4 | 6.5 |
| ***Dosage 2*** | 10% | 100 | 10 | 16.3 |
| ***Dosage 3*** | 15% | 100 | 15 | 24.5 |

Table 4.6: Geopolymer dosage w.r.t. mix ingredients

| **GP Mix Ingredient** | **% to dry weight of soil** | | |
|---|---|---|---|
| | ***Dosage 1*** | ***Dosage 2*** | ***Dosage 3*** |
| MK | 4% | 10% | 15% |
| K431 AAS | 6.5% | 16.3% | 24.5% |
| MK + K431 AAS | 10.5% | 26.4% | 39.5% |
| GP solids | 8% | 20% | 30% |
| Total GP | 12.7% | 31.7% | 47.5% |

### *4.5.2 Specimen Preparation and Testing*

The soils were initially oven-dried, crushed and then pulverized before being treated with geopolymer. The geopolymer slurry is prepared by combining metakaolin and K431 AAS in the required proportions determined by the mass of dry soil to be treated and the dosage needed. The geopolymer slurry is manually combined with dry soil to make sure they are well mixed (Figure 4.27), after which additional water is added as needed to bring the moisture of the soil-geopolymer

mix to its OMC. Once the geopolymer slurry is prepared, it is mixed with soil without delay and molded to form test specimens to ensure no moisture loss occurs.

Figure 4.27: Process of mixing geopolymer slurry with soil to make test specimen

Geopolymer-treated soils were statically compacted at the OMC of respective soil-geopolymer mixtures and 95% of its MDD. Molded test specimens were placed for curing in a moisture room at 100% RH for the prescribed curing periods. Subsequently, the specimens were subjected to different engineering characterization tests to determine the effects of geopolymer treatment. The different parameters tested for engineering characteristics of both geopolymer-treated soils in this study are given in Table 4.7.

Table 4.7: Engineering test variables for geopolymer-treated soils

| **Test performed** | **Dosage** | **Curing Periods (days)** |
|---|---|---|
| UCS | 4%, 10%, 15% | 0, 7, 28 |
| RLT | 4%, 10%, 15% | 7, 28 |
| 1-D Swell | 4%, 10%, 15% | 0, 3, 7 |
| Linear shrinkage | 4%, 10%, 15% | 0, 3, 7 |
| Modified Durability | 4%, 10%, 15% | 0, 3, 7, 14, 28 |
| Modified Leachability | 4%, 15% | 7, 28 |

## 4.6 Lime Treatment of Expansive Soils

Lime is the most common method of stabilization for expansive soils. In this study, geopolymers are proposed as an alternative to traditional soil stabilizers like lime. As such, the control soils were treated with lime to correlate the effects of lime-treated soils with that of geopolymer-treated soils. As part of lime treatment of soils, it is important to determine the appropriate dosage of lime needed for each control soil, which is described in detail in the following sections.

### *4.6.1 Soluble Sulfate Determination*

Determination of soluble sulfate in soils is of paramount importance when discussing lime treatment of soils. The calcium in lime is known to react with soil sulfates to form the highly expansive mineral ettringite, which is capable of expanding to about 140% of its original volume (Talluri et al. 2013, Puppala et al. 2018b). Ettringite formation in lime-treated soils results in extensive sulfate heave, which could negate the purpose of lime treatment of expansive soils. As such, it is necessary to determine the soluble sulfate concentration in expansive soils to choose the right plan of action for stabilization treatment. Threshold sulfate levels in sulfate-bearing clays used as reference for this study and its associated risk due to lime stabilization are given in Table 4.8; although the Texas Department of Transportation (TxDOT) recommends a safety limit of 0.2 percent by mass as a threshold separating a safe acceptable risk from low to moderate risk (Little and Nair 2009b).

Table 4.8: Threshold sulfate levels and associated risk of lime treatment in sulfate-bearing clays (Little and Nair 2009b)

| Risk Level | Soluble Sulfate Concentration | |
|---|---|---|
| | Parts per million | Percent dry weight |
| Low Risk | < 3,000 | < 0.3 % |
| Moderate Risk | 3,000 – 5,000 | 0.3 – 0.5% |
| Moderate to High Risk | 5,000 – 8,000 | 0.5 – 0.8% |
| High to unacceptable Risk | > 8,000 | > 0.8 % |
| Unacceptable Risk | > 10,000 | > 1.0% |

Soluble sulfate determination in this study was conducted using the colorimetric method in accordance with TEX 145-E, using a Thermo Scientific Orion AQUAfast AQ3700 colorimetry meter (Figure 4.28). The colorimetry meter uses the turbidimetric technique wherein the cloudiness of a liquid is converted into a concentration, based on the degree of absorbance of a specific wavelength of transmitted light. A sulfate test tablet is used as the reagent in this method to cause turbidity in the solution.

An initial dilution ratio of 1:20 was obtained for the test by mixing a representative soil specimen passing the No. 40 sieve with 400 ml of distilled water in a high-density polyethylene (HDPE) bottle. The colorimetry meter reading was multiplied with the dilution ratio to obtain the sulfate concentration in parts per million (ppm). If the test yielded a sulfate reading exceeding the equipment limit using the 1:20 dilution ratio, the test was redone using higher dilution ratios.


Figure 4.28: Thermo Scientific colorimetry meter used for sulfate testing

Soluble sulfate testing was performed on both control soils and the low-plasticity Alvarado soil was found to have sulfate levels below 100 ppm, while the high-plasticity Lewisville soil was found to have a sulfate level of 7,000 ppm. According to Table 4.8, the Lewisville soil places in the 'moderate to high risk' zone, while the Alvarado soil has 'low risk'. According to the NCHRP document 145, sulfate-bearing soils in the moderate to high-risk zone can be stabilized using the modified treatment technique, wherein an extended mellowing period using lime is recommended along with the application of at least 3 percent above OMC during mixing (Little and Nair 2009b). The extent of the mellowing period as well as the moisture content required during the process is usually determined using the mix design process (Talluri et al. 2013). Several soil-lime mixtures at different

moisture contents were tested for sulfate concentration at different mellowing periods, to determine the appropriate moisture content and mellowing period.

### *4.6.2 Lime Dosage Determination*

The lime dosage rates needed for the control soils were determined using the Eades and Grim pH test as per TEX 121-E. According to this method, a soil-lime pH of 12.4 is required to sustain pozzolanic reactions that result in cementitious products (Eades and Grim 1966). The lowest percentage of lime that gives a pH of 12.4 is the minimum percentage of lime required to stabilize the soil.

For this test, about 30 gm of dry soil passing the 425-um (No. 40) sieve is placed in six HDPE bottles. Six different dosages of lime are added to each of the six bottles at 0, 2, 4, 6, 8, and 10% of dry weight of soil. Subsequently, 150 ml of water is added to each of the containers and mixed thoroughly. The bottles are stirred every 15 minutes for up to an hour, after which the pH of its supernatant is recorded. The lime dosage and pH are plotted to obtain the lowest dosage rate with a pH of 12.4 (Figure 4.29). Table 4.9 shows the lime dosage used for treatment of the control soils in this study.

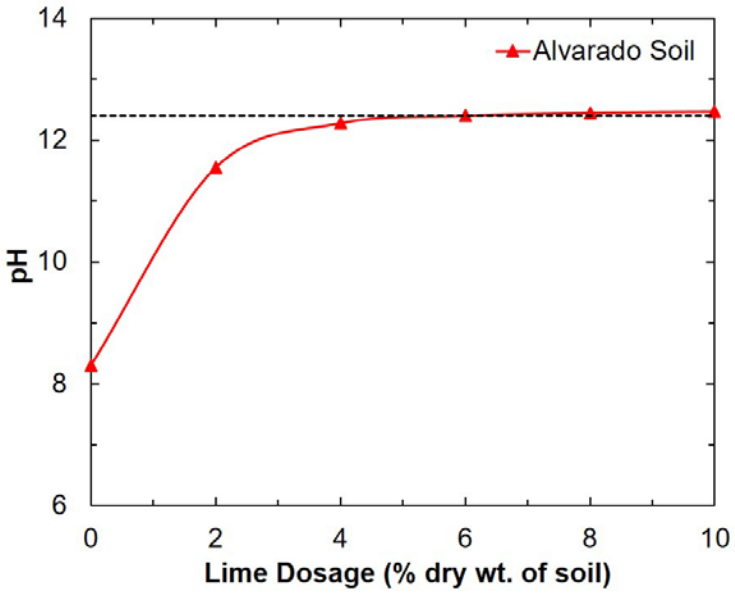


(a)

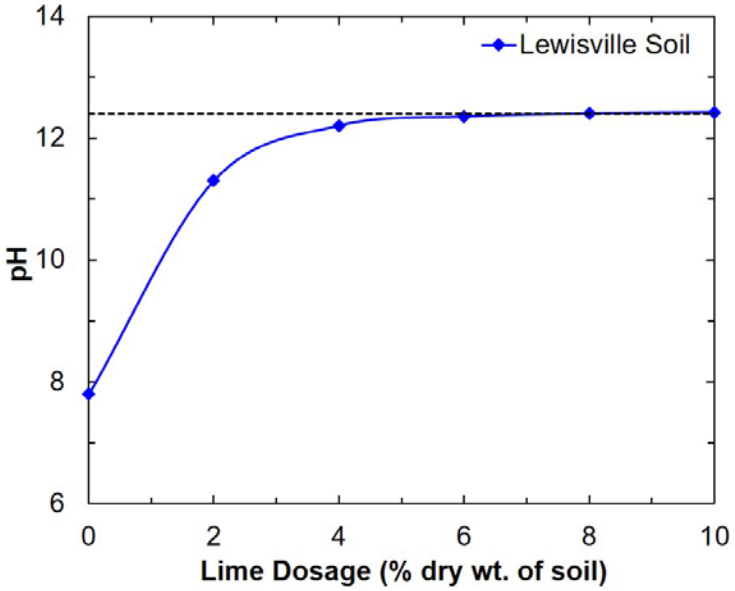


(b)

Figure 4.29: Variation of pH with time after lime treatment for (a) Alvarado soil, and (b) Lewisville soil

### *4.6.3 Specimen Preparation and Testing*

As part of this comparative analysis, lime-treated soils were subjected to UCS, 1-D swell, and modified durability testing. Moisture content – dry density relationship curves of lime-treated soils were determined using Harvard miniature compaction to obtain OMC and MDD. All lime-treated soil specimens were statically compacted at the OMC of the respective soil-lime mixtures and to 95% of its MDD. The high-plasticity Lewisville soil was mellowed for a period of 7 days at 5% above its OMC, before being cured and molded to form test specimens, due to its high sulfate content. UCS and modified durability soil specimens were molded to cylinders of approximate diameter and height of 1.31 inches (33.3 mm) and 2.85 inches (72.4 mm), respectively, while 1-D swell specimens were molded to form specimens with diameter and height of 2.5 inches (63.5 m) and 1.13 inches (28.7 mm), respectively. Molded test specimens were placed for curing in a moisture room at 100% RH for the prescribed curing periods. The parameters tested for comparing engineering characteristics of both lime-treated soils in this study are given in Table 4.9.

Table 4.9: Engineering test variables for lime-treated soils

| **Soil type and Dosage** | **Test** | **Curing Periods (days)** |
|---|---|---|
| Alvarado soil (CL): 6%<br>Lewisville soil (CH): 8% | UCS | 0, 7, 28 |
| | 1-D Swell | 0, 3, 7 |
| | Modified Durability | 0, 3, 7, 14, 28 |

The engineering properties of lime-treated soils are compared with those of geopolymer-treated soils, to provide a reasonable justification for the use of geopolymer as an alternative sole binder for stabilizing expansive soils.

## 4.7 Summary

The experimental methodology followed for analyzing the effects of metakaolin-based geopolymer treatment on two expansive soils from North Texas were presented in detail in this chapter. A series of soil characterization tests were initially conducted to classify the control soils obtained. In addition to basic geotechnical characterization tests, chemical and microstructural tests were also conducted to characterize soils. Subsequently, a series of engineering characterization tests were conducted to evaluate the effects of varying geopolymer treatments on the engineering properties of soils. The engineering tests performed focused on the strength and stiffness, volume change, and long-term performance of geopolymer-treated soils. Moreover, control soils were also subjected to lime treatment so as to compare some of their engineering properties with those of geopolymer-treated soils. The results of the test procedures described in this chapter are presented in detail in the next few chapters that follow.

# CHAPTER 5

# EFFECT OF GEOPOLYMER TREATMENT ON GEOTECHNICAL PROPERTIES OF EXPANSIVE SOILS

## 5.1 Introduction

The performance of a metakaolin-based geopolymer as the sole stabilizer of expansive clays, was analyzed using the different test methodologies detailed in Chapter 4. Two expansive soils from the North Texas area were treated with the K431 GP at three different dosages (4%, 10%, and 15% MK). This chapter presents the results of the basic and engineering tests performed on control and geopolymer-treated soils, to analyze the modifications in their geotechnical properties to evaluate the effectiveness of geopolymer as the sole stabilizer for the tested expansive soils. Additionally, some engineering test results performed on lime-treated soils are also presented to analyze comparative effectiveness of the geopolymer and lime as sole stabilizers.

## 5.2 Basic and Chemical Tests

Control soils and geopolymer-treated soils were tested for moisture content – dry density relationship, Atterberg limits and pH test at different dosages.

### *5.2.1 Moisture content – dry density relationship test*

Moisture content – dry density relationship curves were determined for both control soils and geopolymer-treated soils at the specific dosages, and are presented in Figure 5.1. These curves provided the OMC and MDD of the geopolymer-treated

soils for each dosage, which are of utmost importance for specimen preparation for all further testing procedures. Specimens for all tests were molded at the OMC and to 95% of the MDD for the specific dosage for the particular soil type. The high-plasticity Lewisville soil (CH) has higher OMC and lower MDD than the low-plasticity Alvarado soil (CL), which is expected. For both expansive soils, the lowest geopolymer dosage of 4% MK resulted in a higher OMC and lower MDD than the control soils.

The mixing of the geopolymer slurry with the soils causes agglomeration and flocculation of soil particles, resulting in a geopolymer-soil mixture with reduced dry density and higher water holding capacity than the control soil. Interestingly, the intermediate and highest geopolymer dosages reverse this trend by lowering the OMC and increasing the MDD compared to that of the lowest geopolymer dosage. The increased geopolymer dosages are observed to significantly reduce the water holding capacity of the soils, due to chemical or morphological changes in the mixture, thereby lowering the OMC of the soil-geopolymer mix. This is one of the primary objectives of stabilizing high PI soils, where the OMC reduces and the MDD increases.

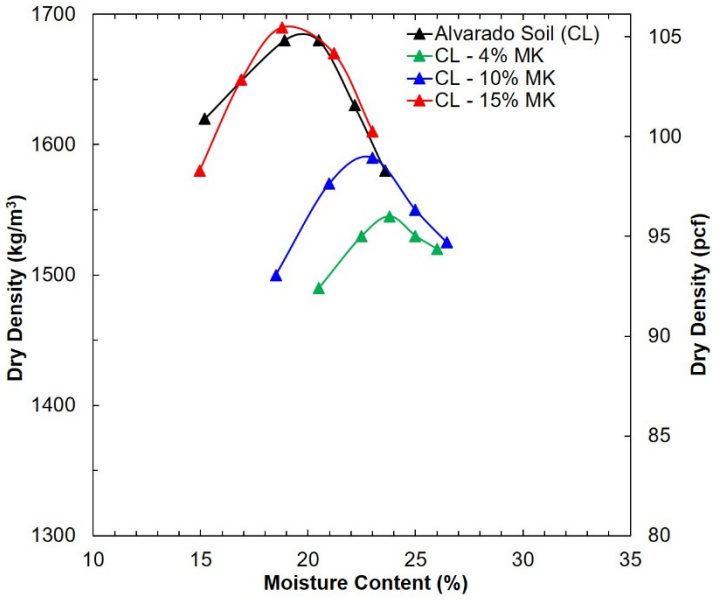


(a)

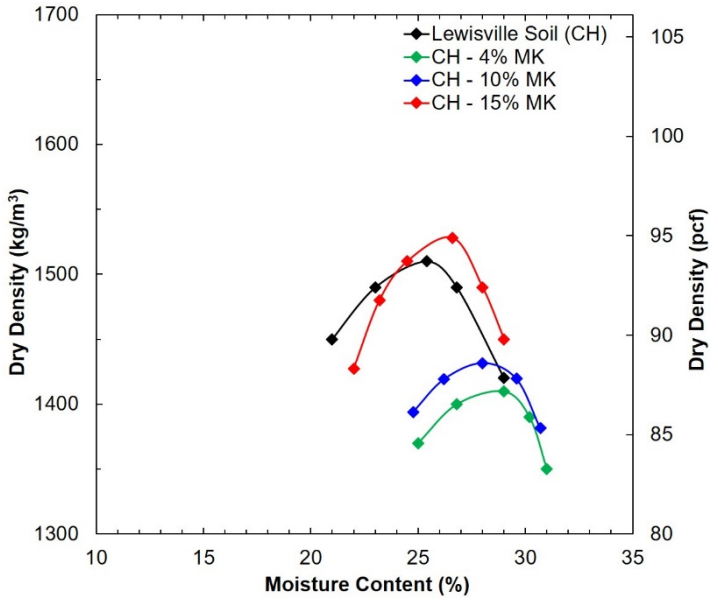


(b)

Figure 5.1: Moisture content – dry density relationship curves for control and geopolymer-treated soils: (a) Alvarado soil (CL), (b) Lewisville soil (CH)

### *5.2.2 Atterberg limit test*

The Atterberg limits (LL, PL, and PI) provide insight into the water holding capacity and swell potential of soils. As such, variation in Atterberg limits were monitored for control soils and soils treated with each geopolymer dosage after a curing period of 0 (2 hours), and 7 days (see Table 5.1). Figure 5.2 shows the variation of PI for both soils at the different dosages and curing periods. After 28 days of curing, the soils were observed to lose its plasticity and hence were described as non-plastic soils.

Geopolymer treatment was found to significantly reduce the plasticity index of both expansive soils. The 4% MK dosage was found to be effective in reducing the PI of CL below 15% after a curing period of a few hours, while the highest dosage of 15% MK was needed to reduce the PI of CH below 15%. A curing period of 7 days proved more effective in further reducing the PI of CH by about 20 to 35%, than in CL were no significant reduction was observed. The lowest dosage reduced the PI of CL and CH by about 50% and 40%, respectively, while the highest application reduced the PI of CL and CH by about 90% and 85%, respectively. The immediate reduction of PI is possibly due to a rapid cation exchange reaction occurring between the geopolymer and clay particles. The need for higher dosage and curing time needed for reduction of PI in CH can be attributed to the higher montmorillonite content in CH than CL.

Table 5.1: Variation of Atterberg limits for control soils and GP-treated soils

| **Alvarado soil - CL** | | | | | | |
|---|---|---|---|---|---|---|
| *Dosage (%MK to dry soil)* | *0 day cured* | | | *7 day cured* | | |
| | *LL (%)* | *PL (%)* | *PI (%)* | *LL (%)* | *PL (%)* | *PI (%)* |
| 0% (Control soil) | 40 | 16 | 25 | 40 | 16 | 25 |
| 4% | 36 | 23 | 13 | 33 | 22 | 12 |
| 10% | 33 | 27 | 7 | 31 | 25 | 6 |
| 15% | 33 | 28 | 5 | 30 | 27 | 4 |
| **Lewisville soil - CH** | | | | | | |
| *Dosage (%MK to dry soil)* | *0 day cured* | | | *7 day cured* | | |
| | *LL (%)* | *PL (%)* | *PI (%)* | *LL (%)* | *PL (%)* | *PI (%)* |
| 0% (Control soil) | 80 | 27 | 53 | 80 | 27 | 53 |
| 4% | 74 | 30 | 44 | 55 | 24 | 31 |
| 10% | 50 | 28 | 22 | 43 | 26 | 17 |
| 15% | 41 | 27 | 14 | 37 | 28 | 9 |

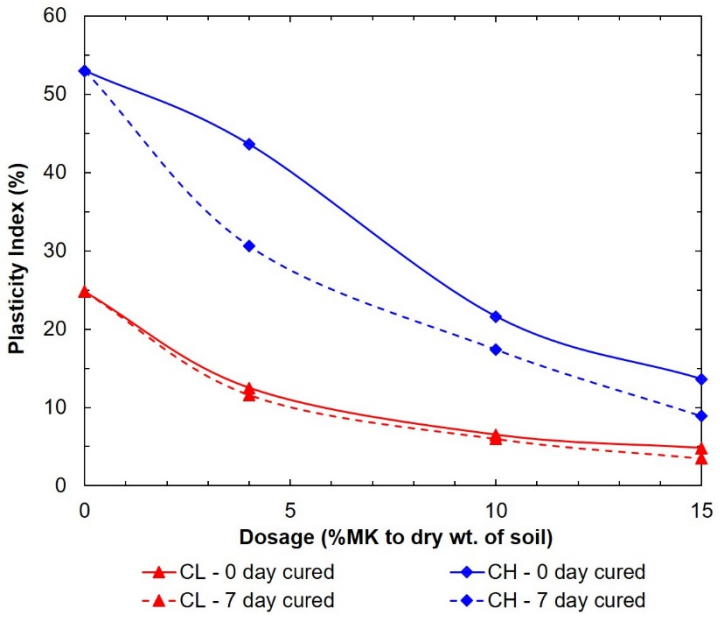


Figure 5.2: Variation of PI for two expansive soils at different GP dosages and curing periods

### *5.2.3 pH test*

It is known that a high alkaline environment is necessary to activate the reactive alumina and silica of the raw materials to form geopolymers. The K431 AAS used in this study was found to have a pH of about 13.5, thereby establishing the high alkaline reaction setting. The control soils were tested for their initial pH as per ASTM D4972-19 and was found to be about 8 and 7.5 for CL and CH, respectively. The change in pH of the soil-GP mixture is an indicator of a progressive chemical reaction, in addition to giving insight into the environmental impact of the geopolymer on soil. The variation in pH was monitored for geopolymer-treated soils at the different dosages after a curing period of 0 (2 hours), 7, 14, 21 and 28 days, and is presented in Figure 5.3.

A modest reduction in pH, in the range of about 6 to 9%, was observed in all geopolymer-treated soils over the course of the 28-day curing period, corroborating a progressive chemical reaction. The lowest dosage had the lowest initial pH in both soils and vice versa. The lowest dosage required for maximum percentage reduction of pH was observed to be 4% MK and 10% MK for CL and CH, respectively. The final pH values are observed to be lower for GP treated CH (between 9.5 and 12), than GP treated CL (between 11 and 12.5).

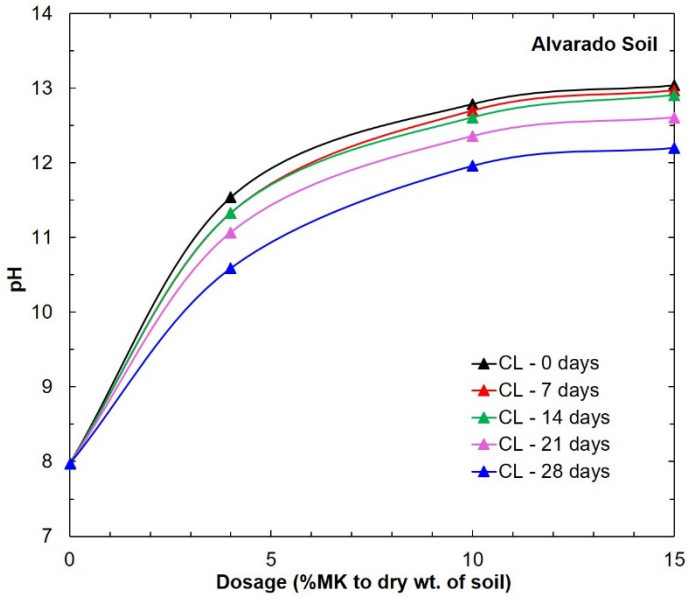


(a)

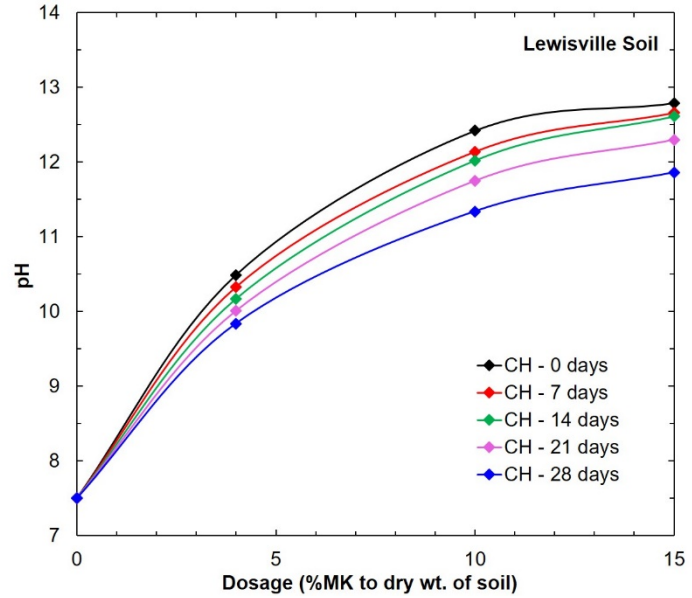


(b)

Figure 5.3: Variation of pH for control and GP-treated soils at different curing periods. (a) Alvarado soil (CL), (b) Lewisville soil (CH)

## 4.1 Engineering Tests

Control soils and geopolymer-treated soils were tested for UCS, $M_R$, 1-D swell, linear shrinkage, modified durability, and modified leachability characteristics. These results are presented in the sections to follow.

### *5.2.4 UCS*

UCS tests were performed on control and geopolymer-treated soils as per ASTM D2166-16, for three geopolymer dosages (4%, 10%, and 15% MK) after curing periods of 0 (2 hours), 7, and 28 days. All UCS specimens were of the miniature dimension, compacted at 95% of their respective MDDs and OMCs and cured in air-tight chambers with no moisture-loss at 100% RH. The UCS tests were conducted at a strain rate of 0.03 in/min (0.762 mm/min), so as to negate the influence of the different shearing rate on the peak stress. Triplicate specimens were prepared for each soil type, dosage, and curing period to ensure reliability of data. The results presented here are the average values of the triplicate specimens, with a coefficient of variation less than 20%.

UCS test results for low-plasticity Alvarado soil (CL) and high-plasticity Lewisville soil (CH) are presented in Figures 5.4 and 5.5, respectively. GP treatment was observed to cause significant strength improvement in both CL and CH. The CL control soil specimens were found to have UCS value of around 15 psi, which upon the treatment with the lowest dosage (4% MK) increased to about 45 psi after 28 days of curing, which is about a 200% increase in its UCS value

compared to the control CL. Similarly, the 10% and 15% MK dosages increased the UCS of CL by about 375% and 770%, respectively, after a curing period of 28 days. The 375% increase in UCS of the control CL equates to an increase in just over 55 psi. According to ASTM D4609-94, an increase in UCS of 50 psi or more is suggested for a chemical treatment to be considered effective.

The CH control soil specimens were found to have UCS value of around 20 psi, which upon treatment with the 4% MK dosage resulted in a 100% increase in UCS after 28 days of curing. The 10% and 15% MK dosages increased the UCS of control CH by about 225% and 520%, respectively, after a curing period of 28 days.

For both CL and CH, immediate strength gain was observed within a few hours of the geopolymer treatment, except for the highest geopolymer dosage. The highest dosage was found to have OMC and MDD quite similar to that of its respective control soils, which explains the similar values of strength for control soils and soils treated with 15% MK. As such, significant strength increase is not attained until after a curing period of 7 days for soils treated with 15% MK. It was observed that for the lowest dosage (4% MK), strength increase is almost immediate, while for the higher dosages, the highest UCS was observed after 28 days of curing. As such, increased curing days did not significantly boost the UCS of soils treated with 4% MK. Overall, UCS values are observed to be higher for geopolymer-treated CL than CH.

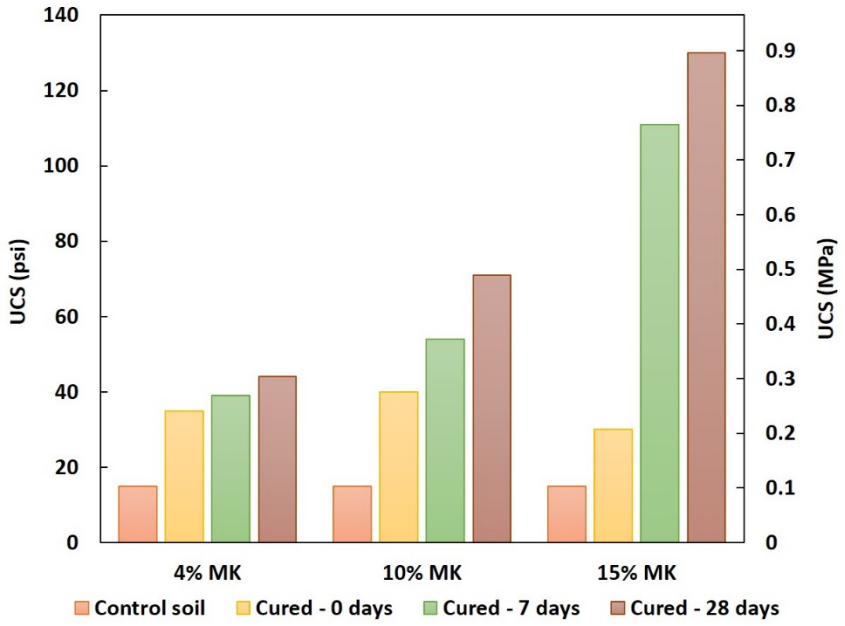


Figure 5.4: Effect of GP treatment on UCS of Alvarado soil (CL)

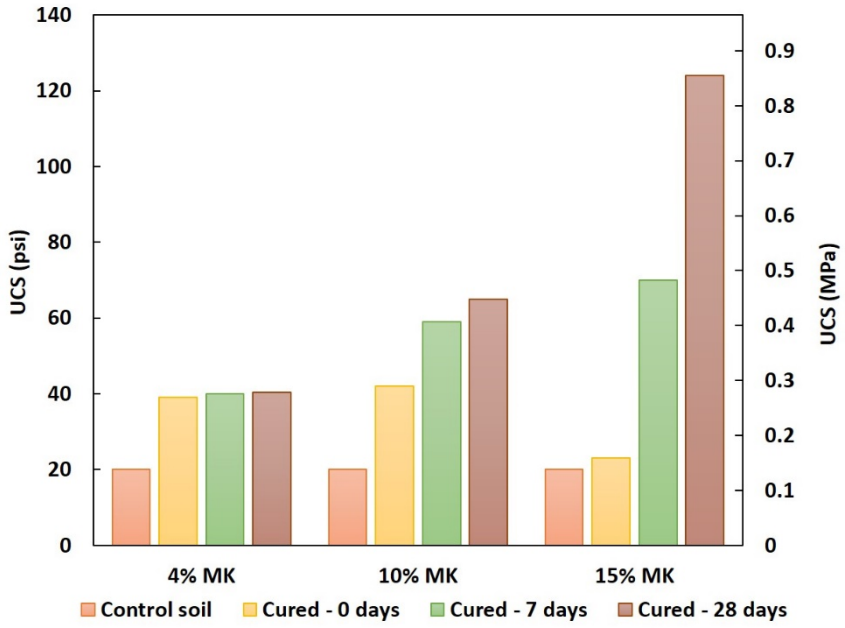


Figure 5.5: Effect of GP treatment on UCS of Lewisville soil (CH)

### *5.2.5 Resilient Modulus*

The resilient modulus of control and geopolymer-treated soils were obtained by performing a series of repeated load triaxial tests as per AASHTO T307, for three geopolymer dosages (4%, 10%, and 15% MK) after curing periods of 7 and 28 days. All $M_R$ specimens were of the larger dimension, compacted at 95% of their respective MDDs and OMCs and cured in air-tight chambers with no moisture-loss at 100% RH. $M_R$ values for low-plasticity Alvarado soil (CL) and high-plasticity Lewisville soil (CH) are presented in Figures 5.6 and 5.7, respectively. Figures 5.6 and 5.7 show $M_R$ results from test sequence 7 with applied confining pressure and maximum deviator stress of 4 psi (27.6 kPa) each, as it represents intermediate stresses that most closely simulate real-world traffic loading, among the 15 test sequences.

Geopolymer treatment was observed to cause significant improvement in $M_R$ of both CL and CH. Overall $M_R$ was observed to increase with increasing net confining pressure and deviator stress, as well as increasing geopolymer dosage and curing period. For the specific test sequence results presented here, the dosages of 4%, 10%, and 15% MK resulted in an increase in $M_R$ of CL control soil by about 12%, 45%, and 430%, respectively, after a curing period of 28 days. Similarly, the 4%, 10%, and 15% MK dosages increase the $M_R$ of control CH by about 45%, 100%, and 120%, respectively, after a curing period of 28 days. While the 15% MK dosage in CL provided the highest $M_R$ value of about 23.2 ksi (160 MPa), the 4%

and 10% MK dosages resulted in only low to moderate increase in $M_R$ values from that of control CL. Geopolymer treatment of CH showed more consistent increase with respect to dosages and curing periods.

For both CL and CH, the highest $M_R$ values were obtained for the highest geopolymer dosage after the 28 day curing period. Increased curing periods of 28 days did not significantly boost the $M_R$ for most geopolymer-treated soils except for CL treated with 15% MK dosage. The highest geopolymer dosage was found to have much lower OMC and higher MDD than other dosages, which explains the high $M_R$ values associated with high geopolymer dosages. Overall, $M_R$ values were observed to be higher for CH at dosages of 4% and 10% MK, and for CL at dosage of 15% MK.

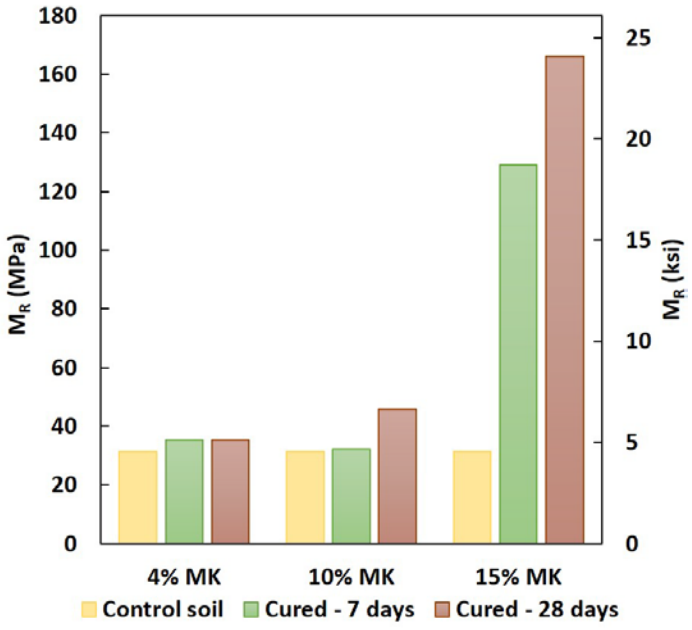


Figure 5.6: $M_R$ results for GP-treated Alvarado soil (CL) at Sequence 7

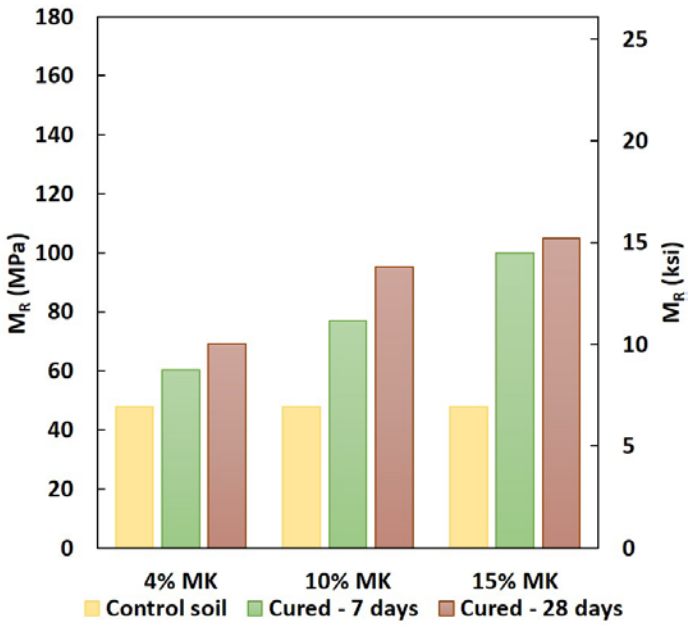


Figure 5.7: $M_R$ results for GP-treated Lewisville soil (CH) at Sequence 7

### *5.2.6 1-D swell*

1-D swell tests were performed on control and geopolymer-treated soils as per ASTM D4546-14e1, for three geopolymer dosages (4%, 10%, and 15% MK) after curing periods of 0 (2 hours), 3, and 7 days. All swell specimens were compacted at 95% of their respective MDDs and OMCs and cured in air-tight chambers with no moisture-loss at 100% RH. Triplicate specimens were prepared for each soil type, dosage, and curing period to ensure reliability of data. Swell test plots for low-plasticity Alvarado soil (CL) at 4%, 10%, and 15% MK dosages are presented in Figures 5.8, 5.9, and 5.10, respectively; while swell test plots for high-plasticity Lewisville soil (CH) at 4%, 10%, and 15% MK dosages are presented in

Figures 5.11, 5.12, and 5.13, respectively. Swell potential is equated to the percentage vertical swell strain in all figures.

Geopolymer treatment was observed to significantly reduce the swell potential of both expansive soils. CL control soil specimens with a moderate swell potential of about 3.5%, was reduced by about 95% with the lowest dosage (4% MK) after 7 days of curing. Similarly, CH control soil specimens with a very high swell potential of about 15%, was reduced by about 98% with the lowest dosage after 7 days of curing. Swell was observed to be negligible for both CL and CH treated with higher dosages of geopolymer.

For both CL and CH, immediate swell reduction was observed within a few hours of the geopolymer treatment. Significant percentage swell reduction in the range of 65% to 90% and 80% to 95% was observed in geopolymer-treated CL and CH, respectively, within 2 hours of curing for all geopolymer dosages. For both soils, maximum swell reduction occurs within a curing period of 3 days. It is possible that the immediate swell reduction is a result of rapid cation exchange of geopolymer with clay minerals, which reduces the water adsorption capacity of the clay minerals. The lowest geopolymer dosage is found to be sufficient in reducing the swell potential of both expansive soils by more than 95% within 3 days of curing.

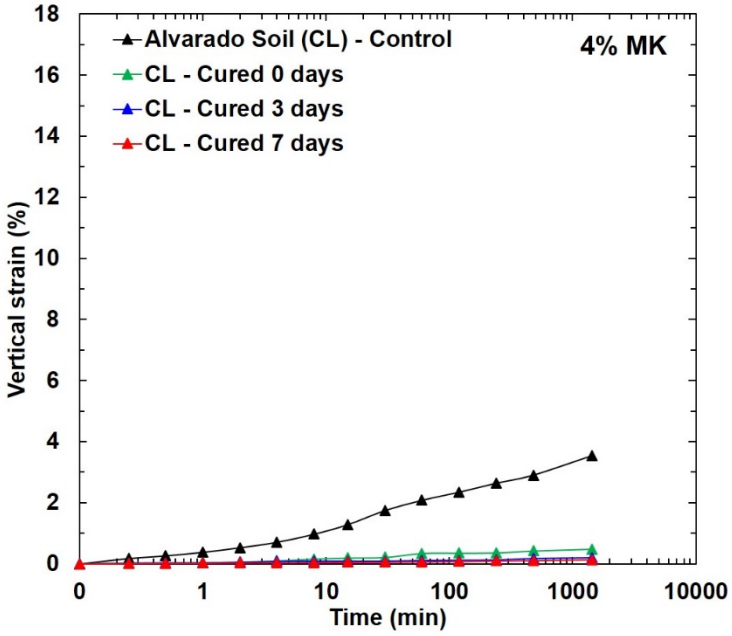


Figure 5.8: Swell potential of Alvarado soil at 4% MK dosage

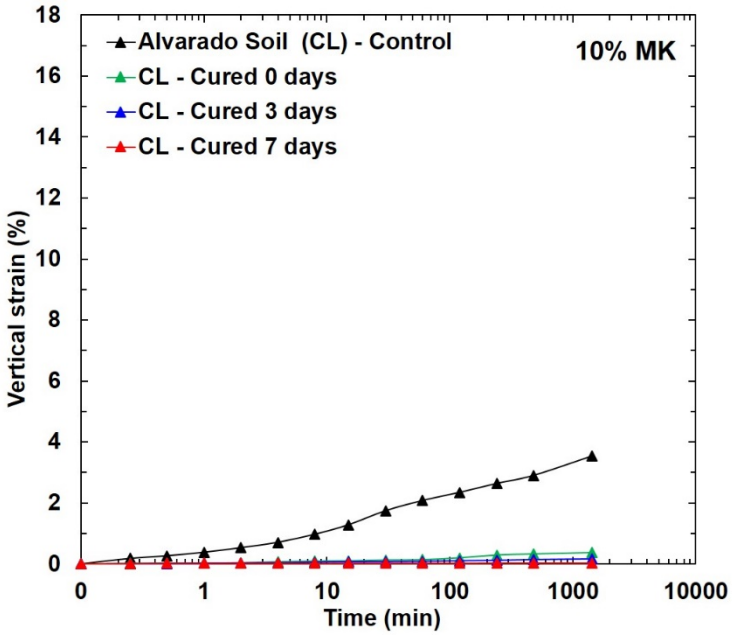


Figure 5.9: Swell potential of Alvarado soil at 10% MK dosage

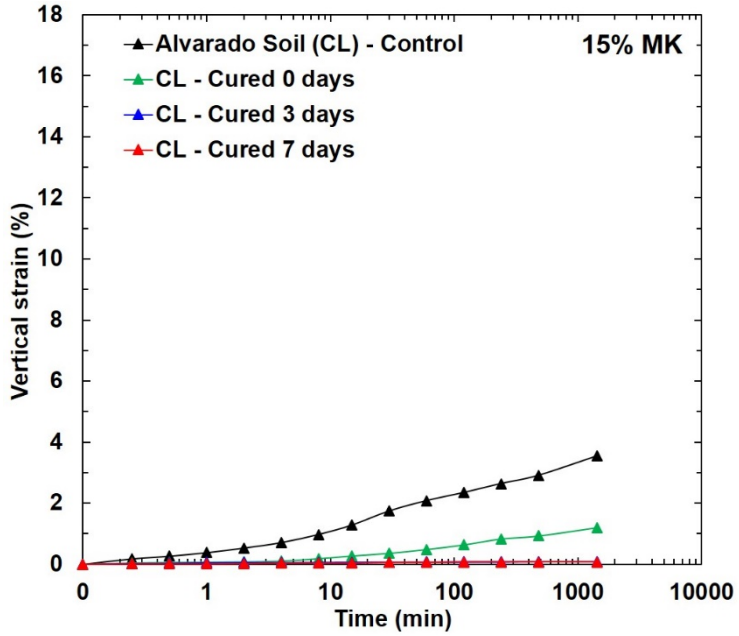


Figure 5.10: Swell potential of Alvarado soil at 15% MK dosage

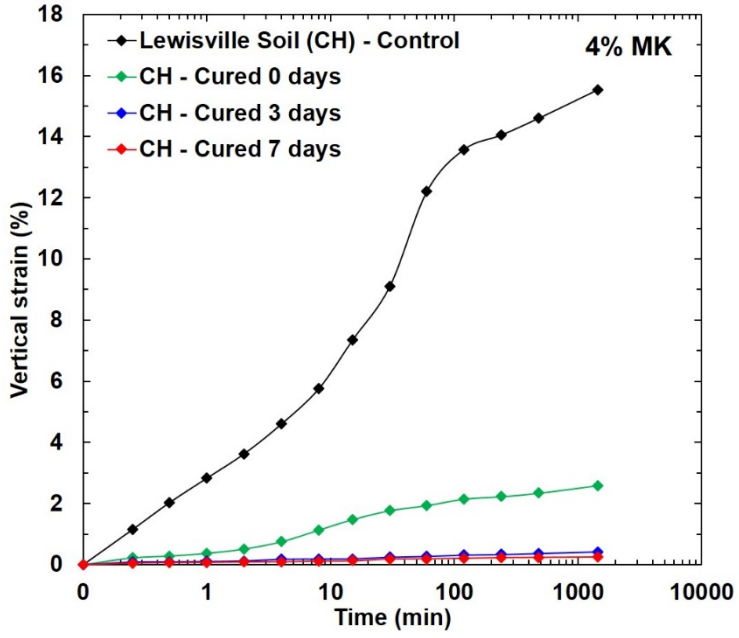


Figure 5.11: Swell potential of Lewisville soil at 4% MK dosage

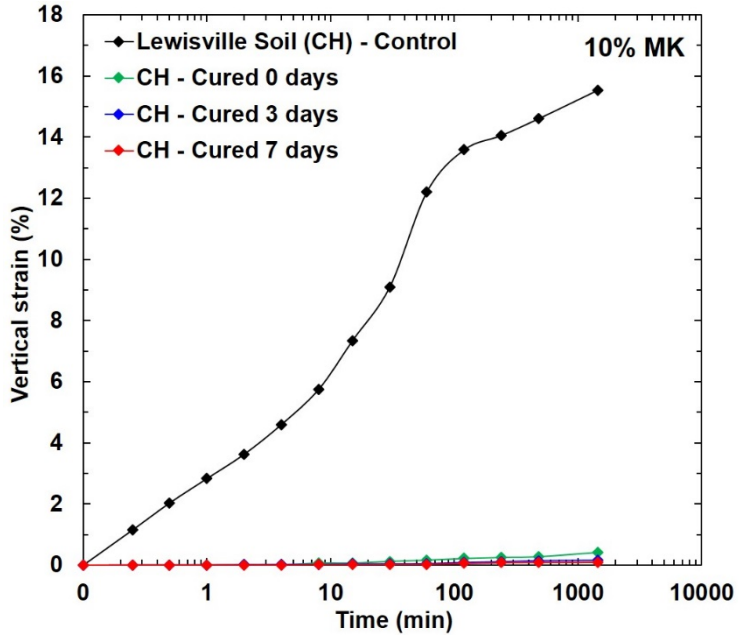


Figure 5.12: Swell potential of Lewisville soil at 10% MK dosage

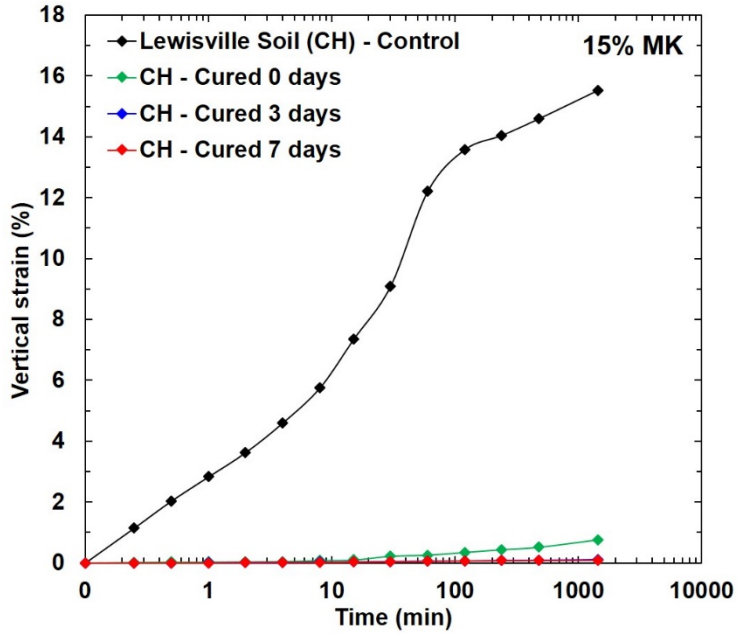


Figure 5.13: Swell potential of Lewisville soil at 15% MK dosage

### *5.2.7 Linear shrinkage*

Linear shrinkage tests were performed on control and geopolymer-treated soils as per TEX-107-E, for three geopolymer dosages (4%, 10%, and 15% MK) after curing periods of 0 (2 hours), 3, and 7 days. Triplicate specimens were prepared for each soil type, dosage, and curing period to ensure reliability of data. Shrinkage test results for low-plasticity Alvarado soil (CL) and high-plasticity Lewisville soil (CH) are presented in Figures 5.14 and 5.15, respectively, where shrinkage potential is represented as the percentage linear shrinkage.

Geopolymer treatment was observed to significantly reduce the shrinkage potential of both expansive soils. The CL control soil specimens with a shrinkage potential of about 16%, was reduced by about 65%, 66%, and 92% on being treated with dosages of 4%, 10%, and 15% MK, respectively after 3 days of curing. Similarly, the CH control soil specimens with a shrinkage potential of about 22%, were reduced by about 50%, 80%, and 88% on being treated with dosages of 4%, 10%, and 15% MK, respectively. An increase in geopolymer dosages and curing periods were observed to reduce the shrinkage potential of the expansive soils. Shrinkage potential of both soils were unable to be evaluated for the highest dosage after a curing period of 7 days, as it was observed to have become cohesionless.

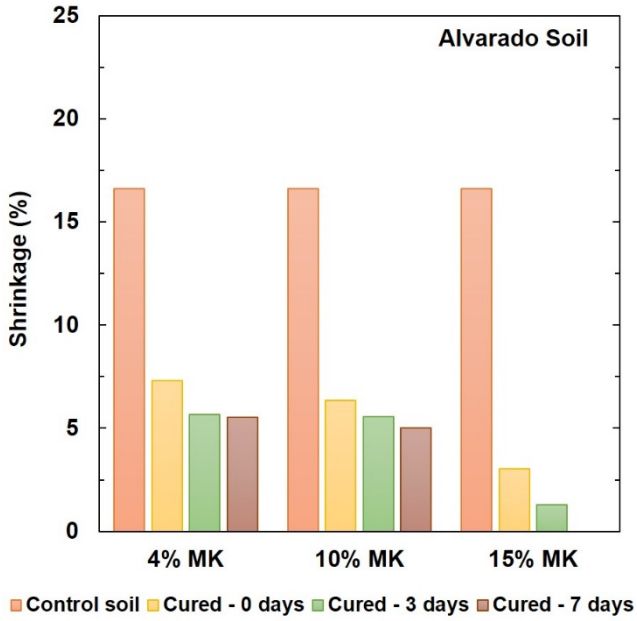


Figure 5.14: Shrinkage plot for control and GP-treated Alvarado soil

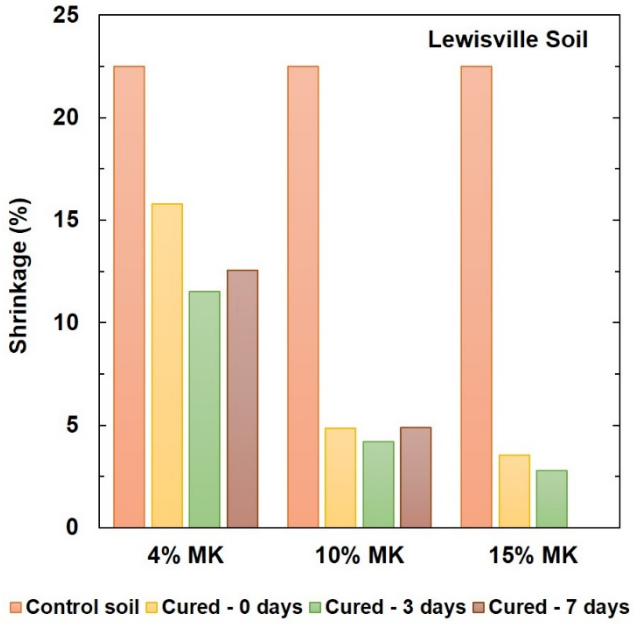


Figure 5.15: Shrinkage plot for control and GP-treated Lewisville soil

### *5.2.8 Modified Durability*

Modified durability testing was performed by capillary soaking method, wherein soil specimens were allowed to undergo capillary soaking for 24 hours as detailed in Chapter 4. These tests were conducted on control and geopolymer-treated soils for three geopolymer dosages (4%, 10%, and 15% MK) after curing periods of 0 (2 hours), 3, 7, 14, and 28 days. All modified durability specimens were compacted at 95% of their respective MDDs and OMCs; and were cured in air-tight chambers with no moisture-loss at 100% RH. Triplicate specimens were prepared for each soil type, dosage, and curing period to ensure reliability of data. The effect of ingress of water due to capillary soaking was determined by monitoring changes in UCS, mass, and volume of control and geopolymer-treated specimens.

Modified durability test results for low-plasticity Alvarado soil (CL) are presented in Figures 5.16, 5.17, 5.18, and 5.19, where changes in UCS, mass, and volume are presented with respect to different geopolymer dosages and curing periods. Some reduction in UCS values were observed for CL specimens after being subjected to durability testing. As expected, control CL underwent significant strength loss from 15 psi to 3 psi after modified durability testing in comparison to UCS before testing. Higher geopolymer dosages show lower reduction in UCS values as compared to those CL specimens not subjected durability testing. Final strength loss of same-day cured CL specimens before and after modified durability

testing was found to be 55%, 60%, and 15%, for geopolymer dosages of 4%, 10% and 15% MK, respectively.

Despite modified durability testing, UCS of geopolymer-treated CL were observed to increase with increasing geopolymer dosages and curing periods. In comparison to control CL subjected to modified durability testing, dosages of 4%, 10%, and 15% MK resulted in strength increase by about 6, 8, and 25 times, respectively, after 7 days of curing.

Control CL experienced considerable increase in mass and volume by about 7% and 2%, respectively, due to intake of water during modified durability testing. Significant reduction in mass and volume change by under 2% and 0.2%, respectively was observed for CL after only 7 days of curing. The lowest geopolymer dosage of 4% MK is observed to be sufficient to significantly reduce mass and volume change in Alvarado soil.

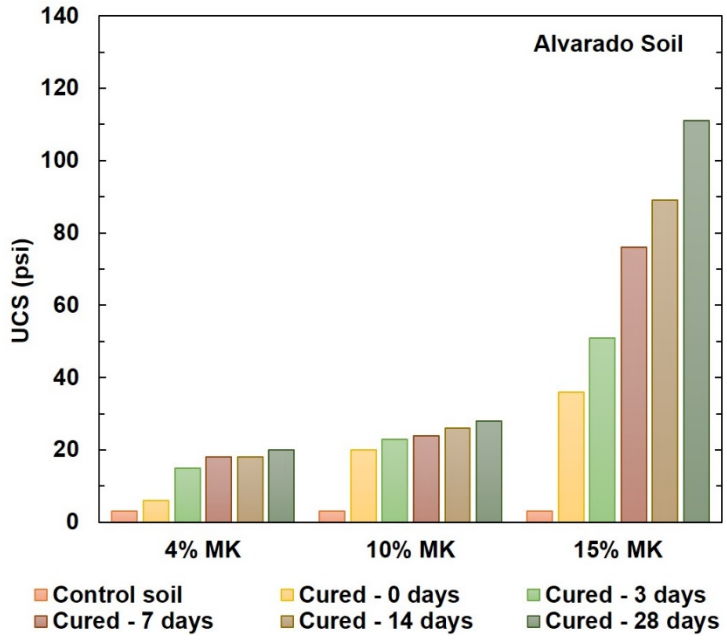


Figure 5.16: UCS of Alvarado soil after modified durability tests

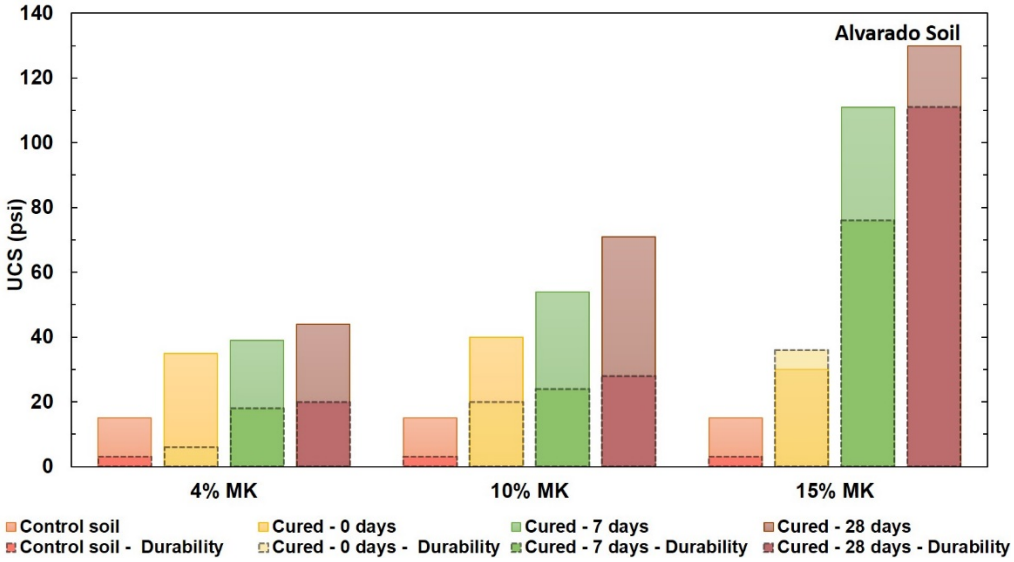


Figure 5.17: UCS of Alvarado soil before and after modified durability test

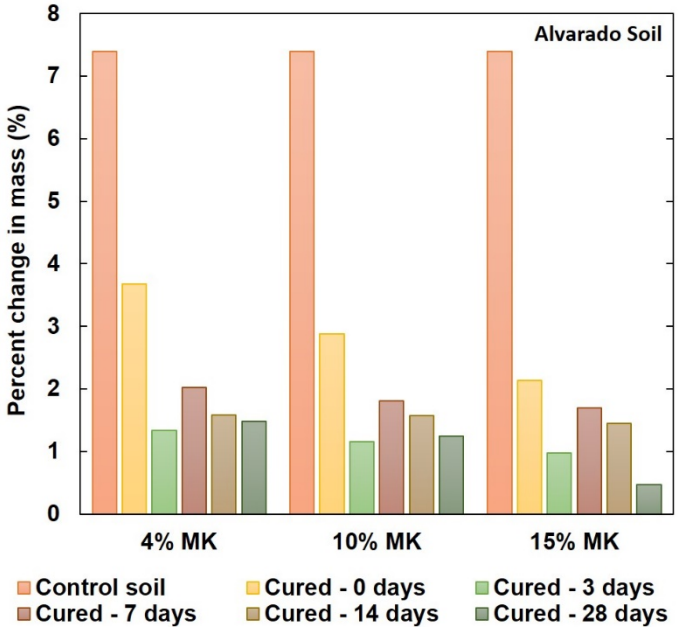


Figure 5.18: Effect of modified durability test on mass of Alvarado soil

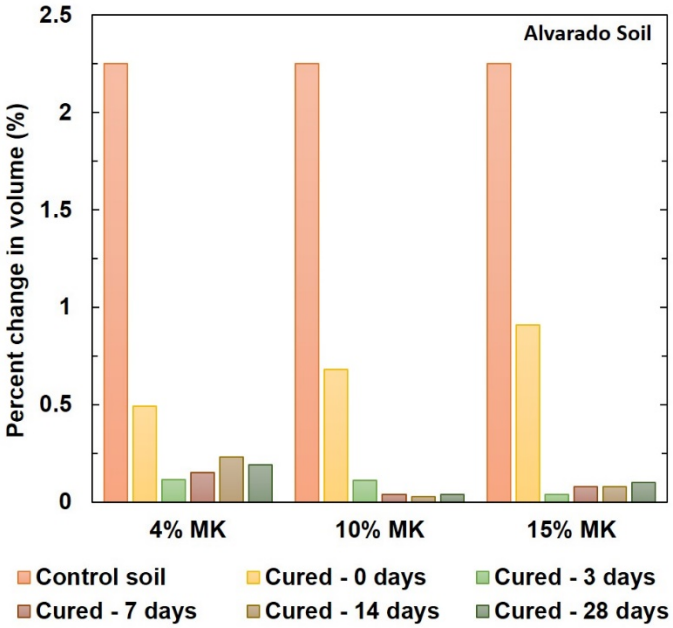


Figure 5.19: Effect of modified durability test on volume of Alvarado soil

Modified durability test results for high-plasticity Lewisville soil (CH) are presented in Figures 5.20, 5.21, 5.22, and 5.23. Strength reduction was observed in CH specimens after being subjected to durability testing. As expected, control CH underwent significant strength loss from 20 psi to 1 psi after modified durability testing in comparison to UCS before testing. Higher geopolymer dosages show lower reduction in UCS values as compared to those CH specimens not subjected durability testing. Final strength loss of same-day cured CH specimens before and after modified durability testing was found to be 55%, 40%, and 15%, for geopolymer dosages of 4%, 10% and 15% MK, respectively. Interestingly, the 0-day and 7-day curing of 15% MK GP treated CH resulted in increased strength after durability testing.

UCS of geopolymer-treated CH were observed to increase with increasing geopolymer dosages and curing periods, after modified durability testing. In comparison to control CH subjected to modified durability testing, dosages of 4%, 10%, and 15% MK resulted in strength increase by about 14, 49, and 100 times, respectively, after 7 days of curing.

Control CH experienced considerable increase in mass and volume by about 20% and 10%, respectively, due to intake of water during modified durability testing. Significant reduction in mass and volume change by under 3% and 0.5%, respectively was observed for CH after only 7 days of curing. The 10% and 15% MK dosages reduce the percentage mass and diameter change in Lewisville soil to

under 2% within a few hours of curing. The lowest GP dosage of 4% MK is observed to be sufficient to significantly reduce mass and volume change in Lewisville soil.

Overall, geopolymer treatment was observed to significantly reduce the ability of soil to absorb water as compared to both control soils. Increased geopolymer dosages and curing periods were observed to significantly reduce mass and volume change for both soils. The 10% MK dosage resulted in lower UCS for CL than CH, while the 15% MK dosage resulted in higher UCS for CL than CH. The 15% MK dosage resulted in a difference of 30 psi of 0-day strength in CL and CH, with CL starting much lower and increasing exponentially to finally outdo CH at 28 days. Compared to the control soils subjected to modified durability testing, geopolymer-treated CL and CH subjected to the same testing show momentous increase in UCS by the final curing period.

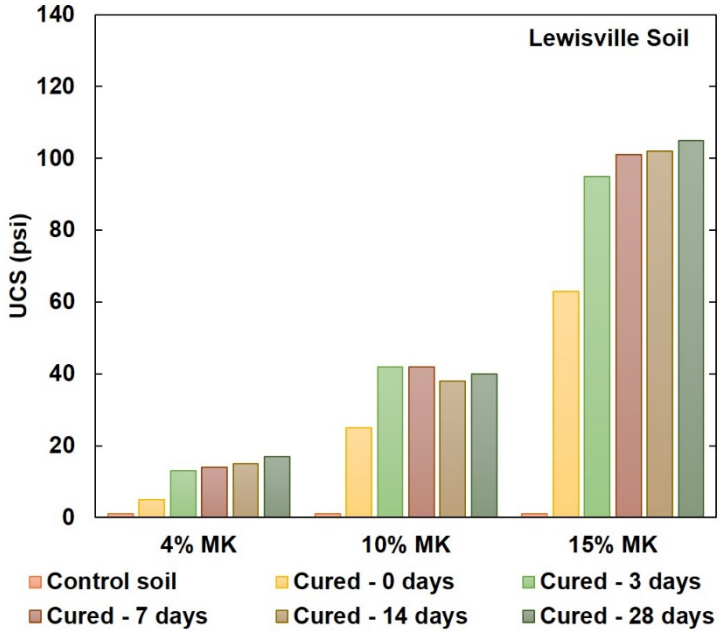


Figure 5.20: UCS of Lewisville soil after modified durability tests

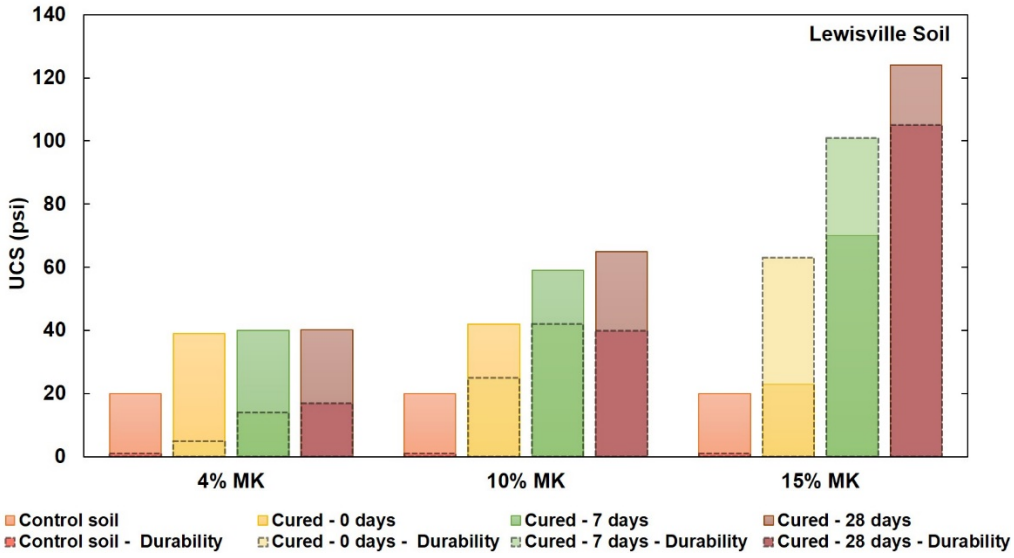


Figure 5.21: UCS of Lewisville soil before and after modified durability test

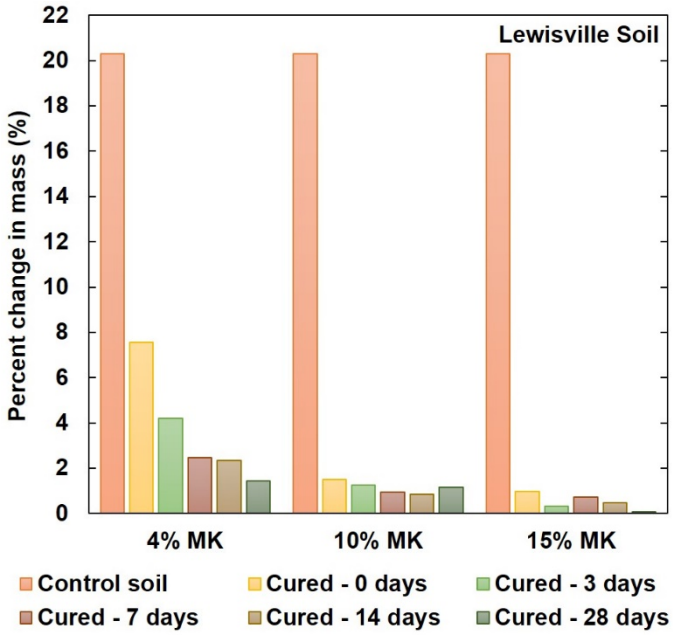


Figure 5.22: Effect of modified durability test on mass of Lewisville soil

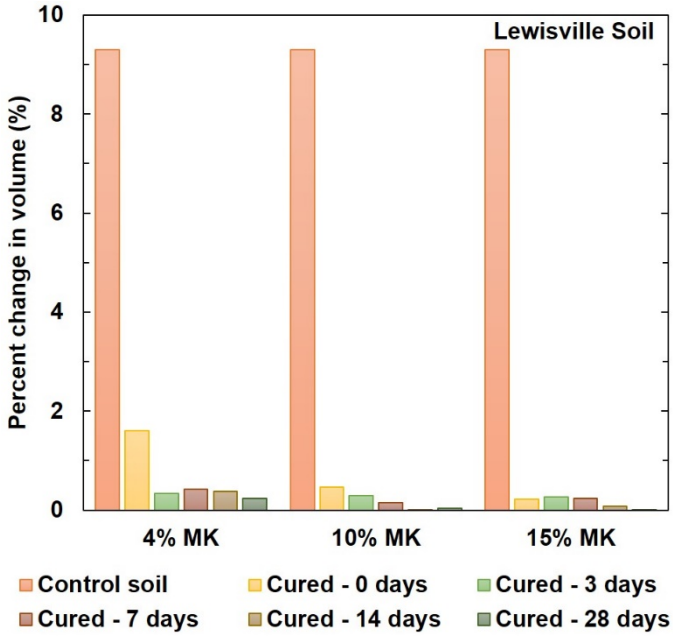


Figure 5.23: Effect of modified durability test on volume of Lewisville soil

### *5.2.9 Modified Leachability*

Modified leachability testing was conducted on soils treated with 4%, and 15% MK geopolymer dosages after curing periods of 7 and 28 days. All leachability specimens were compacted at 95% of their respective MDDs and OMCs and cured at 100% RH. Leachate was collected for a period of 5 hours to determine the volume of leachate discharged. The effect of leaching was determined by monitoring the UCS of control and geopolymer-treated specimens. Results of the leachability tests for both soils are presented in Table 5.2 below.

Table 5.2: Leachability results for control and geopolymer-treated soils

| **Alvarado soil – CL** | | | | | |
|---|---|---|---|---|---|
| *Geopolymer dosage (%MK to dry soil)* | *0% (Control)* | *4%* | | *15%* | |
| *Curing period* | *0 day* | *7 day* | *28 day* | *7 day* | *28 day* |
| Leachate (ml) | 95 | 70 | 100 | 210 | 65 |
| $K^+$ ion (ppm) | 24 | 22,000 | 19,000 | 165,000 | 117,500 |
| **Lewisville soil – CH** | | | | | |
| *Geopolymer dosage (%MK to dry soil)* | *0% (Control)* | *4%* | | *15%* | |
| *Curing period* | *0 day* | *7 day* | *28 day* | *7 day* | *28 day* |
| Leachate (ml) | 160 | 125 | 88 | 135 | 390 |
| $K^+$ ion (ppm) | 18 | 13,500 | 11,000 | 155,000 | 57,000 |

Increasing geopolymer dosages and curing periods were observed to lower leachate volume, by about 15 to 30% after 7 days of curing. The 15% MK dosage shows an anomalous spike in leachate volume of CL and CH after 7 and 28 days of curing, respectively. It can be hypothesized that lower amounts of leachate produced correspond to specimens where soil has bonded well with the

geopolymer, resulting in less voids and therefore less pathways for water to leach through.

The potassium ion ($K^+$) concentration in leachate was determined using a spectrophotometer. According to the World Health Organization, $K^+$ concentration of less than 82 ppm is considered acceptable for drinking water (WHO 1993). Control CL and CH soils were found to have 24 and 18 ppm of $K^+$ in their respective leachates. The 4% MK dosage results in $K^+$ concentration between 10,000 ppm and 22,000 ppm; 15% MK dosage escalates $K^+$ exponentially in both soils. Interestingly, the high $K^+$ concentrations in the leachate of CL and CH treated with 15% MK dosage reduces by about 30% and 60%, respectively after the 28 day curing period. The $K^+$ concentration was observed to be much lower for geopolymer-treated CH than CL.

Figures 5.24 and 5.25 present a comparison of UCS before and after leachability testing in Alvarado and Lewisville soils. Some reduction in UCS values were observed for both soil specimens after being subjected to leachability testing. Final strength loss of CL subjected to leachability testing after 28 days curing for dosages of 4% and 15% MK was observed to be about 30% and 15%, respectively; while for CH strength loss was observed to be about 13% for both dosages. Overall, increasing geopolymer treatments and curing periods were observed to increase UCS values of specimens subjected to leachability tests.

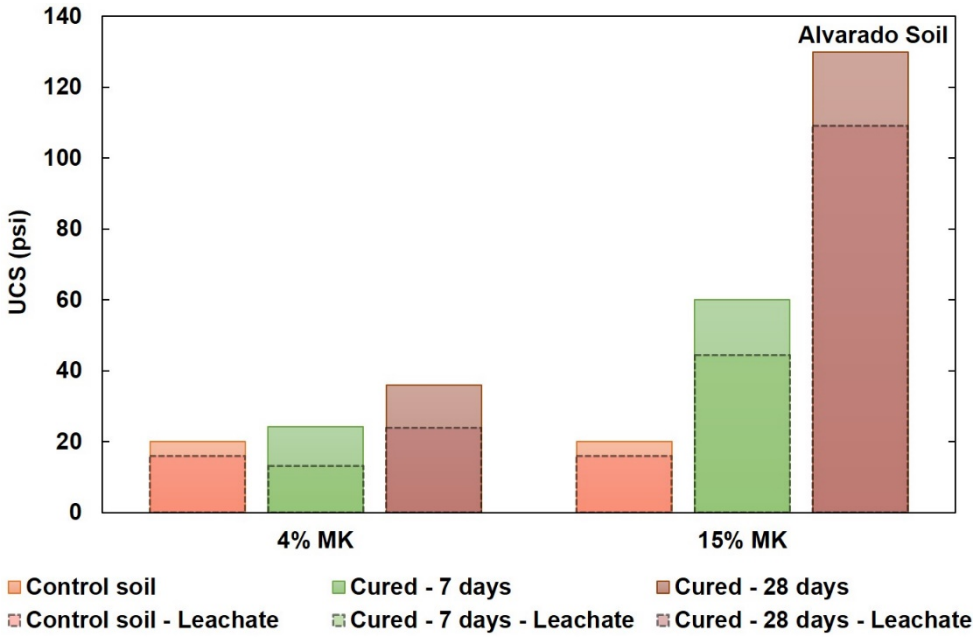


Figure 5.24: UCS comparison of Alvarado soil before and after leachability test

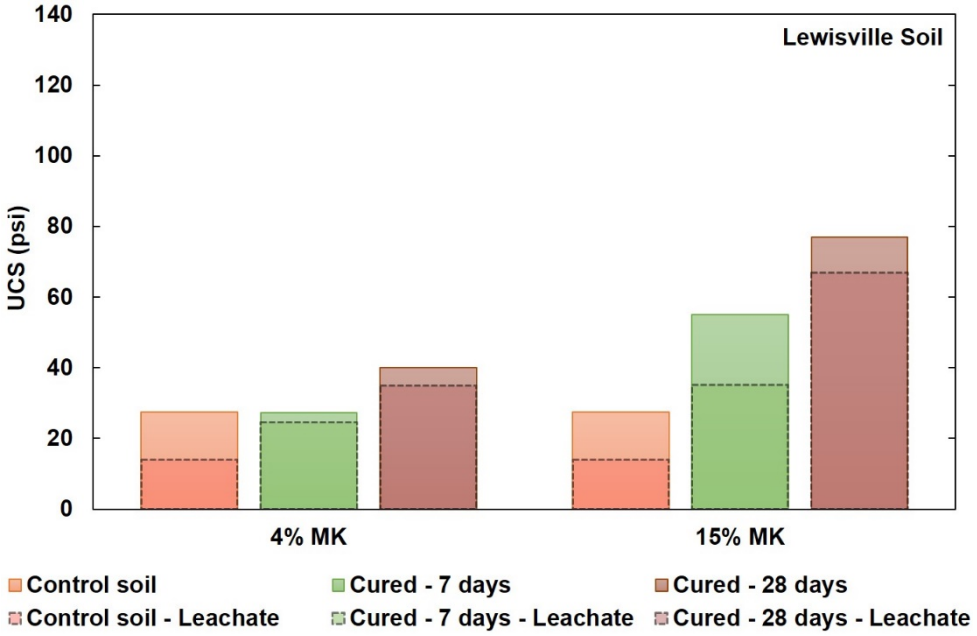


Figure 5.25: UCS comparison of Lewisville soil before and after leachability test

## 5.3 Effect of lime treatment on expansive soils

Both control soils were treated with lime to correlate some engineering properties of lime-treated and geopolymer-treated soils. The low-plasticity Alvarado soil (CL) was treated with 6% lime, while the high-plasticity Lewisville soil (CH) was treated with 8% lime. Moisture content – dry density relationship tests were performed on lime-treated soils to establish their MDD and OMC. Lewisville soil was observed to have a soluble sulfate concentration in the moderate to high risk range (7000 ppm), and was therefore mellowed for 7 days at 5% above its OMC.

Lime-treated soils were tested for UCS, 1-D swell, and modified durability testing at different curing periods as specified in Chapter 4. All lime-treated specimens were molded to 95% of its MDD, and cured in air-tight chambers with no moisture-loss at 100% RH. The results presented here are average values of triplicate specimens, with a coefficient of variation less than 20%. The following sections discuss the results of these tests.

### *5.3.1 Moisture content – dry density relationship test*

Moisture content – dry density relationship curves were determined for both lime-treated soils at their predetermined dosage, and are presented in Figure 5.26. As expected, lime treatment was observed to increase the OMC and decrease the MDD of the soils. The reduced dry density and higher water holding capacity of

lime-treated soils is caused due to the agglomeration and flocculation of soil particles by lime, which is traditionally observed for lime-treated soils (Little 1998).

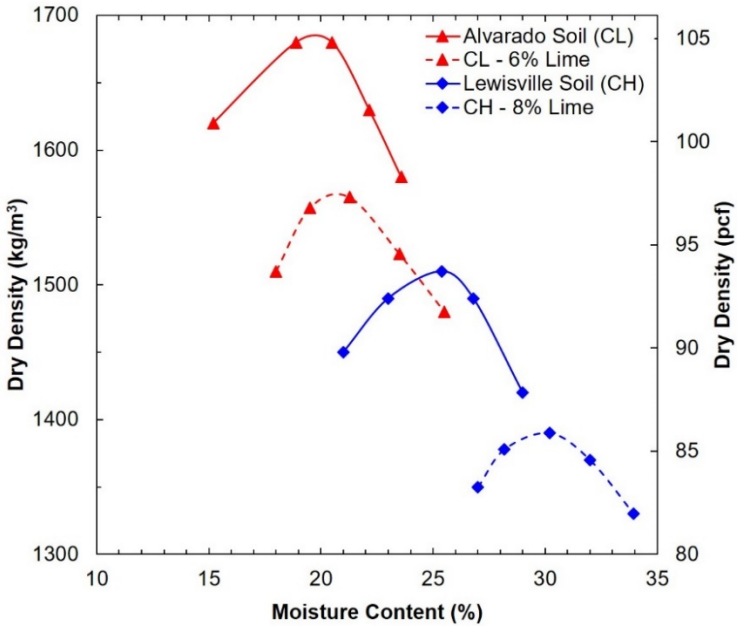


Figure 5.26: Moisture content – dry density relationship curves for control and lime-treated expansive soils

### *5.3.2 UCS*

UCS tests were performed on lime-treated soils as per ASTM D2166-16, after curing periods of 0 (2 hours), 7, and 28 days. Specimens were molded to the miniature dimension and tested at a strain rate of 0.03 in/min. UCS test results for lime-treated CL and CH are presented in Figure 5.27. As expected, lime treatment was observed to cause significant strength improvement in both CL and CH. A strength increase of about 6.7 and 4 times were observed after 28 days of curing in lime-treated CL and CH, respectively. A curing period of only 7 days was needed

for lime-treated CL to have a strength increase of more than 50 psi, while a curing period of 28 days was needed for lime-treated CH.

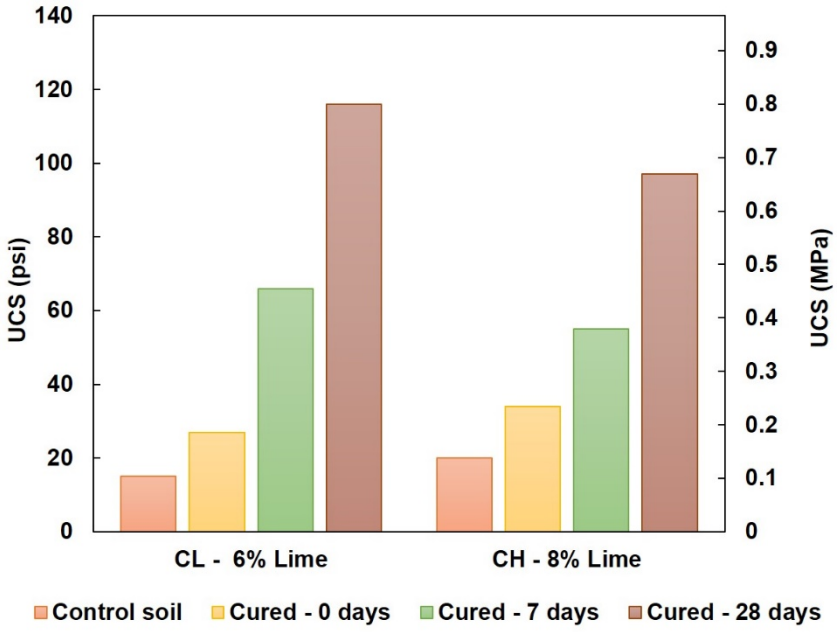


Figure 5.27: Effect of lime treatment on UCS of expansive soils

*5.3.3 1-D swell*

1-D swell tests were performed on lime-treated soils as per ASTM D4546-14e1, after curing periods of 0 (2 hours), 7, and 28 days. Specimens were molded to diameter of 2.5 inches (63.5 mm) and height of 1.13 inches (28.7 mm). Swell test results for Alvarado soil and Lewisville soil treated with lime are presented in Figures 5.28 and 5.29, respectively. As expected, lime treatment was observed to significantly reduce the swell potential of both expansive soils. The CL and CH control soil specimens with moderate and high swell potential were found to have reduced to negligible swell within a few hours of lime treatment.

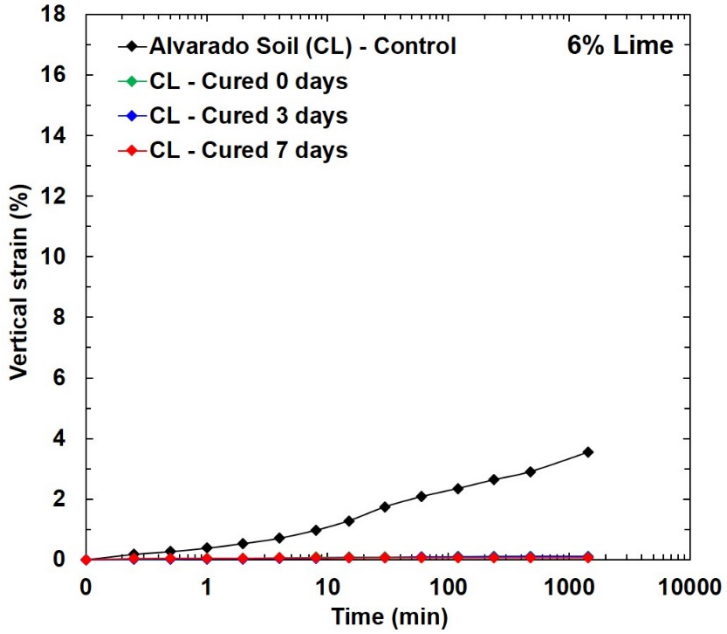


Figure 5.28: Swell potential of Alvarado soil at 6% lime treatment

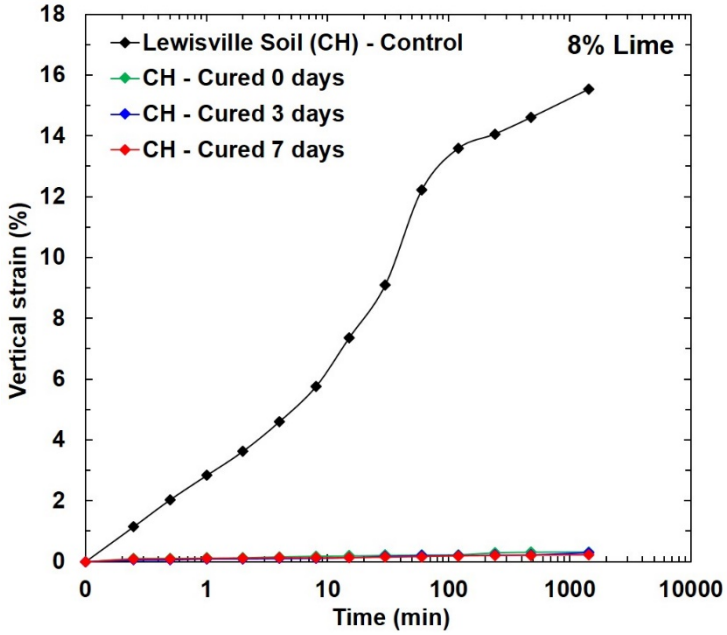


Figure 5.29: Swell potential of Lewisville soil at 8% lime treatment

### *5.3.4 Modified Durability test*

Modified durability testing of lime-treated soils was performed by capillary soaking method, wherein soil specimens were allowed to undergo capillary soaking for 24 hours as detailed in Chapter 4, for specified lime dosages for each soil type after curing periods of 0 (2 hours), 3, 7, 14 and 28 days. The effect of ingress of water due to capillary soaking was determined by monitoring changes in UCS, mass, and volume of control and lime-treated specimens. Figures 5.30, 5.31, 5.32, and 5.33 present these results with respect to different curing periods.

Figure 5.30 shows that while longer curing periods increase UCS for both soils, lime treatment resulted in higher strength gain in CL than CH, after modified durability testing. Final UCS values of 90 psi for CL and 55 psi for CH correspond to an increase of about 30 and 55 times, respectively, from their control values. Figure 5.31 shows some strength loss in both soils after modified durability testing. Final strength loss of same-day cured CL and CH specimens before and after modified durability testing was found to be about 20%, and 45%, respectively.

The percentage change in mass and volume of soil specimens are presented in Figures 5.32 and 5.33, respectively. The percentage change in mass was reduced from 7.4% in control CL to 0.5% in lime-treated CL, and from 20% in control CH to 1.7% in lime-treated CH. Similarly, lime treatment reduced the percentage change in volume from 2.2% in control CL and 9.3% in control CH to negligible, within 7 days of curing.

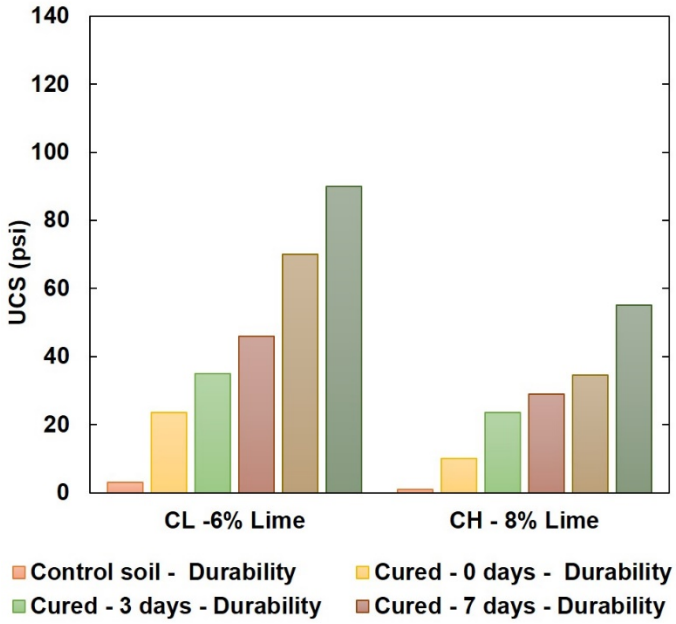


Figure 5.30: Effect of durability testing on UCS of lime-treated soils

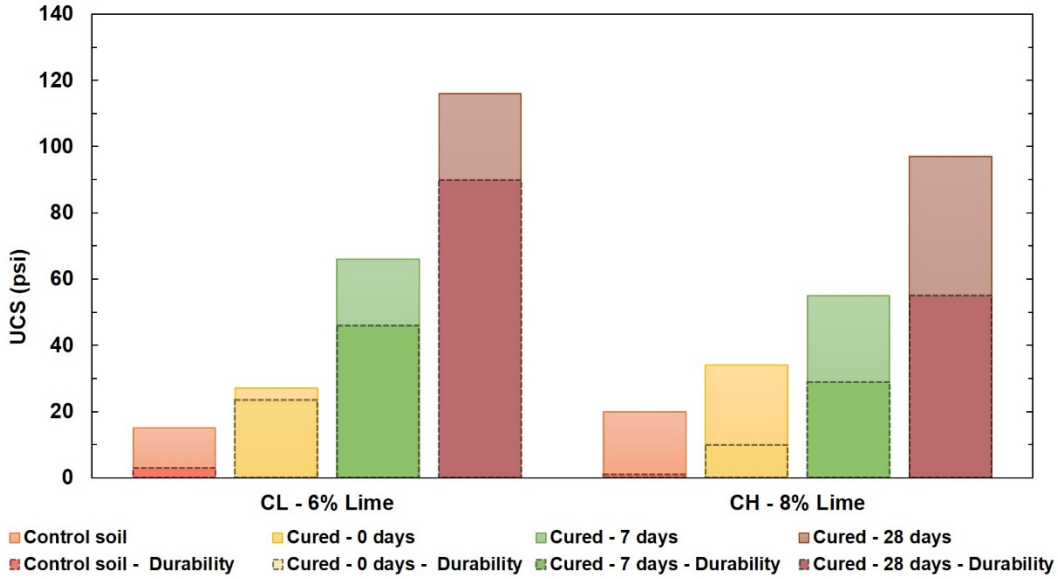


Figure 5.31: UCS comparison of lime-treated soils before and after durability test

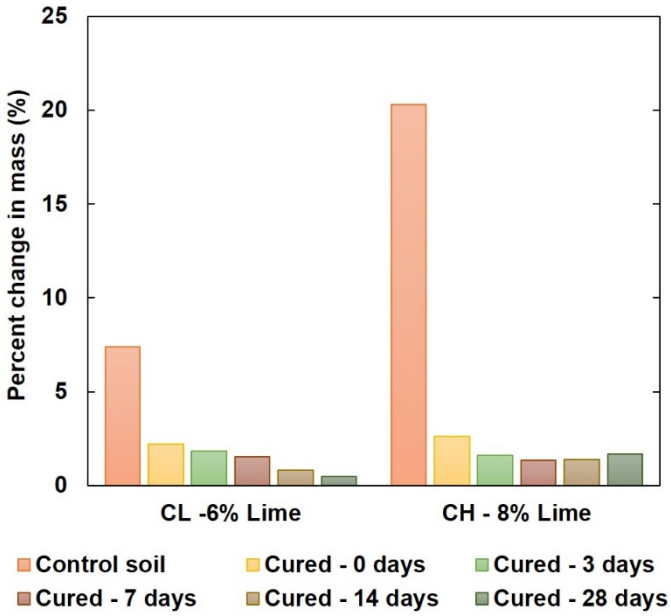


Figure 5.32: Effect of durability testing on mass of lime-treated soils

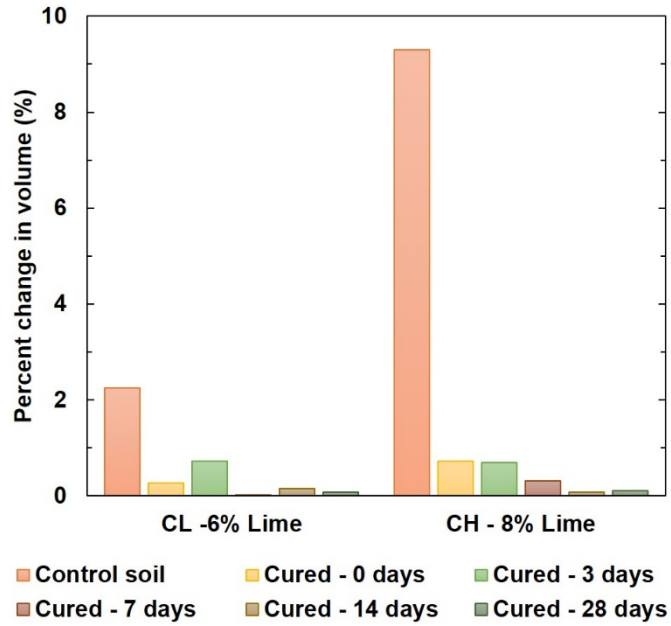


Figure 5.33: Effect of durability testing on volume of lime-treated soils

### *5.3.5 Comparison of geopolymer and lime treatment*

Lime-treated soils tested for UCS, 1-D swell, and modified durability were compared with geopolymer-treated soils for these engineering properties. The test results used for comparison in this section were obtained from soils treated with the highest geopolymer dosage (15% MK).

Figure 5.34 presents a UCS comparison of GP-treated and lime-treated soils, where final strength gain was observed to be higher in geopolymer-treated soils than lime-treated soils. Geopolymer treatment resulted in an increase of about 100% in CL and 150% in CH than lime treatment. Overall, both geopolymer and lime treatment of expansive soils yield comparable results for strength gain. It is important to note that lime-treated CH specimens were molded at 5% over its OMC value to control ettringite formation.

Figure 5.35 presents a comparison of swell potential of GP-treated and lime-treated soils. Both treatments reduced swell rapidly, although swell potential was observed to be slightly higher in geopolymer-treated soils than lime-treated soils within the first few hours of treatment application. Swell potential was made negligible using both treatments within the first 3 days of curing. Geopolymer treatment was found to be slightly more effective in reducing the final swell potential of CH than lime treatment. Overall, both geopolymer and lime treatment of expansive soils yield comparable results for swell potential reduction.

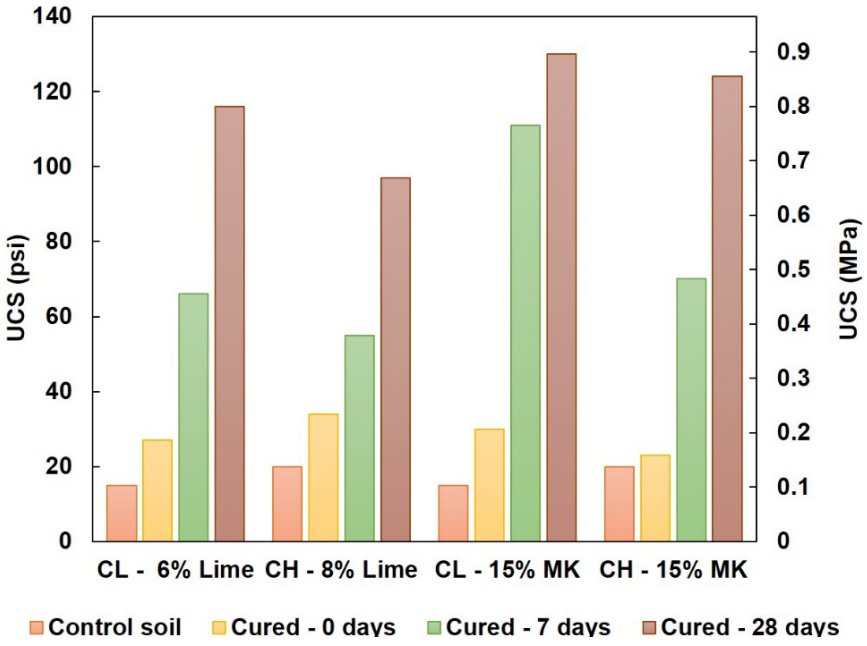


Figure 5.34: UCS comparison of GP-treated (15% MK) and lime-treated soils

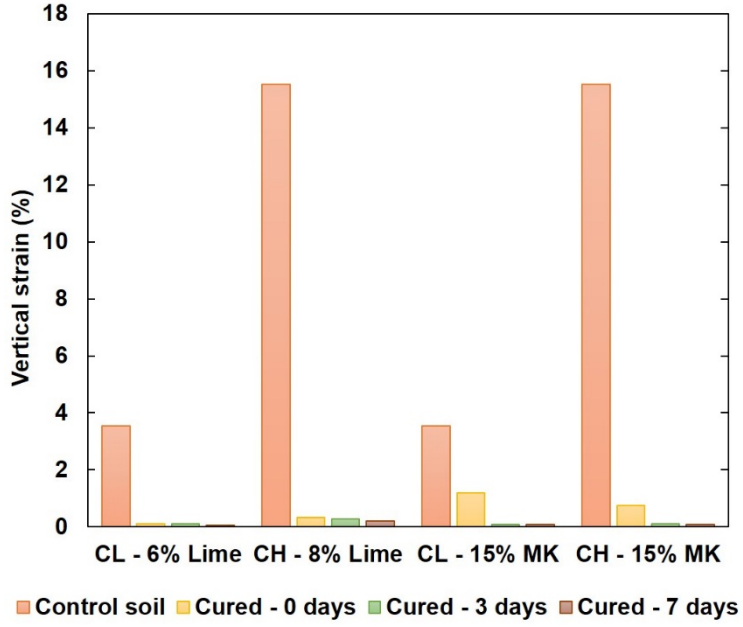


Figure 5.35: Swell comparison of GP-treated (15% MK) and lime-treated soils

Figure 5.36 presents the UCS comparison of both treatments before and after modified durability testing, while Figures 5.37 and 5.38 show comparative reduction in mass and volume of specimens from both treatments. Geopolymer-treated soils were observed to have lower strength loss of only 15% after modified durability testing, while lime-treated soils shows strength reduction by 22% and 44% in CL and CH, respectively. Both treatments significantly reduced the changes in mass and volume of specimens due to ingress of water. Both mass and volume change were made negligible by geopolymer treatment in CH, after 28 days of curing. Geopolymer treatment was found to be more effective in limiting mass and volume change than lime, especially in CH.

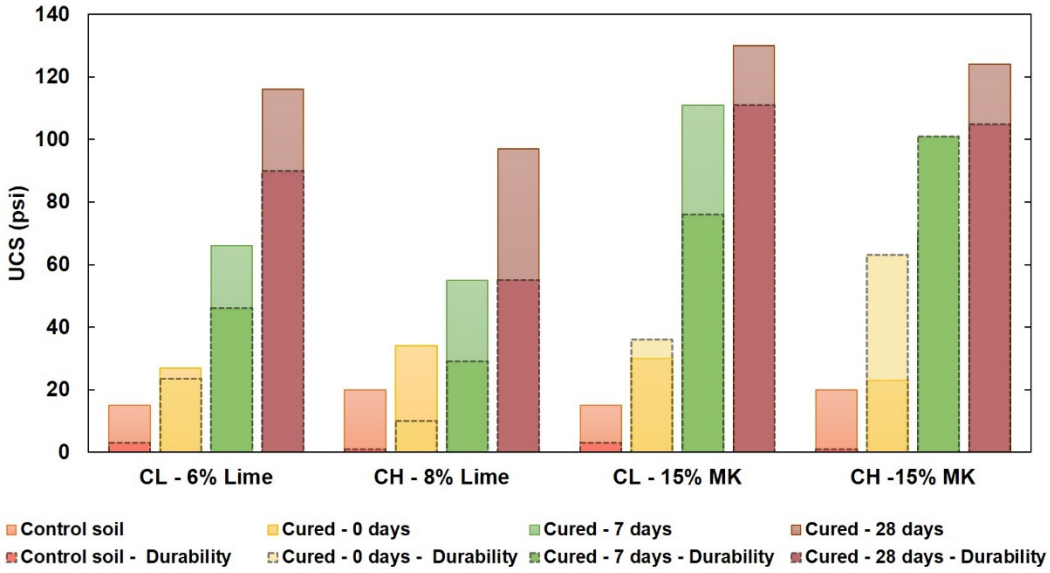


Figure 5.36: UCS comparison of GP-treated (15% MK) and lime-treated soils before and after durability test

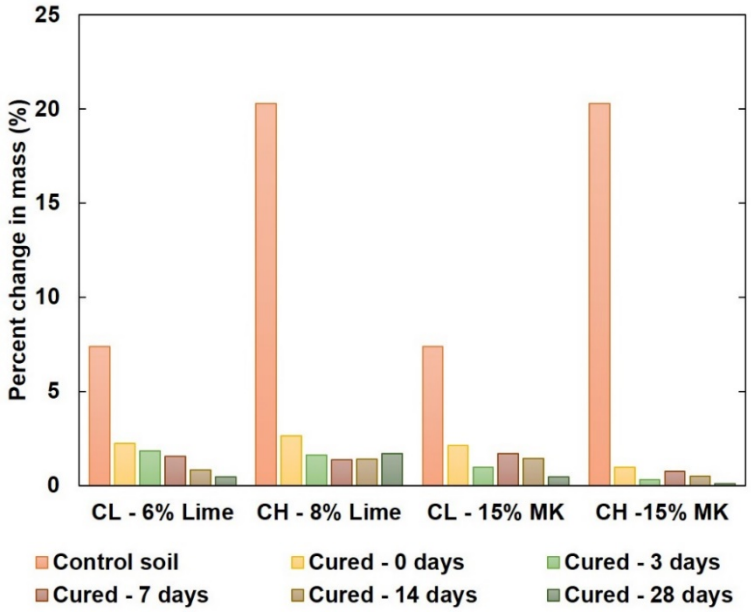


Figure 5.37: Comparison of effect of modified durability testing on mass of GP-treated (15% MK) and lime-treated soils

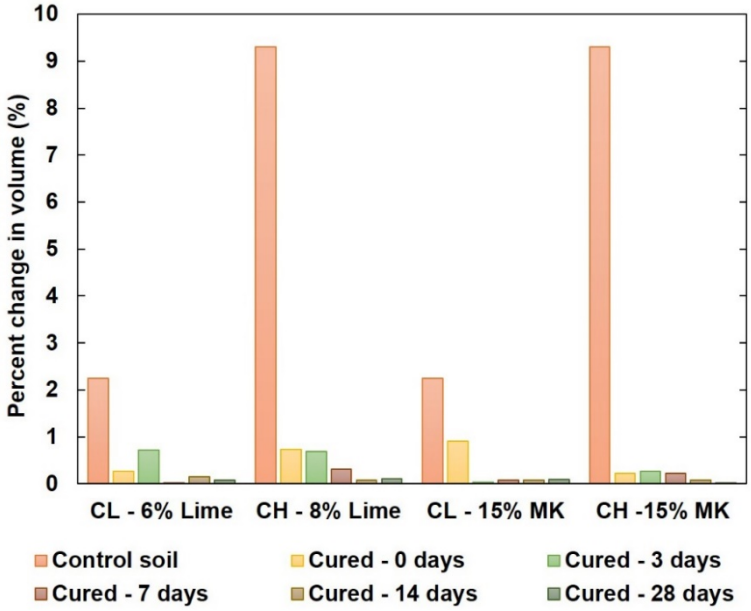


Figure 5.38: Comparison of effect of modified durability testing on volume of GP-treated (15% MK) and lime-treated soils

## 5.4 Summary

This chapter discussed the results of the basic and engineering tests performed on two expansive soils treated with a metakaolin-based geopolymer at three different dosages. Geopolymer treatment resulted in immediate reduction of plasticity index by about 20% and 50% in CH and CL, respectively with the lowest geopolymer dosage. Significant compressive strength enhancement was observed in both soils, although higher strength gain was observed in CL than CH. Final strength gain for the highest geopolymer dosage was about 750% in CL and 500% in CH. Geopolymer treatment also caused improvement in stiffness of soils. Swell potential of both soils were made negligible by the lowest geopolymer dosage, within a few days of curing. Significant reduction in linear shrinkage by about 50% and 90% were observed with the lowest and highest geopolymer dosages, respectively. Strength loss after modified durability testing was found to be reasonable (around 50%) using the lowest geopolymer dosage. Overall, geopolymer was found to be an excellent sole soil stabilizer. While the highest geopolymer dosage yields the best outcomes, the intermediate geopolymer dosage of 10% MK was found to be adequate for enhancement of relevant engineering properties. Additionally, expansive soils treated with lime and tested for UCS, 1-D swell, and modified durability properties were compared with geopolymer-treated soils. The comparative analysis show that geopolymer and lime treatment yield comparable results.

# CHAPTER 6

# MICROSTRUCTURAL CHARACTERIZATION AND ASSESSEMENT OF SUSTAINABILITY AND RESILIENCY BENEFITS OF GEOPOLYMER

## 6.1 Introduction

The metakaolin-based geopolymer synthesized in this study performed well as the sole stabilizer of two expansive soils from North Texas. As shown in Chapter 5, the metakaolin-based geopolymer significantly improved the UCS, $M_R$, and durability characteristics of geopolymer-treated soils, in addition to reducing swelling and shrinkage potential to almost negligible values. This chapter presents the results of the microstructural characterization studies of the MK-based geopolymer as well as the soils treated with it. The microstructural studies are anticipated to shed light on the micro characteristics of geopolymer and geopolymer-treated soils which could correlate to the macro-behavior of enhancing soil properties. In addition, an assessment of the sustainability and resiliency benefits of the MK-based geopolymer in comparison to a conventional soil stabilizer is conducted.

## 6.2 Microstructural Characterization

Microstructural investigation of geopolymer and geopolymer-treated soils were accomplished using the FESEM method. FESEM images were analyzed for formation of geopolymer gels and other reaction products that could aid the stabilization mechanisms of geopolymers in expansive soils.

Two expansive soils from the North Texas area, Alvarado soil, and Lewisville soil, were tested using FESEM for changes in microstructural characteristics of their control and geopolymer-treated specimens. The geopolymer-treated soils tested using FESEM were treated with the highest GP dosage (15% MK), and cured for a period of 28 days at room temperature and 100% RH, to ensure maximum geopolymerization. The K431 geopolymer specimens were also cured for 28 days, before being subject to FESEM testing. FESEM images were obtained for specimens at different magnifications in order to obtain a clearer perspective.

The FESEM images of both control soils are presented in Figures 6.1 and 6.2, and exhibit layered, sheet-like structuring as expected of clays. While MK-based geopolymers have been investigated for their microstructural properties using FESEM, most studies were observed to suspend their investigation at 5000 magnification or lower (Duxson et al. 2005, Liyana et al. 2013, Yun-Ming et al. 2016). FESEM images of the MK-based geopolymer were obtained at higher magnifications and are presented in Figure 6.3. Additionally, FESEM images of GP-treated Alvarado soil and Lewisville soil are presented in Figures 6.4 and 6.5, respectively.

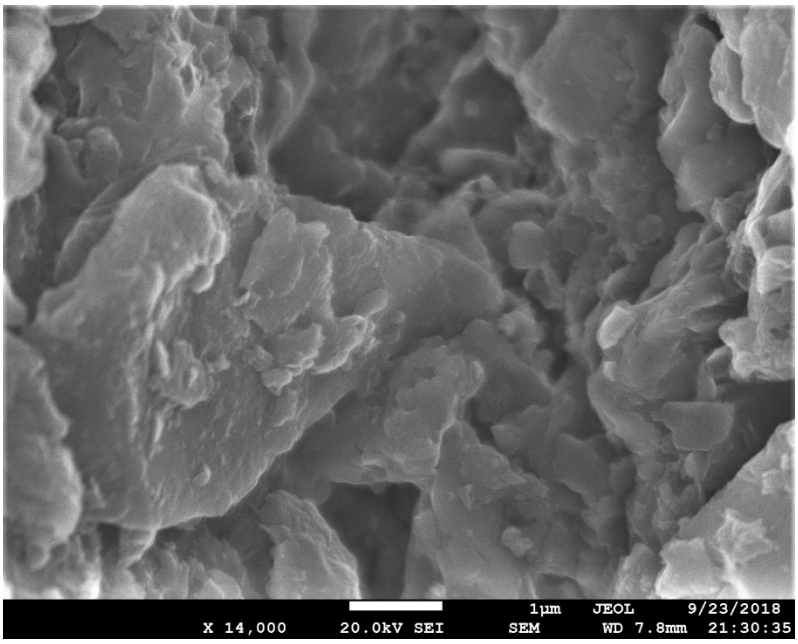


Figure 6.1: FESEM image of control Alvarado soil (Mag. 14k)

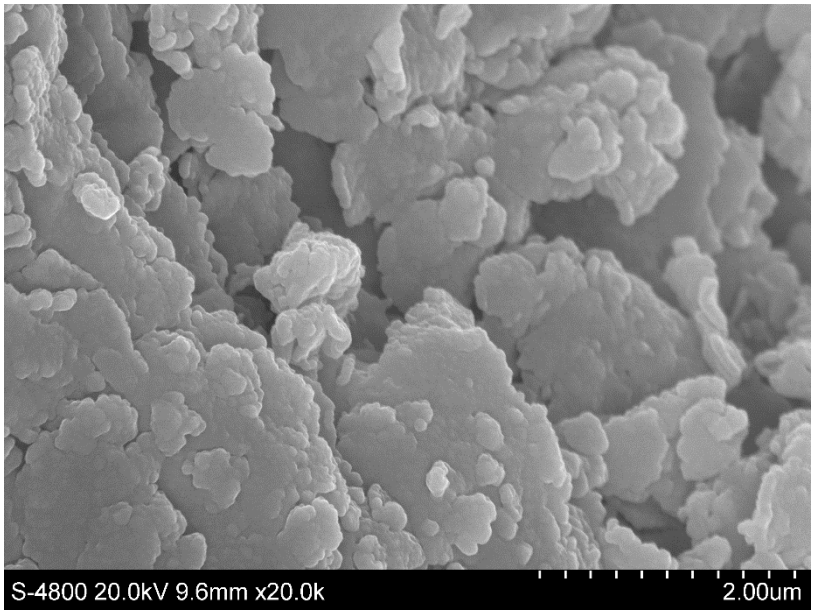


Figure 6.2: FESEM image of control Lewisville soil (Mag. 20k)

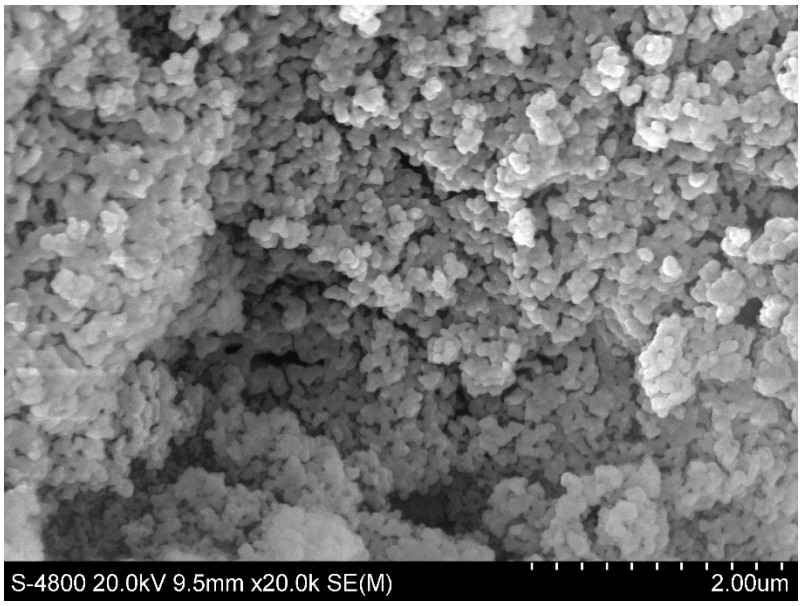


(a)

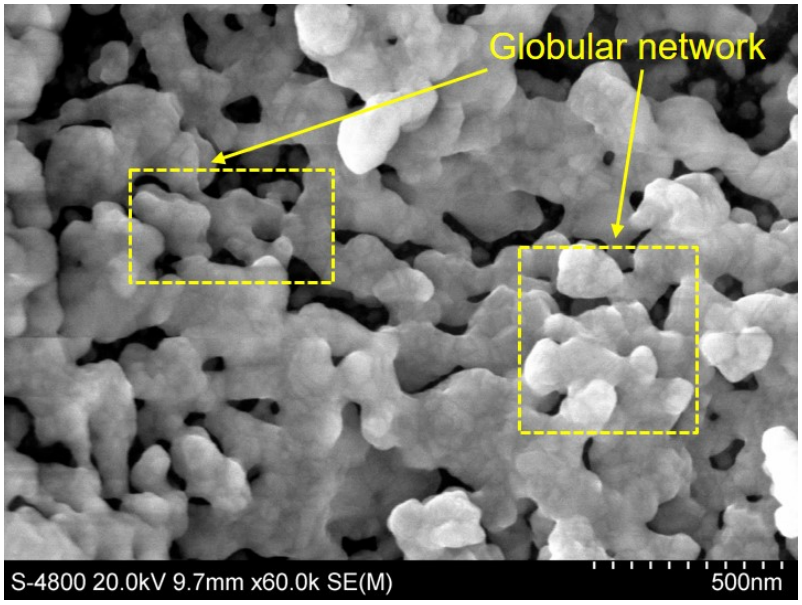


(b)

Figure 6.3: FESEM images of 28 day-cured geopolymer at (a) 20k and (b) 60k magnification

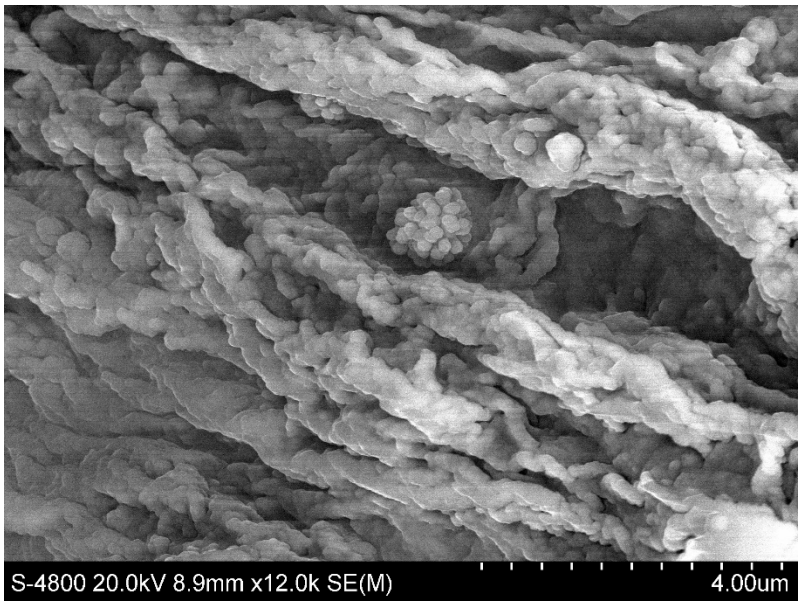


(a)

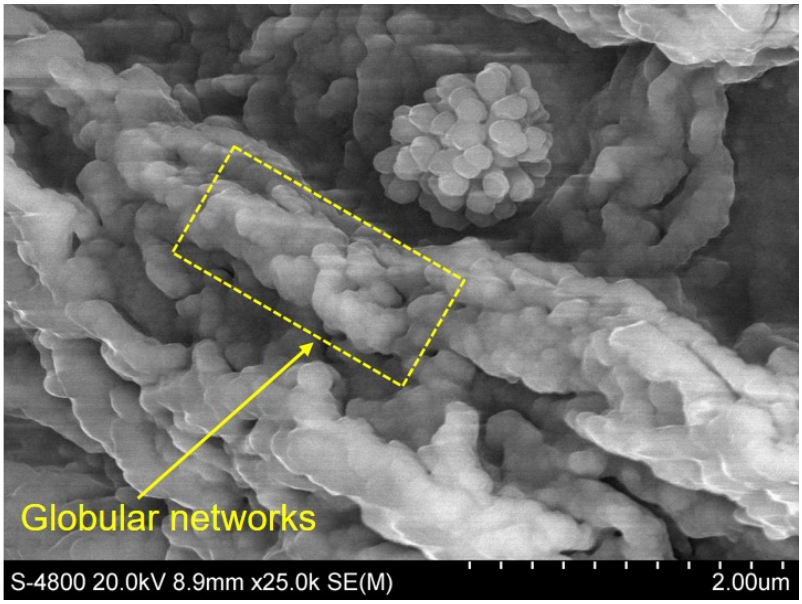


(b)

Figure 6.4: FESEM images of 28-day cured geopolymer-treated Alvarado soil at (a) 12k and (b) 25k magnification

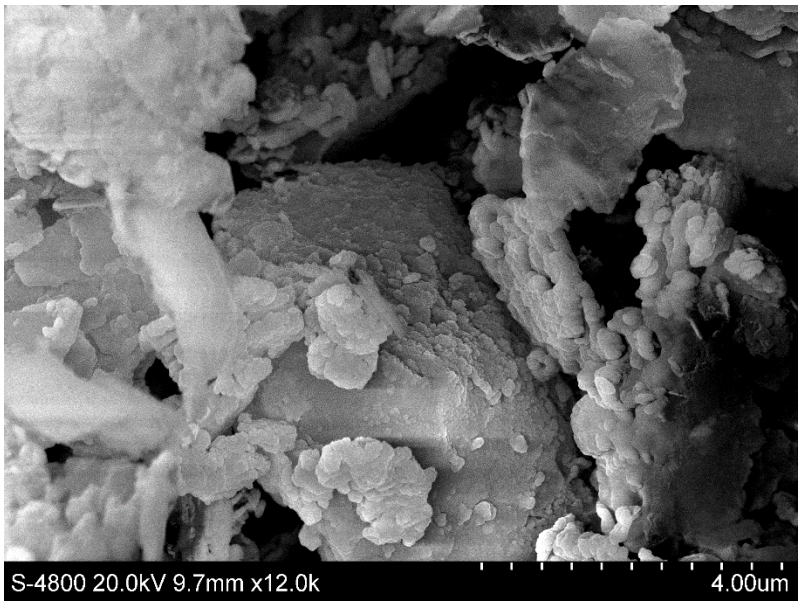


(a)

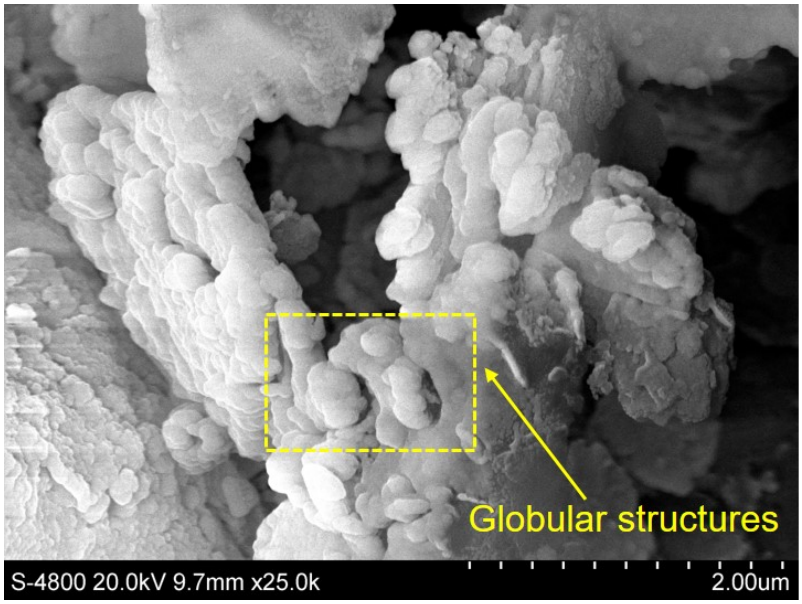


(b)

Figure 6.5: FESEM images of 28-day cured geopolymer-treated Lewisville soil at (a) 12k and (b) 25k magnification

Figures 6.1 and 6.2 show microstructures of control soils detailing its micro-fabric at the clay-particle level with individual particles ranging in dimension around 1 to 2 microns or less. Soil particles were observed to be irregular in shape, flaky, and layered, as is observed in montmorillonite (Mitchell and Soga 2005). The soil particles appeared flocculated and randomly oriented and no definite particle alignment was observed.

The hardened MK-based K431 geopolymer specimens shown in Figure 6.3, appear much more densely packed at the 2 micron scale. The densely-packed structures appear to be consisted of many follicle-like units, that can be described as either bulbous or globular in shape, as confirmed by some researchers (Yun-Ming et al. 2016). On further magnification, the globular units were observed to be interconnected, 3-D networks of geopolymer gels, which appeared to closely resemble the microstructure of some sea sponges and cucumbers (Reich 2015). A few researchers have observed similar globular structures forming at elevated temperatures (900°C to 975°C) of potassium-activated MK-based geopolymers, and interpreted them to be leucite crystals in formation (Kriven et al. 2003, Bell et al. 2009).

Figures 6.4 and 6.5 showing geopolymer-treated expansive soils, were observed to have similar globular structures overlaying the platy, clay-particles, confirming the formation of geopolymer gels and its integration into the clay microstructure. The low-plasticity Alvarado soil was observed to have a higher

concentration of geopolymer gels than the high-plasticity Lewisville soil. The formation of these geopolymer gels can be attributed to enhanced soil properties of geopolymer-treated soils.

### 6.3 Sustainability and Resiliency Benefits Assessment

Geopolymers have been hailed as sustainable alternatives to conventional soil stabilization techniques, owing to the usage of industry by-products in the formulation of geopolymers. An assessment of the sustainability and resiliency benefits of the MK-based geopolymer used in this study and lime was conducted, as per the combined framework recently introduced at UTA (Das et al. 2016, 2018a, 2018b, 2019, Das 2018, Puppala et al. 2018a).

The concept of sustainability is relatively new and is usually met with a lot of apprehension, as it has a myriad of different interpretations. Even so, the Brundtland Declaration's definition is widely accepted and states that "sustainable development is development that meets the needs of the present without compromising the ability of future generations to meet their own needs" (Brundtland 1987). The engineering perspective of sustainability often incorporates cost-efficiency and reasonable control of harmful emissions in addition to prudent resource consumption (Graedel 1994, Kibert 2016). As such, a comprehensive sustainability approach includes environmental protection, economic development and social development (Das 2018).

Resiliency can be defined as “the measure of the persistence of systems and of their ability to absorb change and disturbance and still maintain the same relationships between populations or state variables” (Holling 1996). Robustness, redundancy, resourcefulness, and rapidity were identified as four parameters that can be used to measure infrastructure resilience (Bruneau et al. 2003). Resiliency of infrastructure is important at normal and extraordinary loading conditions. Loss of functionality of critical infrastructures due to any event, can result in catastrophic losses. In this study, probability of failure is selected as indicator of infrastructure resilience (Das 2018).

Both sustainability and resiliency are complementary attributes that are indicative of infrastructure quality (Das 2018). An evaluation of sustainability disregarding resiliency would provide a flawed perspective of sustainable development (Puppala et al. 2017). The combined framework developed at UTA was intended for assessing transportation infrastructure and focuses on its geotechnical components, to estimate a quality index value for different applications, which is a function of both its sustainability and resiliency indices. The best alternative is the one with the lowest quality index value. A flowchart of the combined assessment framework used for this study is presented in Figure 6.6.

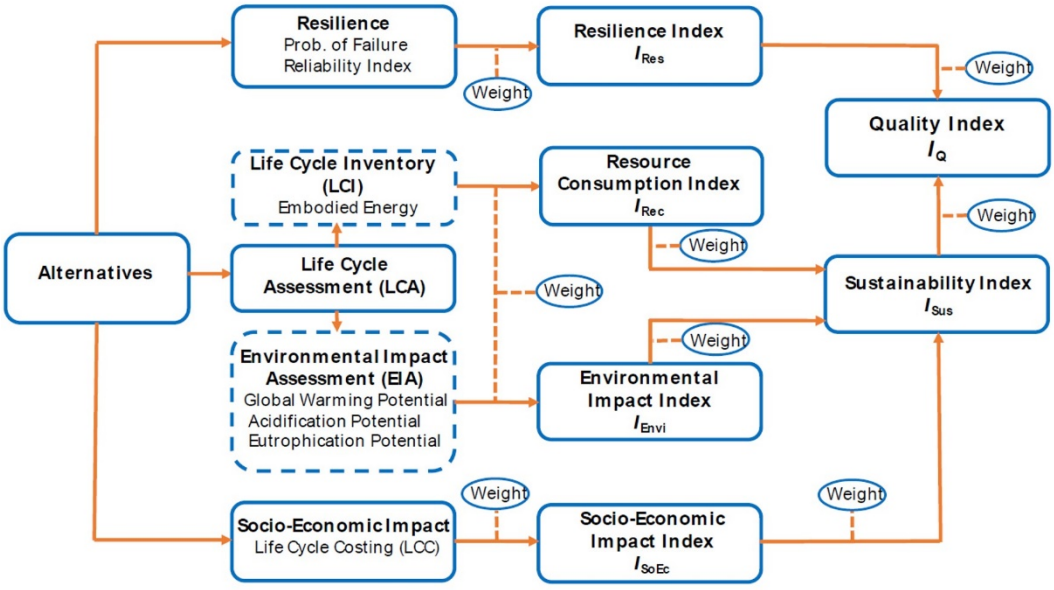


Figure 6.6: Combined assessment framework (Das, 2018)

### *6.3.1 Sustainability Index*

The sustainability index ($I_{Sus}$) is determined by evaluating the resource consumption, environmental impact, and socio-economic impact of a treatment alternative. A life cycle assessment (LCA) is one of the preliminary steps taken to assess the resource consumption and environmental impact of a material. The $I_{Sus}$ was estimated using equation 6.1 as follows (Das 2018):

$$I_{Sus} = (W_1 \times I_{Rec}) + (W_2 \times I_{Env}) + (W_3 \times I_{SoEc}) \quad \text{(Eqn. 6.1)}$$

Where, $I_{Rec}$ is the resource consumption index, $I_{Env}$ is the environmental impact indec, $I_{SoEc}$ is the socio-economic impact index, and $W_1$, $W_2$, $W_3$ are weighted values for each associated index. Different treatment alternatives can be assessed for their sustainability index, and the alternative with the lowest $I_{SUS}$ value

contributes the least to the three impact categories, and is therefore considered most sustainable.

The resource consumption index ($I_{Rec}$) is evaluated using the embodied energy or the energy expended in the construction, operation, and maintenance of an infrastructure. For specific materials, the $I_{Rec}$ can be evaluated using the embodied energy utilized in the production and transportation of a material, usually using a 'cradle to gate' approach. The embodied energy values are determined using energy accounting methods through life cycle inventory (LCI) analysis, which is a part of LCA (Das 2018). The embodied energy values in this study are measured in megajoules (MJ).

The environmental impact index ($I_{Env}$) is evaluated using three major impact factors known as global warming potential, acidification potential, and eutrophication potential. The global warming potential provides an estimated impact of the raw materials on the production of greenhouse gases. In this study, the global warming potential is measured as the global warming potential of carbon dioxide measured as gram equivalent of $CO_2$ ($gCO_2$ eq.). The acidification potential is the tendency of a material to increase the acidity of soil or nearby water and is usually measured as gram equivalent of $SO_2$ ($gSO_2$ eq.). The eutrophication potential is an indicator of biodiversity and ecological health and is measured as the gram equivalent $PO4^{3-}$ equivalent ($gPO_4^{3-}$ eq.).

The socio-economic impact index ($I_{SoEc}$) is evaluated using a cost-benefit analysis of different project alternatives. A life cycle cost analysis (LCCA) is used to quantify costs associated with each alternative usually including purchase, construction, operation, maintenance, rehabilitation, and other residual costs (Das 2018). This study will focus on the initial costs of materials, as this pilot study compares geopolymers with conventional soil stabilizers like lime.

### *6.3.2 Resiliency Index*

The resiliency index ($I_{Res}$) of infrastructure can be determined by the robustness of a system to withstand normal operating loads as well as extreme events. The functional integrity of infrastructure can be maintained at normal operating loads, when reliability-based designs that establish acceptable factors of safety are implemented (Das 2018). For pavement systems, fatigue cracking and rutting are crucial indicators of pavement life.

In this study, $I_{Res}$ was determined for the two different soil stabilizers using a hypothetical scenario of pavement subgrade stabilization. A probabilistic approach was used to analyze resiliency (Bocchini et al. 2014), instead of a factor of safety approach. $I_{Res}$ in this study was estimated using equation 6.2 as follows (Das 2018):

$$I_{Res} = (W_4 \times P_{Ff}) + (W_5 \times P_{Fr}) \quad \text{(Eqn. 6.2)}$$

Where, $P_{Ff}$ is the probability of fatigue cracking, $P_{Fr}$ is the probability of rutting failure, and $W_4$, and $W_5$, are weighted values for each associated parameter. The

treatment alternative with the lower $I_{Res}$ value corresponds to a more resilient stabilization method.

### *6.3.3 Combined Quality Index*

The quality index ($I_Q$) is a measure of the sustainability index as well as resiliency index of a design alternative. The $I_Q$ is calculated using equation 6.3 as follows (Das 2018):

$$I_Q = (W_s \times I_{Sus}) + (W_R \times I_{Res}) \quad \text{(Eqn. 6.3)}$$

Where, $W_S$ and $W_R$ are the weighted values for $I_{Sus}$ and $I_{Res}$, respectively. A lower $I_Q$ value corresponds to lower impact for both sustainability and resiliency aspects, and therefore a better alternative. It is to be noted that, each weight assigned to the individual parameters in the combined framework are based on the discretion of the author.

### *6.3.4 Comparative assessment of geopolymer and lime*

This section assesses the sustainability and resiliency benefits of two different treatment methods for soils stabilization, using the aforementioned combined assessment framework. The MK-based geopolymer treatment and lime treatment used in this study, were evaluated on the basis of a laboratory-scale scenario.

Although two different soil types, and varying dosages of geopolymer and lime treatment were applied on the expansive soils in this study, the combined assessment evaluates the effect of geopolymer and lime treatment solely on the

high-plasticity Lewisville soil (CH). Based on the results of the engineering tests in the previous chapter, a dosage of 10% MK geopolymer and 8% lime were found to be appropriate for stabilization of CH. The combined assessment only considers the effects of metakaolin on the geopolymer production process, as the other materials (silica fume, KOH) are used in much smaller quantities. The amount of dry CH to be stabilized in the laboratory for the combined assessment was assumed to be 100 kg. Table 6.1 provides a summary of the treatments methods to be assessed.

Table 6.1: Treatment methods assessed using combined framework

| | **Treatment 1** | **Treatment 2** |
|---|---|---|
| Soil type | CH | CH |
| Treatment type | Geopolymer | Lime |
| Primary component (PC) | Metakaolin (MK) | Lime |
| Dry soil (kg) | 100 | 100 |
| Dosage | 10% MK | 8% |
| PC quantity (kg) | 10 | 8 |

The determination of $I_{Sus}$ was based on the effect of the production of the materials on the three impact categories. Values for embodied energy, global warming potential, acidification potential, and eutrophication potential for metakaolin were reported in literature (Heath et al. 2014). The global warming potential values for lime were obtained from The Inventory of Carbon and Energy (ICE) database (Hammond et al. 2011) that utilizes a 'cradle-to-gate' approach. The embodied energy, acidification potential, and eutrophication potential values for lime were obtained from previous studies (da Rocha et al. 2016). $I_{SoEc}$ of the two

treatments were estimated using the unit price of the materials obtained from the respective manufacturers.

The resource consumption of both treatments and their corresponding $I_{Rec}$ values are summarized in Table 6.2. Additionally, the embodied energy of transportation of the material from the source to site was obtained from the GREET model (Wang 1999) to be 1.5 MJ/metric ton-km. The $I_{Rec}$ for the treatments were calculated using equation 6.4 as follows (Das 2018):

$$I_{Rec} = w_{1a} \times E_{E(GP)} + w_{1b} \times E_{E(lime)} + w_{1c} \times E_{E(transportation)} \quad \text{(Eqn. 6.4)}$$

Where, $w_{1a}$, $w_{1b}$, $w_{1c}$ are weighted values of each parameter and $E_E$ is the embodied energy. The distance travelled by the truck to transport the material from production source to site was assumed to be 50 miles (80km) for both geopolymer and lime. A higher weightage was placed on $E_E$ of lime to highlight the significantly higher resource consumption per kg of lime than geopolymer. Treatment 1 was found to have a lower $I_{Rec}$ value of 46.67.

Table 6.2: Calculation of resource consumption index

| Resource Category | Embodied energy consumed (MJ) | | Per cent consumption of embodied energy (%) | | Weights | Weighted resource use | |
|---|---|---|---|---|---|---|---|
| | Treatment 1 | Treatment 2 | Treatment 1 | Treatment 2 | | Treatment 1 | Treatment 2 |
| | (1) | (2) | (3)=[(1)/((1)+(2))] × 100 | (4)=[(2)/((1)+(2))] × 100 | (5) | (6)=(5)×(3) | (7)=(5)×(4) |
| Geopolymer | 25 | 0 | 100.00 | 0.00 | 0.30 | 30.00 | 0.00 |
| Lime | 0 | 63 | 0.00 | 100.00 | 0.40 | 0.00 | 40.00 |
| Transportation | 1.2 | 0.96 | 55.56 | 44.44 | 0.30 | 16.67 | 13.33 |
| **Resource Consumption Index ($I_{Rec}$)** | | | | | | 46.67 | 53.33 |

The environmental impact of both treatments and their corresponding $I_{Env}$ values are summarized in Table 6.3, and the $I_{Env}$ for the treatments were calculated using equation 6.5 as follows (Das 2018):

$$I_{Env} = w_{2a} \times GW_P + w_{2b} \times A_P + w_{2c} \times E_P \quad \text{(Eqn. 6.5)}$$

Where, $w_{2a}$, $w_{2b}$, $w_{2c}$ are weighted values of each parameter, $GW_P$ is the global warming potential, $A_P$ is the acidification potential, and $E_P$ is the eutrophication potential. A higher weightage was placed on the $GW_P$ of the treatments as carbon dioxide emissions are a more imminent concern on a global scale. Treatment 1 was found to have a lower $I_{Env}$ value of 38.73.

The socio-economic impact, $I_{SoEc}$ values are summarized in Table 6.4, and were calculated using equation 6.6 as follows (Das 2018):

$$I_{SoEc} = w_3 \times C \quad \text{(Eqn. 6.6)}$$

Where, $w_3$ =1.0, and C is the cost of the treatment. The cost of geopolymer was assumed to be 50% more than the current cost of lime. $I_{SoEc}$ of Treatment 2 was lower with a value of 34.78.

$I_{Sus}$ was calculated using Equation 6.1 as mentioned earlier, by assigning appropriate weights to each parameter. $I_{Sus}$ values of both treatments are summarized in Table 6.5. Treatment 1 was found to have a lower $I_{Sus}$ value of 47.2. A lower weightage was placed on $I_{SoEc}$ of the treatments as this study considers cost to be a secondary aspect that can be further adjusted based on future supply and demand.

Table 6.3: Calculation of environmental impact index

| Environmental impact category | Emission category contribution | | Per cent contribution in emission category (%) | | Weights | Weighted environmental impact | |
|---|---|---|---|---|---|---|---|
| | Treatment 1 | Treatment 2 | Treatment 1 | Treatment 2 | | Treatment 1 | Treatment 2 |
| | (1) | (2) | (3)=[(1)/((1)+(2))] × 100 | (4)=[(2)/((1)+(2))] × 100 | (5) | (6)=(5)×(3) | (7)=(5)×(4) |
| Global Warming Potential ($gCO_2$ eq.) | 3300 | 6240 | 34.59 | 65.41 | 0.60 | 20.75 | 39.25 |
| Acidification Potential ($gSO_2$ eq.) | 3.24 | 4.95 | 39.55 | 60.45 | 0.20 | 7.91 | 12.09 |
| Eutrophication Potential ($gPO_4^{3-}$ eq.) | 0.65 | 0.64 | 50.30 | 49.70 | 0.20 | 10.06 | 9.94 |
| **Environmental Impact Index ($I_{Env}$)** | | | | | | 38.73 | 61.27 |

Table 6.4: Calculation of socio-economic impact index

| Socio-Economic impact category | Cost category contribution | | Per cent contribution in cost category (%) | | Weights | Weighted socio-economic impact | |
|---|---|---|---|---|---|---|---|
| | Treatment 1 | Treatment 2 | Treatment 1 | Treatment 2 | | Treatment 1 | Treatment 2 |
| | (1) | (2) | (3)=[(1)/((1)+(2))] × 100 | (4)=[(2)/((1)+(2))] × 100 | (5) | (6)=(5)×(3) | (7)=(5)×(4) |
| Cost of treatment (US$) | 1.80 | 0.96 | 65.22 | 34.78 | 1.0 | 65.22 | 34.78 |
| **Socio-Economic Impact Index ($I_{SoEc}$)** | | | | | | 65.22 | 34.78 |

Table 6.5: Calculation of sustainability index

| Sustainability indicator | Index value | | Weights | Weighted index | |
|---|---|---|---|---|---|
| | Treatment 1 | Treatment 2 | | Treatment 1 | Treatment 2 |
| | (1) | (2) | (3) | (4)=(1)×(3) | (5)=(2)×(3) |
| Resource Consumption ($I_{Rec}$) | 46.67 | 53.33 | 0.40 | 18.67 | 21.33 |
| Environmental Impact ($I_{Env}$) | 38.73 | 61.27 | 0.40 | 15.49 | 24.51 |
| Socio-Economic Impact ($I_{SoEc}$) | 65.22 | 34.78 | 0.20 | 13.04 | 6.96 |
| **Sustainability Index ($I_{Sus}$)** | | | | 47.20 | 52.80 |

$I_{Res}$ of both treatments were evaluated using equation 6.2. The probability of fatigue cracking ($P_{Ff}$) and the probability of rutting failure ($P_{Fr}$) for treated subgrades were estimated for a hypothetical pavement section. The pavement section used for this study consisted of 6 inches of asphalt concrete pavement, followed by 6 inches of flexible base, and 8 inches of stabilized subgrade. The FPS 21 flexible pavement design system (Liu and Scullion 2011) was used to determine the fatigue cracking life and rutting life of the pavement section. The modulus and thickness of the layers were varied to obtain the reliability of each treatment type. The reliability index and probability of failure for each treatment is given in Table 6.6. These values were obtained by assuming an average daily traffic (ADT) of 2000 vehicles per day and an 18-kip (80 kN) ESAL value of 1.2 million over 20 years. $I_{Res}$ values for both treatments are summarized in Table 6.7. Treatment 1 was found to have a lower $I_{Res}$ value of 48.04.

Table 6.6: Resiliency metrics

| Resilience Indicator | | Control | Treatment 1 | Treatment 2 |
|---|---|---|---|---|
| Fatigue (Cracking) | $FoS_f$ | 1.242 | 1.525 | 1.425 |
| | $\beta_f$ | 0.414 | 1.878 | 0.915 |
| | $P_{Ff}$ | 0.339 | 0.164 | 0.18 |
| Rutting | $FoSr$ | 0.167 | 0.337 | 0.432 |
| | $\beta r$ | 0.469 | 0.742 | 0.595 |
| | $P_{Fr}$ | 0.976 | 0.183 | 0.195 |

Table 6.7: Calculation of resiliency index

| Resilience indicator | Impact category contribution | | Per cent contribution in impact category (%) | | Weights | Weighted impact | |
|---|---|---|---|---|---|---|---|
| | Treatment 1 | Treatment 2 | Treatment 1 | Treatment 2 | | Treatment 1 | Treatment 2 |
| | (1) | (2) | (3)=[(1)/((1)+(2))] × 100 | (4)=[(2)/((1)+(2))] × 100 | (5) | (6)=(5)×(3) | (7)=(5)×(4) |
| Probability of Fatigue Cracking | 0.164 | 0.180 | 47.67 | 52.33 | 0.50 | 23.84 | 26.16 |
| Probability of Rutting Failure | 0.183 | 0.195 | 48.41 | 51.59 | 0.50 | 24.21 | 25.79 |
| **Resilience Index ($I_{Res}$)** | | | | | | 48.04 | 51.96 |

The combined assessment of sustainability and resiliency of both treatments were calculated using the individual indices of sustainability and resiliency from Tables 6.5 and 6.7, to yield the Quality index ($I_Q$). $I_Q$ values for both treatments are presented in Table 6.8, with treatment 1 (geopolymer) shown to have a lower $I_Q$ of 47.62, making it the more sustainable and resilient stabilization alternative based on the assumptions stated in this study. A radar chart of the combined framework assessment is presented in Figure 4.7. The area under the radar chart was estimated to be about 0.64 square units for geopolymer treatment, and 0.86 square units for lime treatment. This confirms that geopolymer treatment is more sustainable and resilient than lime treatment based on the assumptions followed for the combined framework study. It is to be noted that a radar chart does not reflect the unequal individual weights applied to each of the parameters to evaluate the sustainability and resiliency indices (Das 2018).

The combined framework assessment is dependent on weights applied by the user on each impact factor. This study placed more weightage on environmental impact and resource consumption than on socio-economic impact, as there is quite a disparity between current cost of geopolymer treatment and prevalent cost of lime treatment. For this study, cost of the geopolymer was assumed to be 50% more than the prevalent cost of lime, when current geopolymer treatment costs are about 6 to 7 times that of lime treatment. This large difference in cost is primarily due to the fact that geopolymers are not mass produced on a large scale like lime. While the

environmental benefits of geopolymers significantly outweigh that of lime, the low cost of production of lime offsets these benefits by a very large margin, thereby overshadowing the environmental benefits that geopolymers offer. This study attempts to level the playing field by adjusting the weights to highlight environmental benefits of geopolymers.

Table 6.8: Calculation of quality index

| Quality indicator | Index value | | Weights | Weighted index | |
|---|---|---|---|---|---|
| | Treatment 1 | Treatment 2 | | Treatment 1 | Treatment 2 |
| | (1) | (2) | (3) | (4)=(1)×(3) | (5)=(2)×(3) |
| Sustainability Index ($I_{Sus}$) | 47.20 | 52.80 | 0.5 | 23.60 | 26.40 |
| Resilience Index ($I_{Res}$) | 48.04 | 51.96 | 0.5 | 24.02 | 25.98 |
| **Quality Index ($I_Q$)** | | | | 47.62 | 52.38 |

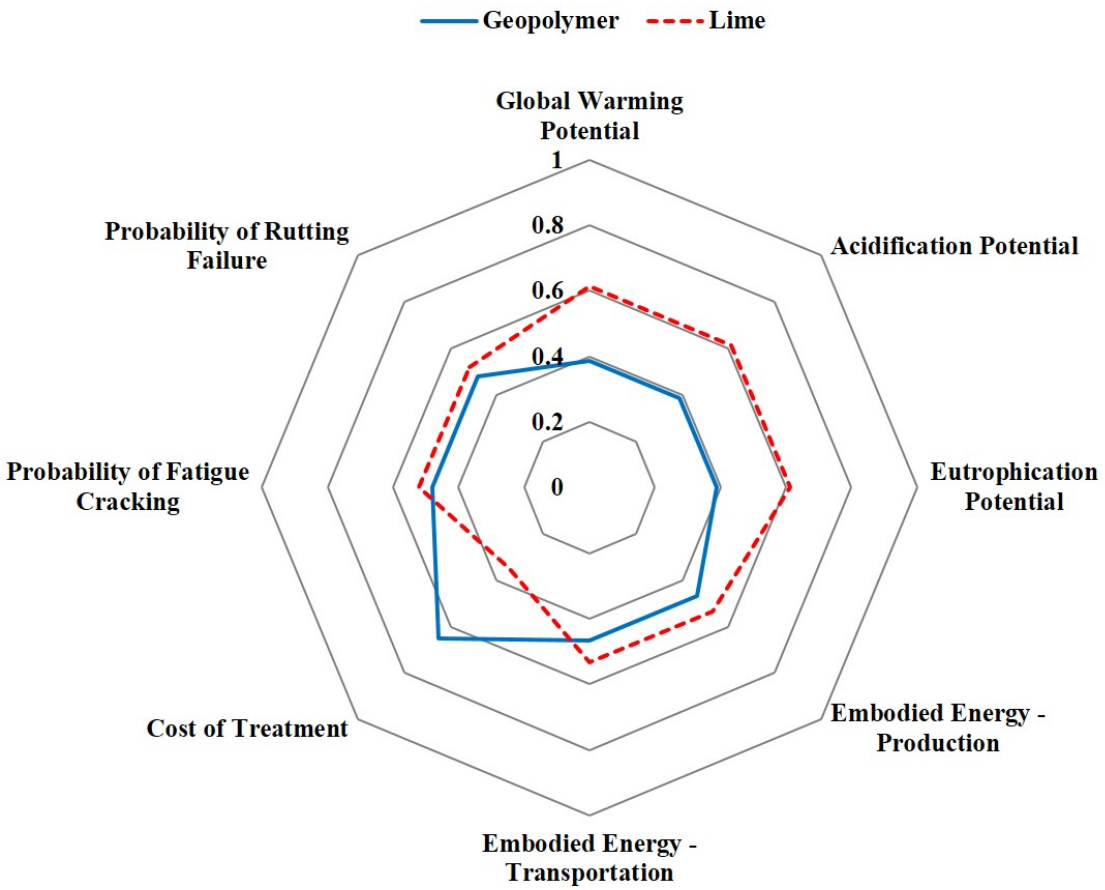


Figure 6.7: Radar chart for combined framework assessment

## 6.4 Summary

This chapter presented the results of the microstructural studies performed using FESEM on the metakaolin-based geopolymer used in this study, as well as the soils treated with the geopolymer. The FESEM of the geopolymer revealed densely packed, 3-D networks of globular geopolymer gels, which were interpreted by some researchers to be phases of leucite formation. The globular formations were also observed on both geopolymer-treated soils, confirming the formation of geopolymer gels.

A sustainability and resiliency assessment based on the combined framework proposed at UTA was conducted for the metakaolin-based geopolymer and lime treatment of Lewisville soil (CH). The assessment was performed for the primary components of the treatments – metakaolin and lime. The embodied energy of production and the global warming potential of a kilogram of lime were found to be significantly higher than metakaolin. Additionally, the transportation distance and cost of metakaolin were adjusted to represent values similar to that of lime, when in reality, they are significantly higher than lime, since metakaolin is not as widely produced. The environmental benefits of metakaolin far outweigh lime and the weighted values assigned for each parameter were adjusted to highlight these differences. Based on the assumptions of this study, metakaolin treatment was found to be the more sustainable and resilient alternative.

# CHAPTER 7

# SUMMARY, CONCLUSIONS, AND FUTURE RECOMMENDATIONS

## 7.1 Introduction

Expansive soils have been effectively treated using calcium-based chemical soil stabilizers, such as lime and OPC, for the past several decades. These conventional stabilizers while effective in improving strength and stiffness properties of expansive soils, are known to be major contributors of carbon dioxide emissions worldwide. Additionally, the effectiveness of these calcium-based stabilizers are limited by issues caused due to the formation of ettringite in sulfate-rich soils. A relatively new class of materials known as geopolymers have been claimed as a more sustainable alternative to conventional soil stabilizers. This study evaluates the effectiveness of a metakaolin-based geopolymer as the sole binder in stabilizing expansive soils.

Several metakaolin-based geopolymers were synthesized in-house to determine the ideal geopolymer to be used as soil stabilizer. The effect of two alkali metal cation sources (KOH and NaOH) were considered for geopolymer synthesis. Eight different geopolymer mixes with varying $SiO_2$:$Al_2O_3$ and water to solids ratios were prepared for this study. The alkali metal cation to aluminum oxide ratio was maintained at 1 for all mixes, to allow for optimal geopolymer formation. Geopolymer slurry was cured at room temperature of around 22°C and 50% RH to form hardened geopolymer specimen. Each geopolymer mix was analyzed for its

setting time, workability, and compressive strength. The sodium-based geopolymer mixtures synthesized for this study were observed to have lower workability than the potassium-based geopolymer mixtures, therefore the potassium-based geopolymer was optimized for increasing the strength and stiffness while mitigating the swell-shrink potential of the stabilized soil. The potassium-based K431 mix with $SiO_2$:$Al_2O_3$ ratio of 4, water to solids ratio of 3, and $K_2O$:$Al_2O_3$ ration of 1, was selected as the geopolymer to be used as soil stabilizer in this study.

Two native expansive soils from north Texas were obtained and treated with the K431 geopolymer at three dosages and tested at different curing periods. A comprehensive testing program involving physical, chemical, and engineering tests were performed on control soils and geopolymer-treated soils. These tests determined the effectiveness of the geopolymer in enhancing the compressive strength, stiffness, volume-change, and long-term performance characteristics of the expansive soils. The expansive soils were also treated with lime and tested for a few engineering characteristics, to evaluate their comparative soil enhancement properties along with geopolymer-treated soil. Microstructural tests were conducted on geopolymer, control soils, and geopolymer-treated soils to detect micro-characteristics of geopolymer and geopolymer-treated soils that could be correlated to their macro-behavior. Furthermore, an assessment of the sustainability and resiliency benefits of geopolymer and lime were conducted.

## 7.2 Summary of Findings

The major findings of this research study are summarized in this section.

1. The Alvarado soil was classified as a low plasticity clay (CL) with a PI of 17% and clay content of about 32%, while the Lewisville soil was classified as a high plasticity clay (CH) with a PI of 53% and clay content of about 52%. CEC and SSA tests performed on expansive soils showed higher montmorillonite content in Lewisville soil.
2. The K431 geopolymer was applied to both expansive soils at dosages of 4%, 10%, and 15% MK. The moisture content – dry density relationship tests performed on control and geopolymer-treated expansive soils revealed that the lowest GP dosage resulted in higher OMC and lower MDD than control soils, while the intermediate and high GP dosage treated soils showed an increasing MDD and decreasing OMC trend than the lowest GP dosage. This is similar to the compaction curves of lime-stabilized soils.
3. Geopolymer treatment was observed to reduce the PI of both expansive soils almost immediately. Significant reduction in PI by about 50 to 90% was observed for the lowest and highest GP dosages, respectively, after a 7 day curing period. The pH of geopolymer-treated soils was observed to reduce modestly, indicative of a progressive chemical reaction, and was found to be between 9.5 and 12.5 after 28 days of curing.

4. Geopolymer-treated soils were observed to have significantly higher unconfined compressive strength than control soils, especially for the higher GP dosages after 28 days of curing. Strength gain was observed to be immediate for lower GP dosages for both soils. Higher compressive strength was observed in geopolymer-treated Alvarado soil than Lewisville soil.
5. Stiffness was evaluated from $M_R$ values of geopolymer-treated soils after curing periods of 7 and 28 days. Overall, increasing net confining pressure and deviator stress resulted in higher $M_R$ values for both soils. Significant improvement in $M_R$ was observed for the highest GP dosages, especially for Alvarado soil. Increasing dosages and curing periods resulted in consistent increase of $M_R$ values, especially for Lewisville soil.
6. Immediate and significant reduction of swell potential was observed in both geopolymer-treated expansive soils. The swell potential of Alvarado and Lewisville control soils were determined to be about 4% and 15%, respectively, and were found to be negligible after being treated with the lowest geopolymer dosage after only 3 days of curing.
7. Shrinkage of both soils was significantly reduced upon geopolymer treatment.
8. Geopolymer-treated specimens fared well under modified durability testing. Strength loss ranging from 15 to 60% was observed in geopolymer-treated

specimens after undergoing modified durability testing. Significant reduction in mass and volume change was also observed, after only 7 days of curing. Geopolymer treatment was also observed to significantly reduce the water absorption capacity of soil specimens.

9. Based on modified leachability testing of geopolymer-treated specimens, increasing GP dosages and curing periods were observed to mostly lower the leachate volume produced after 7 days of curing. The $K^+$ ion concentration was observed to increase with increasing GP dosage, and decrease with increasing curing periods. The $K^+$ ion concentration for geopolymer-treated soils was observed to be much lower for Lewisville soil than for Alvarado soil.
10. Both soils were treated with lime and tested for UCS, 1-D swell, and durability characteristics. Both lime-treated and geopolymer-treated soils were found to have comparable UCS and swell properties. Geopolymer-treated soils were observed to cause a lower percentage decrease of strength after durability testing compared to lime-treated soils, especially at the highest dosage. Lime was found to be more effective in reducing changes in mass and volume in Alvarado soil, while the higher GP dosages were found to be more effective in Lewisville soil for the same conditions.
11. XRD tests performed on MK as well as hardened K431 GP produced broad diffuse halos characteristic of amorphous materials, rendering the use of

XRD for further investigation of reaction products ineffective. FESEM imaging was performed on K431 GP, control soils, and GP-treated soils. GP-treated soils show the presence of globular structures similar to those present in K431 GP, establishing the formation of geopolymer gels and their integration into the clay microstructure. These microstructural changes can be attributed to the enhanced macro behavior of GP-treated soils.

12. A combined benefits assessment of the sustainability and resiliency of the MK-based GP was conducted in comparison to lime treatment of Lewisville soil. The embodied energy of production and the global warming potential of a kilogram of lime were found to be significantly higher than MK. Certain assumptions were made related to cost and transportation of MK, based on which MK-based GP was found to be a more sustainable and resilient alternative than lime for soil stabilization.

## 7.3 Concluding Remarks

This study clearly demonstrates the potential of the metakaolin-based geopolymer as the sole binder for stabilization of expansive soils. Geopolymer treatment shows significant improvement in strength, stiffness, volume change, and long-term performance characteristics of expansive soils. Definite evidence of evolution of the metafabric of geopolymer-treated soils obtained from microstructural imaging, validates its enhanced characteristics. A comparison of lime-treated soils with geopolymer-treated soils show that their strength, swell, and

durability characteristics are comparable. Production of metakaolin-based geopolymers is found to be more environmentally sustainable than lime, although its prevailing cost of production is considerably higher than lime. The pervasive presence of lime production units and its low cost can be attributed to the colossal consumption of lime in different industries. This further proves the need for use of more environmentally sustainable alternatives, such as geopolymer, in place of lime for soil stabilization.

## 7.4 Future Recommendations

This research presents a pilot study of metakaolin-based geopolymers for the purpose of stabilization of expansive soils from North Texas. The following recommendations are suggested to further advance the concept of geopolymers as effective and environmentally sustainable stabilizers of expansive soils:

1. Additional chemical and microstructural analyzes, such as CEC, SSA, thermogravimetry, and differential scanning calorimetry, could be used to analyze geopolymer-treated soils to comprehend the geopolymerization mechanism in soils.
2. For lower geopolymer dosages where improvements are deemed to be not substantial, explore the use of metakaolin-based geopolymer as a co-stabilizer along with other conventional stabilizers.
3. Perform direct shear or triaxial tests on geopolymer-treated soils to analyze changes in its shear strength parameters.

4. Perform soil-water characteristic curve tests to see water retention properties of geopolymer-treated soils and to conduct a study on variation of permeability with geopolymer treatment.
5. Design and perform aggressive durability and leachate testing programs to better characterize long-term performance of geopolymer-treated soils.
6. Investigate the effects of different geopolymer compositions and dosages on different expansive and high-sulfate soils, to detect effect of geopolymers on ettringite formation.
7. Perform pavement design analysis for geopolymer-treated and lime-treated subgrade soils.

# REFERENCES


Abdullah, H.H., Shahin, M.A., and Sarker, P. 2017. Stabilisation of clay with fly-ash geopolymer incorporating GGBFS. World Congress on Civil, Structural, and Environmental Engineering,: 1–8. doi:10.11159/icgre17.141.

Adem, H.H., and Vanapalli, S.K. 2015. Review of methods for predicting in situ volume change movement of expansive soil over time. Journal of Rock Mechanics and Geotechnical Engineering, **7**(1): 73–86. Elsevier.

Atahu, M.K., Saathoff, F., and Gebissa, A. 2019. Strength and compressibility behaviors of expansive soil treated with coffee husk ash. Journal of Rock Mechanics and Geotechnical Engineering, **11**(2): 337–348. Elsevier.

Bailey, S.W. 1980. Summary of recommendations of AIPEA nomenclature committee on clay minerals. American Mineralogist, **65**(1–2): 1–7. Mineralogical Society of America.

Banerjee, A. 2017. Response of Unsaturated Soils under Monotonic and Dynamic Loading over moderate Suction States. Doctoral Dissertation, Department of Civil Engineering, University of Texas at Arlington, Arlington, Texas.

Banerjee, A., Patil, U.D., Puppala, A.J., and Hoyos, L.R. 2018a. Evaluation of Liquefaction Resistance in Silty Sand via Suction Controlled Cyclic Triaxial Tests. *In* PanAm Unsaturated Soils 2017. pp. 543–552. doi:10.1061/9780784481684.055.

Banerjee, A., Patil, U.D., Puppala, A.J., and Hoyos, L.R. 2018b. Suction-controlled

repeated load triaxial test of subgrade soil at high suction states. *In* Unsaturated Soils, Proceeding of Seventh International Conference on Unsaturated Soils. Hong Kong. pp. 667–672.

Banerjee, A., and Puppala, A.J. 2015. Influence of Rate of Shearing on Strength Characteristics of Saturated and Unsaturated Silty Soil. *In* Proc. 50th Indian Geotechnical Conference. Pune, India.

Banerjee, A., Puppala, A.J., and Hoyos, L.R. 2019a. Suction-controlled multistage triaxial testing on clayey silty soil. Engineering Geology,: 105409. doi:10.1016/j.enggeo.2019.105409.

Banerjee, A., Puppala, A.J., Hoyos, L.R., Likos, W.J., and Patil, U.D. 2019b. Resilient Modulus of Expansive Soils at High Suction Using Vapor Pressure Control. Geotechnical Testing Journal, **43**(3). doi:10.1520/GTJ20180255.

Banerjee, A., Puppala, A.J., Patil, U.D., Hoyos, L.R., and Bhaskar, P. 2018c. A Simplified Approach to Determine the Response of Unsaturated Soils Using Multistage Triaxial Test. *In* IFCEE 2018: Advances in Geomaterial Modeling and Site Characterization, GSP 295. pp. 332–342. doi:10.1061/9780784481585.033.

Barbosa, V.F.F., and MacKenzie, K.J.D. 2003. Thermal behaviour of inorganic geopolymers and composites derived from sodium polysialate. Materials research bulletin, **38**(2): 319–331. Elsevier.

Barbosa, V.F.F., MacKenzie, K.J.D., and Thaumaturgo, C. 2000. Synthesis and

characterisation of materials based on inorganic polymers of alumina and silica: sodium polysialate polymers. International Journal of Inorganic Materials, **2**(4): 309–317. Elsevier.

Bell, F. 1993. Engineering Treatment of Soils. CRC Press.

Bell, J.L., Driemeyer, P.E., and Kriven, W.M. 2009. Formation of ceramics from metakaolin-based geopolymers. Part II: K-based geopolymer. Journal of the American Ceramic Society, **92**(3): 607–615. doi:10.1111/j.1551-2916.2008.02922.x.

Bhat, G., and Kandagor, V. 2014. Synthetic polymer fibers and their processing requirements. *In* Advances in Filament Yarn Spinning of Textiles and Polymers. Elsevier. pp. 3–30.

Biswas, N., and Ghosh, P. 2018. Interaction of adjacent strip footings on reinforced soil using upper-bound limit analysis. Geosynthetics International, **25**(6): 599–611. doi:10.1680/jgein.18.00020.

Biswas, N., and Ghosh, P. 2019. Bearing Capacity Factors for Isolated Surface Strip Footing Resting on Multi-layered Reinforced Soil Bed. Indian Geotechnical Journal, **49**(1): 37–49. doi:10.1007/s40098-017-0293-z.

Bocchini, P., Frangopol, D.M., Ummenhofer, T., and Zinke, T. 2014. Resilience and Sustainability of Civil Infrastructure: Toward a Unified Approach. Journal of Infrastructure Systems, **20**(2): 04014004. doi:10.1061/(ASCE)IS.1943-555X.0000177.

Bohn, H.L., McNeal, B.L., and O'Connor, G.A. 1985. Soil chemistry. Wiley.

Boynton, R.S. 1980. Chemistry and technology of lime and limestone. Wiley.

Brundtland, G.H. 1987. Report of the World Commission on environment and development:" our common future.". United Nations.

Bruneau, M., Chang, S.E., Eguchi, R.T., Lee, G.C., O'Rourke, T.D., Reinhorn, A.M., Shinozuka, M., Tierney, K., Wallace, W.A., and von Winterfeldt, D. 2003. A framework to quantitatively assess and enhance the seismic resilience of communities. Earthquake spectra, **19**(4): 733–752.

Buchanan, S. 2007. Resilient Modulus: What, Why, and How. Vulcan Materials Company, **8**(31): 7.

Buchwald, A., Hilbig, H., and Kaps, C. 2007. Alkali-activated metakaolin-slag blends—performance and structure in dependence of their composition. Journal of materials science, **42**(9): 3024–3032. Springer.

Caballero, S., Acharya, R., Banerjee, A., Bheemasetti, T. V, Puppala, A., and Patil, U. 2016. Sustainable Slope Stabilization Using Biopolymer-Reinforced Soil. *In* Geo-Chicago 2016. American Society of Civil Engineers, Reston, VA. pp. 116–126. doi:10.1061/9780784480120.013.

Caldrone, M.A., Gruber, K.A., and Burg, R.G. 1994. High reactivity MEtakaolin: a new generation mineral admixture for high performance concrete. Concrete International, **16**: 11.

Carter, D.L., Mortland, M.M., and Kemper, W.D. 1986. Specific surface.

Cerato, A.B., and Lutenegger, A.J. 2002. Determination of surface area of fine-grained soils by the ethylene glycol monoethyl ether (EGME) method. Geotechnical Testing Journal, **25**(3): 315–321. ASTM International.

Chakraborty, S., Bheemasetti, T. V., Puppala, A.J., and Nazarian, S. 2019. A rational approach to select the number of field tests required to determine subgrade properties. International Journal of Pavement Engineering, **20**(9): 1118–1126. doi:10.1080/10298436.2017.1394095.

Chakraborty, S., and Nair, S. 2017. Impact of different hydrated cementitious phases on moisture-induced damage in lime-stabilised subgrade soils. Road Materials and Pavement Design,: 1–17. doi:10.1080/14680629.2017.1314222.

Chakraborty, S., and Nair, S. 2018. Impact of curing time on moisture-induced damage in lime-treated soils. International Journal of Pavement Engineering,: 1–13. doi:10.1080/10298436.2018.1453068.

Chen, C., Habert, G., Bouzidi, Y., and Jullien, A. 2010. Environmental impact of cement production: detail of the different processes and cement plant variability evaluation. Journal of Cleaner Production, **18**(5): 478–485. Elsevier.

Chen, F.H. 1988. Foundations on expansive soils. Elsevier.

Cheng, T.W., and Chiu, J.P. 2003. Fire-resistant geopolymer produced by granulated blast furnace slag. Minerals Engineering, **16**(3): 205–210.

doi:10.1016/S0892-6875(03)00008-6.

Chindaprasirt, P., Chareerat, T., Hatanaka, S., and Cao, T. 2011. High-Strength Geopolymer Using Fine High-Calcium Fly Ash. Journal of Materials in Civil Engineering, **23**(3): 264–270. doi:10.1061/(ASCE)MT.1943-5533.0000161.

Chittoori, B. 2009. Clay mineralogy effects on long-term performance of chemically treated expansive clays. Civil & Environmental Engineering.

Chittoori, B., and Puppala, A.J. 2011. Quantitative estimation of clay mineralogy in fine-grained soils. Journal of Geotechnical and Geoenvironmental engineering, **137**(11): 997–1008. American Society of Civil Engineers.

Chittoori, B.C.S., Puppala, A.J., Wejrungsikul, T., and Hoyos, L.R. 2013. Experimental Studies on Stabilized Clays at Various Leaching Cycles. Journal of Geotechnical and Geoenvironmental Engineering, **139**(10): 1665–1675. doi:10.1061/(ASCE)GT.1943-5606.0000920.

Christensen, A.P. 1969. Cement modification of clay soils. Portland Cement Assoc R & D Lab Bull,.

Cioffi, R., Maffucci, L., and Santoro, L. 2003. Optimization of geopolymer synthesis by calcination and polycondensation of a kaolinitic residue. Resources, Conservation and Recycling, **40**(1): 27–38. Elsevier.

Congress, S.S.C., and Puppala, A.J. 2019. Evaluation of UAV–CRP Data for Monitoring Transportation Infrastructure Constructed over Expansive Soils. Indian Geotechnical Journal,. doi:10.1007/s40098-019-00384-4.

Congress, S.S.C., Puppala, A.J., Banerjee, A., Jafari, N.H., and Patil, U.D. 2019. Use of Unmanned Aerial Photogrammetry for Monitoring Low-Volume Roads After Hurricane Harvey. *In* 12th International Conference on Low-Volume Roads. pp. 530–543.

Cristelo, N., Glendinning, S., Miranda, T., Oliveira, D., and Silva, R. 2012. Soil stabilisation using alkaline activation of fly ash for self compacting rammed earth construction. Construction and Building Materials, **36**: 727–735. Elsevier Ltd. doi:10.1016/j.conbuildmat.2012.06.037.

Das, B.M., and Sobhan, K. 2013. Principles of geotechnical engineering. Cengage learning.

Das, J.T. 2018. Assessment of Sustainability and Resilience in Transportation Infrastructure Geotechnics. University of Texas at Arlington.

Das, J.T., Banerjee, A., Chakraborty, S., and Puppala, A.J. 2018a. A Framework for Assessment of Sustainability and Resilience in Subgrade Stabilization for a High-Volume Road. *In* Transportation Research Board, 97th Annual Meeting. Washington, D.C.

Das, J.T., Banerjee, A., Puppala, A.J., and Chakraborty, S. 2019. Sustainability and resilience in pavement infrastructure: a unified assessment framework. Environmental Geotechnics,: 1–13. doi:10.1680/jenge.19.00035.

Das, J.T., Puppala, A.J., Bheemasetti, T. V, Walshire, L.A., and Corcoran, M.K. 2016. Sustainability and resilience analyses in slope stabilisation. Proceedings

of the Institution of Civil Engineers - Engineering Sustainability,: 1–12. doi:10.1680/jensu.16.00054.

Das, J.T., Samuel, R.A., George, A.M., Chakraborty, S., Bheemasetti, T. V., and Puppala, A.J. 2018b. Establishing a Threshold Sustainability Index for a Geotechnical Construction. *In* IFCEE 2018. American Society of Civil Engineers, Reston, VA. pp. 222–232. doi:10.1061/9780784481615.018.

Davidovits, J. 1982, September. Mineral polymers and methods of making them. Google Patents.

Davidovits, J. 1988. Structural characterization of geopolymeric materials with Xray diffractometry and MAS NMR spectroscopy. *In* Geopolymer. pp. 149–166.

Davidovits, J. 1991. Geopolymers - Inorganic polymeric new materials. Journal of Thermal Analysis, **37**(8): 1633–1656. doi:10.1007/BF01912193.

Davidovits, J. 1994. Properties of geopolymer cements. *In* First international conference on alkaline cements and concretes. Scientific Research Institute on Binders and Materials Kiev, Ukraine. pp. 131–149.

Davidovits, J. 2008. Geopolymer chemistry and applications. Geopolymer Institute.

Deb, P.S., and Sarker, P.K. 2016. Effects of ultrafine fly ash on setting, strength, and porosity of geopolymers cured at room temperature. Journal of Materials in Civil Engineering, **29**(2): 6016021. American Society of Civil Engineers.

van Deventer, J.S.J., Provis, J.L., Duxson, P., and Brice, D.G. 2010. Chemical research and climate change as drivers in the commercial adoption of alkali activated materials. Waste and Biomass Valorization, **1**(1): 145–155. doi:10.1007/s12649-010-9015-9.

Diamond, S., and Kinter, E.B. 1956. Surface areas of clay minerals as derived from measurements of glycerol retention. Clays and clay minerals, **5**(1): 334–347. Springer.

Diniz, D.H., de Carvalho, J.M.F., Mendes, J.C., and Peixoto, R.A.F. 2017. Blast oxygen furnace slag as chemical soil stabilizer for use in roads. Journal of materials in civil engineering, **29**(9): 4017118. American Society of Civil Engineers.

Du, Y.-J., Yu, B.-W., Liu, K., Jiang, N.-J., and Liu, M.D. 2016. Physical, hydraulic, and mechanical properties of clayey soil stabilized by lightweight alkali-activated slag geopolymer. Journal of Materials in Civil Engineering, **29**(2): 4016217. American Society of Civil Engineers.

Dungca, J.R., and Codilla, E.E.T. 2018. Fly-ash-based geopolymer as stabilizer for silty sand embankment materials. International Journal of GEOMATE, **14**(46): 143–149. doi:10.21660/2018.46.7181.

Duxson, P. 2009. Geopolymer precursor design. *In* Geopolymers. Elsevier. pp. 37–49.

Duxson, P., Fernández-Jiménez, A., Provis, J.L., Lukey, G.C., Palomo, A., and van

Deventer, J.S.J. 2007a. Geopolymer technology: the current state of the art. Journal of Materials Science, **42**(9): 2917–2933. doi:10.1007/s10853-006-0637-z.

Duxson, P., Mallicoat, S.W., Lukey, G.C., Kriven, W.M., and van Deventer, J.S.J. 2007b. The effect of alkali and Si/Al ratio on the development of mechanical properties of metakaolin-based geopolymers. Colloids and Surfaces A: Physicochemical and Engineering Aspects, **292**(1): 8–20. doi:10.1016/j.colsurfa.2006.05.044.

Duxson, P., Provis, J.L., Lukey, G.C., Mallicoat, S.W., Kriven, W.M., and van Deventer, J.S.J. 2005. Understanding the relationship between geopolymer composition, microstructure and mechanical properties. Colloids and Surfaces A: Physicochemical and Engineering Aspects, **269**(1–3): 47–58. doi:10.1016/j.colsurfa.2005.06.060.

Eades, J.L., and Grim, R.E. 1966. A quick test to determine lime requirements for lime stabilization. Highway research record, (139).

Fan, W.-J., Wang, X.-Y., and Park, K.-B. 2015. Evaluation of the chemical and mechanical properties of hardening high-calcium fly ash blended concrete. Materials, **8**(9): 5933–5952. Multidisciplinary Digital Publishing Institute.

Fernández-Jiménez, A., and Palomo, A. 2003. Characterisation of fly ashes. Potential reactivity as alkaline cements☆. Fuel, **82**(18): 2259–2265. Elsevier.

Fernández-Jiménez, A., Palomo, A., and Criado, M. 2005. Microstructure

development of alkali-activated fly ash cement: a descriptive model. Cement and concrete research, **35**(6): 1204–1209. Elsevier.

Fernández-Jiménez, A., Palomo, A., Sobrados, I., and Sanz, J. 2006. The role played by the reactive alumina content in the alkaline activation of fly ashes. Microporous and Mesoporous Materials, **91**(1–3): 111–119. doi:10.1016/j.micromeso.2005.11.015.

Firoozi, A.A., Olgun, C.G., Firoozi, A.A., and Baghini, M.S. 2017. Fundamentals of soil stabilization. International Journal of Geo-Engineering, **8**(1): 26. Springer.

Fletcher, R.A., MacKenzie, K.J.D., Nicholson, C.L., and Shimada, S. 2005. The composition range of aluminosilicate geopolymers. Journal of the European Ceramic Society, **25**(9): 1471–1477. Elsevier.

Garcia-Lodeiro, I., Palomo, A., and Fernández-Jiménez, A. 2015. An overview of the chemistry of alkali-activated cement-based binders. *In* Handbook of alkali-activated cements, mortars and concretes. Elsevier. pp. 19–47.

Gartner, E. 2004. Industrially interesting approaches to “low-CO2” cements. Cement and Concrete research, **34**(9): 1489–1498. Elsevier.

Gautam, S. 2018. LABORATORY AND FIELD STUDY OF A LIQUID IONIC SOIL STABILIZER.

George, A.M., Banerjee, A., Puppala, A.J., and Praticò, F. 2019a. An Integrated LCA-LCCA Framework for the Selection of Sustainable Pavement Design. *In*

Transportation Research Board, 98th Annual Meeting. Washington, D.C.

George, A.M., Banerjee, A., Puppala, A.J., and Saladhi, M. 2019b. Performance evaluation of geocell-reinforced reclaimed asphalt pavement (RAP) bases in flexible pavements. International Journal of Pavement Engineering,: 1–11. doi:10.1080/10298436.2019.1587437.

George, A.M., Banerjee, A., Taylor, T., and Puppala, A.J. 2019c. Large-Scale Experimental Studies to Evaluate the Resilient Modulus of Geocell-Reinforced Reclaimed Asphalt Pavement Bases. *In* Geosynthetics Conference 2019. Houston, Texas.

George, A.M., Chakraborty, S., Das, J.T., Pedarla, A., and Puppala, A.J. 2018. Understanding Shallow Slope Failures on Expansive Soil Embankments in North Texas Using Unsaturated Soil Property Framework. *In* PanAm Unsaturated Soils 2017. American Society of Civil Engineers, Reston, VA. pp. 206–216. doi:10.1061/9780784481691.021.

Gordon, M., Bell, J.L., and Kriven, W.M. 2005. Comparison of naturally and synthetically-derived potassium-based geopolymers. Ceramic Transactions Series, **165**: 95–106.

Graedel, T. 1994. Industrial ecology: definition and implementation. Industrial ecology and global change,: 23–41. Cambridge University Press: Cambridge.

Granizo, N., Palomo, A., and Fernandez-Jiménez, A. 2014. Effect of temperature and alkaline concentration on metakaolin leaching kinetics. Ceramics

International, **40**(7): 8975–8985. Elsevier.

Gruber, K.A., Ramlochan, T., Boddy, A., Hooton, R.D., and Thomas, M.D.A. 2001. Increasing concrete durability with high-reactivity metakaolin. Cement and concrete composites, **23**(6): 479–484. Elsevier.

Hammond, G., Jones, C., Lowrie, F., and Tse, P. 2011. Embodied carbon: the inventory of carbon and energy (ICE). University of Bath and BSRIA, Bracknell, UK.

Hausmann, M.R. 1990. Engineering principles of ground modification.

He, S., Yu, X., Banerjee, A., and Puppala, A.J. 2018. Expansive Soil Treatment with Liquid Ionic Soil Stabilizer. Transportation Research Record: Journal of the Transportation Research Board, **2672**(52): 185–194. doi:10.1177/0361198118792996.

Heath, A., Paine, K., and McManus, M. 2014. Minimising the global warming potential of clay based geopolymers. Journal of Cleaner Production, **78**: 75–83. Elsevier.

Holling, C.S. 1996. Engineering resilience versus ecological resilience. Engineering within ecological constraints, **31**(1996): 32.

Holtz, W.G. 1969. Volume change in expansive clay soils and control by lime treatment. *In* Proceedings of 2nd International Research and Engineering Conference on Expansive Clay Soils. pp. 157–174.

Huang, O.D., Samuel, R., Banerjee, A., Puppala, A.J., and Radovic, M. 2019.

Development of Alternative Stabilization Methods for Transportation Infrastructure Based on Geopolymers. MATEC Web of Conferences, **271**: 02008. doi:10.1051/matecconf/201927102008.

Hussain, M., Varley, R.J., Cheng, Y.B., and Simon, G.P. 2004. Investigation of thermal and fire performance of novel hybrid geopolymer composites. Journal of materials science, **39**(14): 4721–4726. Springer.

van Jaarsveld, J.G.S., van Deventer, J.S.J., and Lukey, G.C. 2002. The effect of composition and temperature on the properties of fly ash-and kaolinite-based geopolymers. Chemical Engineering Journal, **89**(1–3): 63–73. Elsevier.

Van Jaarsveld, J.G.S., Van Deventer, J.S.J., and Schwartzman, A. 1999. The potential use of geopolymeric materials to immobilise toxic metals: Part II. Material and leaching characteristics. Minerals Engineering, **12**(1): 75–91. doi:10.1016/S0892-6875(98)00121-6.

Jafari, N., Puppala, A., Chakraborty, S., and Boluk, B. 2019a. Integrated Full-Scale Physical Experiments and Numerical Modeling of the Performance and Rehabilitation of Highway Embankments. Available from https://digitalcommons.lsu.edu/transet_pubs/39.

Jafari, N.H., Puppala, A., Boluk, B., Cadigan, J.A., Chakraborty, S., Bheemasetti, T., and Pleasant, J.E. 2019b. Predicting the Performance of Highway Embankment Slopes. MATEC Web of Conferences, **271**: 1–4. doi:10.1051/matecconf/201927102007.

Jones, D.E., and Holtz, W.G. 1973. Expansive soils-the hidden disaster. Civil Engineering, **43**(8).

Julina, M., and Thyagaraj, T. 2019. Quantification of desiccation cracks using X-ray tomography for tracing shrinkage path of compacted expansive soil. Acta Geotechnica, **14**(1): 35–56. Springer.

Karatai, T.R., Kaluli, J.W., Kabubo, C., and Thiong'o, G. 2016. Soil stabilization using rice husk ash and natural lime as an alternative to cutting and filling in road construction. Journal of Construction Engineering and Management, **143**(5): 4016127. American Society of Civil Engineers.

Katz, L., Rauch, A., Liljestrand, H., Harmon, J., Shaw, K., and Albers, H. 2001. Mechanisms of soil stabilization with liquid ionic stabilizer. Transportation Research Record: Journal of the Transportation Research Board, (1757): 50–57. Transportation Research Board of the National Academies.

Kézdi, A. 1979. SOIL PHYSICS-SELECTED TOPICS-DEVELOPMENTS IN GEOTECHNICAL ENGINEERING-25.

Khadka, S.D., Jayawickrama, P.W., and Senadheera, S. 2018. Strength and Shrink/Swell Behavior of Highly Plastic Clay Treated with Geopolymer. Transportation Research Record,: 1–11. doi:10.1177/0361198118797214.

Khoury, N., Brooks, R., Boeni, S.Y., and Yada, D. 2012. Variation of resilient modulus, strength, and modulus of elasticity of stabilized soils with postcompaction moisture contents. Journal of Materials in Civil Engineering,

**25**(2): 160–166. American Society of Civil Engineers.

Kibert, C.J. 2016. Sustainable construction: green building design and delivery. John Wiley & Sons.

Kirsch, K., and Bell, A. 2012. Ground improvement. CRC Press.

Kovalchuk, G., Fernández-Jiménez, A., and Palomo, A. 2007. Alkali-activated fly ash: effect of thermal curing conditions on mechanical and microstructural development–Part II. Fuel, **86**(3): 315–322. Elsevier.

Kriven, W.M., Bell, J.L., and Gordon, M. 2003. Microstructure and microchemistry of fully-reacted geopolymers and geopolymer matrix composites. Ceramic Transactions, **153**(1994).

Kriven, W.M., Gordon, M., and Bell, J.L. 2004. Geopolymers: nanoparticulate, nanoporous ceramics made under ambient conditions. Microscopy and microanalysis, **10**(S02): 404–405. Cambridge University Press.

Krivenko, P. 2017. Why alkaline activation - 60 years of the theory and practice of alkali-activated materials. Journal of Ceramic Science and Technology, **8**(3): 323–333. doi:10.4416/JCST2017-00042.

Kumar, P., and Singh, S.P. 2008. Fiber-reinforced fly ash subbases in rural roads. Journal of transportation engineering, **134**(4): 171–180. American Society of Civil Engineers.

Lad, P.P. 2012. Development of a new device to evaluate stabilization durability of expansive soils by addressing wetting/drying and leachate issues. UMI.

Lade, P. V. 2016. Triaxial testing of soils. John Wiley & Sons.

Little, D.N. 1995. Handbook for Stabilization of Pavement Subgrades and Base Courses With Lime. Kendall Hunt Publishing Company.

Little, D.N. 1996. Evaluation of resilient and strength properties of lime-stabilized soils for the Denver, Colorado area. Report for the Chemical Lime Company,.

Little, D.N. 1998. Evaluation of structural properties of lime stabilized soils and aggregates. National Lime Association.

Little, D.N., and Nair, S. 2009a. Recommended practice for stabilization of subgrade soils and base materials. National Cooperative Highway Research Program, Transportation Research Board ….

Little, D.N., and Nair, S. 2009b. Recommended practice for stabilization for sulfate rich subgrade soils. National Highway Cooperative Research Program, Transportation Research Board ….

Little, D.N., Scullion, T., Kota, P., and Bhuiyan, J. 1995. Guidelines for mixture design and thickness design for stabilized bases and subgrades.

Liu, W., and Scullion, T. 2011. Flexible pavement design system FPS 21: User's manual. Texas Dept. of Transportation, Austin, TX,.

Liu, Z., Cai, C.S., Liu, F., and Fan, F. 2016. Feasibility study of loess stabilization with fly ash-based geopolymer. Journal of Materials in Civil Engineering, **28**(5): 1–8. doi:10.1061/(ASCE)MT.1943-5533.0001490.

Liyana, J., Kamarudin, H., Al Bakri, A.M.M., Binhussain, M., Ruzaidi, C.M., Izzat,

A.M., Unimap, P., Box, P.O., and Besar, D.A.P.P. 2013. Reviews on Fly Ash based Geopolymer Materials for Protective Coating Field Implementations Centre of Excellence Geopolymer & Green Technology ( CEGeoGTech ), School of Materials. **7**(5): 182–186.

Lizcano, M., Gonzalez, A., Basu, S., Lozano, K., and Radovic, M. 2012a. Effects of Water Content and Chemical Composition on Structural Properties of Alkaline Activated Metakaolin-Based Geopolymers. Journal of the American Ceramic Society, **95**(7): 2169–2177. doi:10.1111/j.1551-2916.2012.05184.x.

Lizcano, M., Kim, H.S., Basu, S., and Radovic, M. 2012b. Mechanical properties of sodium and potassium activated metakaolin-based geopolymers. Journal of Materials Science, **47**(6): 2607–2616. doi:10.1007/s10853-011-6085-4.

Madhyannapu, R.S., and Puppala, A.J. 2014. Design and Construction Guidelines for Deep Soil Mixing to Stabilize Expansive Soils. Journal of Geotechnical and Geoenvironmental Engineering, **140**(9). doi:10.1061/(ASCE)GT.1943-5606.0001149.

Mateos, M., and Davidson, D.T. 1962. Lime and fly ash proportions in soil, lime and fly ash mixtures, and some aspects of soil lime stabilization. Highway Research Board Bulletin, (335).

McManis, K.L., and Arman, A. 1989. Class C fly ash as a full or partial replacement for portland cement or lime. Transportation Research Record, (1219): 68–81.

Medri, V., Fabbri, S., Dedecek, J., Sobalik, Z., Tvaruzkova, Z., and Vaccari, A.

2010. Role of the morphology and the dehydroxylation of metakaolins on geopolymerization. Applied Clay Science, **50**(4): 538–545. Elsevier.

Miao, S., Shen, Z., Wang, X., Luo, F., Huang, X., and Wei, C. 2017. Stabilization of highly expansive black cotton soils by means of geopolymerization. Journal of Materials in Civil Engineering, **29**(10): 1–9. doi:10.1061/(ASCE)MT.1943-5533.0002023.

Mitchell, J.K., and Soga, K. 2005. Fundamentals of Soil Behavior. *In* 3rd edition. John Wiley & Sons, Inc., Hoboken, New Jersey.

Mo, B., Zhu, H., Cui, X., He, Y., and Gong, S. 2014. Effect of curing temperature on geopolymerization of metakaolin-based geopolymers. Applied clay science, **99**: 144–148. Elsevier.

Mohammadinia, A., Arulrajah, A., Sanjayan, J., Disfani, M.M., Win Bo, M., and Darmawan, S. 2016. Stabilization of demolition materials for pavement base/subbase applications using fly ash and slag geopolymers: Laboratory investigation. Journal of Materials in Civil Engineering, **28**(7). doi:10.1061/(ASCE)MT.1943-5533.0001526.

Nazarian, S., Mazari, M., Abdallah, I.N., Puppala, A.J., Mohammad, L.N., and Abu-Farsakh, M.Y. 2015. Modulus-Based Construction Specification for Compaction of Earthwork and Unbound Aggregate. *In* NCHRP Project 10–84, National Cooperative Highway Research Program. Transportation Research Board, Washington, D.C. doi:10.17226/22211.

Nelson, J.D., and Miller, D.J. 1992. Expansive Soils: Problems and Practice in Foundation and Pavement Engineering. John Wiley & Sons, Inc.

Nicholson, P.G. 2014. Soil improvement and ground modification methods. Butterworth-Heinemann.

Olive, W.W., Chleborad, A.F., Frahme, C.W., Schlocker, J., Schneider, R.R., and Schuster, R.L. 1989. Swelling clays Map of the Conterminous Unitedm States. United States Geological Survey, Reston, VA.

Parsons, R.L. 2002. Subgrade improvement through fly ash stabilization. Miscellaneous Report,.

Pennell, K.D. 2002. 2.5 Specific Surface Area. Methods of Soil Analysis: Part 4 Physical Methods, (methodsofsoilan4): 295–315. Soil Science Society of America.

Petry, T.M., and Little, D.N. 2002. Review of Stabilization of Clays and Expansive Soils in Pavements and Lightly Loaded Structures—History, Practice, and Future. Journal of Materials in Civil Engineering, **14**(6): 447–460. doi:10.1061/(ASCE)0899-1561(2002)14:6(447).

Petry, T.M., and Wohlgemuth, S.K. 1988. Effects of pulverization on the strength and durability of highly active clay soils stabilized with lime and Portland cement.

Phair, J.W., and Van Deventer, J.S.J. 2002. Effect of the silicate activator pH on the microstructural characteristics of waste-based geopolymers. International

Journal of Mineral Processing, **66**(1–4): 121–143. doi:10.1016/S0301-7516(02)00013-3.

Phetchuay, C., Horpibulsuk, S., Arulrajah, A., Suksiripattanapong, C., and Udomchai, A. 2016. Strength development in soft marine clay stabilized by fly ash and calcium carbide residue based geopolymer. Applied Clay Science, **127**–**128**: 134–142. doi:10.1016/j.clay.2016.04.005.

Phetchuay, C., Horpibulsuk, S., Suksiripattanapong, C., Chinkulkijniwat, A., Arulrajah, A., and Disfani, M.M. 2014. Calcium carbide residue: Alkaline activator for clay-fly ash geopolymer. Construction and Building Materials, **69**: 285–294. Elsevier Ltd. doi:10.1016/j.conbuildmat.2014.07.018.

Phummiphan, I., Horpibulsuk, S., Phoo-ngernkham, T., Arulrajah, A., and Shen, S.-L. 2016. Marginal lateritic soil stabilized with calcium carbide residue and fly ash geopolymers as a sustainable pavement base material. Journal of Materials in Civil Engineering, **29**(2): 4016195. American Society of Civil Engineers.

Poulesquen, A., Frizon, F., and Lambertin, D. 2011. Rheological behavior of alkali-activated metakaolin during geopolymerization. Journal of Non-Crystalline Solids, **357**(21): 3565–3571. Elsevier.

Pourakbar, S., Huat, B.B.K., Asadi, A., and Fasihnikoutalab, M.H. 2016. Model Study of Alkali-Activated Waste Binder for Soil Stabilization. International Journal of Geosynthetics and Ground Engineering, **2**(4): 1–12. Springer

International Publishing. doi:10.1007/s40891-016-0075-1.

Provis, J.L., and Bernal, S.A. 2014. Geopolymers and Related Alkali-Activated Materials. Annual Review of Materials Research, **44**(1): 299–327. doi:10.1146/annurev-matsci-070813-113515.

Provis, J.L., and van Deventer, J.S.J. 2009. Geopolymers: structures, processing, properties and industrial applications. Elsevier.

Provis, J.L., and van Deventer, J.S.J. 2013. Alkali activated materials: state-of-the-art report, RILEM TC 224-AAM. Springer Science & Business Media.

Provis, J.L., and van Deventer, J.S.J. 2014. Alkali avtivated materials: State of Art Report. *In* Rilem Tc 224. doi:10.1007/978-94-007-7672-2.

Provis, J.L., Duxson, P., van Deventer, J.S.J., and Lukey, G.C. 2005. The role of mathematical modelling and gel chemistry in advancing geopolymer technology. Chemical Engineering Research and Design, **83**(7 A): 853–860. doi:10.1205/cherd.04329.

Provis, J.L., Yong, S.L., and Duxson, P. 2009. Nanostructure/microstructure of metakaolin geopolymers. *In* Geopolymers: structures, processing, properties and industrial applications. Elsevier. pp. 72–88.

Prusinski, J.R., and Bhattacharja, S. 1999. Effectiveness of Portland cement and lime in stabilizing clay soils. Transportation research record, **1652**(1): 215–227. SAGE Publications Sage CA: Los Angeles, CA.

Punthutaecha, K., Puppala, A.J., Vanapalli, S.K., and Inyang, H. 2006. Volume

change behaviors of expansive soils stabilized with recycled ashes and fibers. Journal of materials in Civil Engineering, **18**(2): 295–306. American Society of Civil Engineers.

Puppala, A., Wattanasanticharoen, E., and Hoyos, L. 2003a. Ranking of four chemical and mechanical stabilization methods to treat low-volume road subgrades in Texas. Transportation Research Record: Journal of the Transportation Research Board, (1819): 63–71. Transportation Research Board of the National Academies.

Puppala, A.J. 2016. Advances in ground modification with chemical additives: From theory to practice. Transportation Geotechnics, **9**: 123–138. doi:10.1016/j.trgeo.2016.08.004.

Puppala, A.J., Basu, D., Cuisinier, O., and Das, J.T. 2017. General Report of TC 307–Sustainability in Geotechnical Engineering. *In* 19th ICSMGE. Seoul, South Korea. pp. 3353–3360.

Puppala, A.J., and Cerato, A. 2009. Heave distress problems in chemically-treated sulfate-laden materials. Geo-Strata—Geo Institute of ASCE, **10**(2): 28. ASCE.

Puppala, A.J., Congress, S.S.C., and Banerjee, A. 2019a. Research Advancements in Expansive Soil Characterization, Stabilization and Geoinfrastructure Monitoring. *In* Frontiers in Geotechnical Engineering. *Edited by* G.M. Latha. pp. 15–29. doi:10.1007/978-981-13-5871-5_2.

Puppala, A.J., Congress, S.S.C., Talluri, N., and Wattanasanthicharoen, E. 2019b.

Sulfate-Heaving Studies on Chemically Treated Sulfate-Rich Geomaterials. Journal of Materials in Civil Engineering, **31**(6): 04019076. doi:10.1061/(ASCE)MT.1943-5533.0002729.

Puppala, A.J., Das, J.T., Bheemasetti, T. V., and Congress, S.S.C. 2018a. Sustainability and Resilience in Transportation Infrastructure geotechnics: Integrating Advanced Technologies for better Asset Management. Geo-Strata -Geo Institute of ASCE, **22**(3): 42–48.

Puppala, A.J., Hoyos, L.R., and Potturi, A.K. 2011. Resilient Moduli Response of Moderately Cement-Treated Reclaimed Asphalt Pavement Aggregates. Journal of Materials in Civil Engineering, **23**(7): 990–998. doi:10.1061/(ASCE)MT.1943-5533.0000268.

Puppala, A.J., Intharasombat, N., and Vempati, R.K. 2005. Experimental Studies on Ettringite-Induced Heaving in Soils. Journal of Geotechnical and Geoenvironmental Engineering, **131**(3): 325–337. doi:10.1061/(ASCE)1090-0241(2005)131:3(325).

Puppala, A.J., Manosuthikij, T., and Chittoori, B.C.S. 2013. Swell and shrinkage characterizations of unsaturated expansive clays from Texas. Engineering Geology, **164**(17): 187–194. Elsevier. doi:10.1016/j.enggeo.2013.07.001.

Puppala, A.J., Mohammad, L.N., and Allen, A. 1996. Engineering behavior of lime-treated Louisiana subgrade soil. Transportation Research Record, **1546**(1): 24–31. SAGE Publications Sage CA: Los Angeles, CA.

Puppala, A.J., Ramakrishna, A.M., and Hoyos, L.R. 2003b. Resilient Moduli of Treated Clays from Repeated Load Triaxial Test. Transportation Research Record: Journal of the Transportation Research Board, **1821**(1): 68–74. doi:10.3141/1821-08.

Puppala, A.J., Ruttanaporamakul, P., and Congress, S.S.C. 2019c. Design and construction of lightweight EPS geofoam embedded geomaterial embankment system for control of settlements. Geotextiles and Geomembranes, **47**(3): 295–305. doi:10.1016/j.geotexmem.2019.01.015.

Puppala, A.J., Talluri, N., Congress, S.S.C., and Gaily, A. 2018b. Ettringite induced heaving in stabilized high sulfate soils. Innovative Infrastructure Solutions, **3**(1): 72. doi:10.1007/s41062-018-0179-7.

Purdon, A.O. 1940. The action of alkalis on blast-furnace slag. Journal of the Society of Chemical Industry, **59**(9): 191–202.

Raman, V. 1967. Identification of expansive soils from the plasticity index and the shrinkage index data. The Indian Engineer, **11**(1): 17–22.

Rangan, B.V. 2008. Low-calcium, fly-ash-based geopolymer concrete. *In* Concrete construction engineering handbook. CRC press. pp. 21–26.

Rees, C.A., Provis, J.L., Lukey, G.C., and van Deventer, J.S.J. 2008. The mechanism of geopolymer gel formation investigated through seeded nucleation. Colloids and Surfaces A: Physicochemical and Engineering Aspects, **318**(1–3): 97–105. doi:10.1016/j.colsurfa.2007.12.019.

Reich, M. 2015. Different pathways in early evolution of the holothurian calcareous ring. Progress in Echinoderm Palaeobiology, **19**: 137–145. Cuadenos del Museo Geominero.

Rios, S., Ramos, C., Fonseca, A.V. Da, Cruz, N., and Rodrigues, C. 2016. Colombian Soil Stabilized with Geopolymers for Low Cost Roads. Procedia Engineering, **143**(Ictg): 1392–1400. Elsevier B.V. doi:10.1016/j.proeng.2016.06.164.

da Rocha, C.G., Passuello, A., Consoli, N.C., Quiñónez Samaniego, R.A., and Kanazawa, N.M. 2016. Life cycle assessment for soil stabilization dosages: A study for the Paraguayan Chaco. Journal of Cleaner Production, **139**: 309–318. doi:10.1016/j.jclepro.2016.07.219.

Ross, D.S., and Ketterings, Q. 1995. Recommended methods for determining soil cation exchange capacity. Recommended soil testing procedures for the northeastern United States, **2**: 62–70. Northeastern Regional Publication.

Rovnaník, P. 2010. Effect of curing temperature on the development of hard structure of metakaolin-based geopolymer. Construction and building materials, **24**(7): 1176–1183. Elsevier.

Rowles, M., and O'connor, B. 2003. Chemical optimisation of the compressive strength of aluminosilicate geopolymers synthesised by sodium silicate activation of metakaolinite. Journal of materials chemistry, **13**(5): 1161–1165. Royal Society of Chemistry.

Samuel, R., Huang, O., Banerjee, A., Puppala, A., Das, J., and Radovic, M. 2019. Case Study: Use of Geopolymers to Evaluate the Swell-Shrink Behavior of Native Clay in North Texas. *In* Eighth International Conference on Case Histories in Geotechnical Engineering. American Society of Civil Engineers, Philadelphia, PA. pp. 167–178. doi:10.1061/9780784482117.016.

Saride, S., Puppala, A.J., and Williammee, R. 2010. Assessing recycled/secondary materials as pavement bases. Proceedings of the ICE-Ground Improvement, **163**(1): 3–12.

El Sawwaf, M.A. 2007. Behavior of strip footing on geogrid-reinforced sand over a soft clay slope. Geotextiles and Geomembranes, **25**(1): 50–60. doi:10.1016/j.geotexmem.2006.06.001.

Scanlon, J.M. 1994. Factors influencing concrete workability. *In* Significance of tests and properties of concrete and concrete-making materials. ASTM International.

Scavuzzo, R. 1984. Use of the Harvard Miniature Apparatus for obtaining moisture-unit weight relationships of soils. Geotechnical Branch, Division of Research and Laboratory Services ….

Seed, H.B., Mitchell, J.K., and Chan, C.K. 1962. Studies of swell and swell pressure characteristics of compacted clays. Highway Research Board Bulletin, (313).

Shadnia, R., and Zhang, L. 2017. Experimental study of geopolymer synthesized with Class F fly ash and low-calcium slag. Journal of Materials in Civil

Engineering, **29**(10): 1–10. doi:10.1061/(ASCE)MT.1943-5533.0002065.

Sharma, A.K., and Sivapullaiah, P. V. 2016. Ground granulated blast furnace slag amended fly ash as an expansive soil stabilizer. Soils and Foundations, **56**(2): 205–212. Elsevier.

Shuler, E.W. 1918. The geology of Dallas County. The University.

Škvára, F., Jílek, T., and Kopecký, L. 2005. Geopolymer materials based on fly ash. Ceram.-Silik, **49**(3): 195–204.

Snethen, D. 1980. Expansive soils in highway subgrades: summary. US Dept. of Transportation, Federal Highway Administration, Offices of ….

Soltani, A., Taheri, A., Khatibi, M., and Estabragh, A.R. 2017. Swelling potential of a stabilized expansive soil: A comparative experimental study. Geotechnical and Geological Engineering, **35**(4): 1717–1744. Springer.

Steinberg, M.L. 1998. Geomembranes and the Control of Expansive Soils in Construction. McGraw-Hill.

Steins, P., Poulesquen, A., Diat, O., and Frizon, F. 2012. Structural evolution during geopolymerization from an early age to consolidated material. Langmuir, **28**(22): 8502–8510. ACS Publications.

Steveson, M., and Sagoe-Crentsil, K. 2005. Relationships between composition, structure and strength of inorganic polymers. Journal of materials science, **40**(8): 2023–2036. Springer.

Strong, H.M. 1938. A Land Use Record in the Blackland Prairies of Texas. Annals

of the Association of American Geographers, **28**(2): 128–136. Taylor & Francis.

Talluri, N., Puppala, A.J., Chittoori, B.C.S., Gaily, A.H., and Harris, P. 2013. Stabilization of High-Sulfate Soils by Extended Mellowing. Transportation Research Record: Journal of the Transportation Research Board, **2363**(1): 96–104. doi:10.3141/2363-11.

Tayabji, S.D., Nussbaum, P.J., and Ciolko, A.T. 1982. Evaluation of Heavily Loaded Cement-Stabilized Bases. Transportation Research Record, **839**: 6–11.

Temuujin, J., Minjigmaa, A., Rickard, W., Lee, M., Williams, I., and van Riessen, A. 2009. Preparation of metakaolin based geopolymer coatings on metal substrates as thermal barriers. Applied Clay Science, **46**(3): 265–270. doi:10.1016/j.clay.2009.08.015.

Temuujin, J., Rickard, W., Lee, M., and van Riessen, A. 2011. Preparation and thermal properties of fire resistant metakaolin-based geopolymer-type coatings. Journal of Non-Crystalline Solids, **357**(5): 1399–1404. doi:10.1016/j.jnoncrysol.2010.09.063.

Terzaghi, K., and Peck, R.B. 1967. Soil Mechanics in Engineering Practice. *In* Inc., New York, 2nd edition. John Wiley & Sons. Inc., New York.

Thomas, M.D.A., Gruber, K.A., and Hooton, R.D. 1999. The use of high reactivity metakaolin in high performance concrete. *In* First Engineering Foundation

Conference on High Strength ConcreteUnited Engineering Foundation, Incorporated.

Thompson, M.R. 1966. Lime reactivity of Illinois soils. Journal of the Soil Mechanics and Foundations Division, **92**(5): 67–92. ASCE.

Thompson, M.R. 1969. Engineering properties of lime-soil mixtures.

Thompson, M.R. 1970. Soil Stabilization for Pavement Systems - State of the Art. Construction Engineering Reaserch Laboratory,.

Tingle, J.S., Newman, J.K., Larson, S.L., Weiss, C.A., and Rushing, J.F. 2007. Stabilization mechanisms of nontraditional additives. Transportation research record, **1989**(1): 59–67. SAGE Publications Sage CA: Los Angeles, CA.

Tingle, J.S., and Santoni, R.L. 2003. Stabilization of clay soils with nontraditional additives. Transportation Research Record, **1819**(1): 72–84. SAGE Publications Sage CA: Los Angeles, CA.

Usmen, M.A., and Bowders Jr, J.J. 1990. Stabilization characteristics of class F fly ash. Transportation Research Record, (1288).

Wang, M.Q. 1999. Technical Report: GREET 1.5 -Transportation fuel-cycle model: Methodology, development, use, and results. Argonne National Lab., IL (US), Argonne, IL.

Weng, L., Sagoe-Crentsil, K., Brown, T., and Song, S. 2005. Effects of aluminates on the formation of geopolymers. Materials Science and Engineering: B, **117**(2): 163–168. doi:10.1016/j.mseb.2004.11.008.

WHO. 1993. Guidelines for drinking-water quality. World Health Organization.

Williams, H.F.L. 2003. Urbanization pressure increases potential for soils-related hazards, Denton County, Texas. Environmental Geology, **44**(8): 933–938. doi:10.1007/s00254-003-0836-8.

Williams, R.P., Hart, R.D., and van Riessen, A. 2011. Quantification of the Extent of Reaction of Metakaolin-Based Geopolymers Using X-Ray Diffraction, Scanning Electron Microscopy, and Energy-Dispersive Spectroscopy. Journal of the American Ceramic Society, **94**(8): 2663–2670. Wiley Online Library.

Winton, W.M. 1925. The Geology of Denton County. University of Texas at Austin.

Winton, W.M., and Scott, G. 1912. The Geology of Johnson County. The University.

Wray, W.K., and Meyer, K.T. 2004. A widespread and costly geohazard. Geostrata. ASCE GeoInst, **5**(4): 24–28.

Xu, H., and Van Deventer, J.S.J. 2000. The geopolymerisation of alumino-silicate minerals. International Journal of Mineral Processing, **59**(3): 247–266. doi:10.1016/S0301-7516(99)00074-5.

Yun-Ming, L., Cheng-Yong, H., Al Bakri, A.M.M., and Hussin, K. 2016. Structure and properties of clay-based geopolymer cements: A review. Progress in Materials Science, **83**: 595–629. Elsevier Ltd. doi:10.1016/j.pmatsci.2016.08.002.

Zhang, M., Guo, H., El-Korchi, T., Zhang, G., and Tao, M. 2013. Experimental feasibility study of geopolymer as the next-generation soil stabilizer. Construction and Building Materials, **47**: 1468–1478. Elsevier.

Zhang, M., Zhao, M., Zhang, G., Nowak, P., Coen, A., and Tao, M. 2015. Calcium-free geopolymer as a stabilizer for sulfate-rich soils. Applied Clay Science, **108**: 199–207. Elsevier.

Zuhua, Z., Xiao, Y., Huajun, Z., and Yue, C. 2009. Role of water in the synthesis of calcined kaolin-based geopolymer. Applied Clay Science, **43**(2): 218–223. Elsevier.

Zulkifley, M.T.M., Ng, T.F., Raj, J.K., Hashim, R., Bakar, A.F.A., Paramanthan, S., and Ashraf, M.A. 2014. A review of the stabilization of tropical lowland peats. Bulletin of Engineering Geology and the Environment, **73**(3): 733–746. Springer.

# BIOGRAPHICAL INFORMATION

Rinu Ann Samuel received a Bachelor of Science degree in Geological Engineering from the University of Alaska Fairbanks in 2010. Subsequently, she worked as a geological field engineer (EIT) at the Fairbanks, Alaska branch of the geotechnical consulting firm Shannon & Wilson, Inc. She received a Master of Science in Civil Engineering, with a specialization in geotechnical engineering, from the University of Nevada Las Vegas in 2015. She then worked as a staff engineer at G2 Consulting Group, LLC, at Troy, Michigan.

Rinu joined the doctoral program with the Department of Civil Engineering at the University of Texas at Arlington (UTA) in 2016. At UTA, Rinu worked under the able guidance of Dr. Anand Puppala, to investigate the effects of geopolymers as an alternative to conventional soil stabilizers. She is a recipient of the prestigious Dwight D. Eisenhower Transportation Fellowship awarded by the US Department of Transportation. She is a proud member of the American Society of Civil Engineers, and Tau Beta Pi. Rinu's research interests include expansive soils, ground improvement, *in situ* testing, and sustainable geotechnical practices.